AUBURN UNIVERSITY
Samuel Ginn College of Engineering

Research Report

EVALUATION OF ALABAMA LIMESTONE SOURCES FOR USE AS PAVEMENT AGGREGATE BASE

Submitted to

The Alabama Department of Transportation

Prepared by

Dr. Benjamin F. Bowers, P.E.
Dr. J. Brian Anderson, P.E.
Dr. Don Guy Biessan

MARCH 2025

Highway Research Center
Harbert Engineering Center
Auburn, Alabama 36849

1. Report No. 931-052	**2. Government Accession No.**	**3. Recipient Catalog No.**
4. Title and Subtitle EVALUATION OF ALABAMA LIMESTONE SOURCES FOR USE AS PAVEMENT AGGREGATE BASE		**5. Report Date** February 2025 **6. Performing Organization Code**
7. Author(s) Benjamin F. Bowers, J. Brian Anderson, Don Guy Biessan		**8. Performing Organization Report No.**
9. Performing Organization Name and Address Highway Research Center Department of Civil Engineering 238 Harbert Engineering Center Auburn, AL 36849		**10. Work Unit No. (TRAIS)** **11. Contract or Grant No.**
12. Sponsoring Agency Name and Address Highway Research Center Department of Civil Engineering 238 Harbert Engineering Center Auburn, AL 36849		**13. Type of Report and Period Covered** **14. Sponsoring Agency Code**
15. Supplementary Notes		

16. Abstract

In recent years, the number of requests for approval of locally mined limerock in Alabama has increased due to potential economic benefits associated with its use. However, the potential moisture sensitivity of limerock is a concern that has not been fully addressed as it can impact the long-term performance of pavements. The objective of this study was to evaluate the effect of moisture, over a broad spectrum ranging from a very dry state to complete saturation, on the mechanical behavior of crushed limestone and limerock. The second objective is to develop and identify a rapid test method for quality assurance. The resilient modulus of three limestone aggregates and four limerock aggregates were determined at four different moisture contents including 100% saturation. The properties of the base aggregates were also obtained. The results demonstrated that the resilient modulus of limestone and limerock increased significantly with decreasing moisture content when drying from the optimum moisture content. When saturated, limestone and limerock aggregates mostly experienced a reduction in their resilient modulus. A series of statistical and sensitivity analyses of the laboratory test results demonstrated that the fine aggregate content, fines content, fine aggregate angularity, and plastic fines content contribute most to the moisture susceptibility of base aggregates when moisture content exceeds the optimum moisture content. A set of tests was recommended to rapidly obtain these influencing properties, and a threshold chart was developed to assess the moisture susceptibility of unbound base materials. A case study confirmed the validity and reliability of the threshold chart, which can be used during material selection and quality assurance testing in the field or laboratory. This proposed method can help ensure that the unbound base materials selected for construction can retain their stiffness or recover from the effects of climatic events in a timely and efficient manner. These findings are also valuable for pavement design and construction material selection to achieve more sustainable and climate-resilient pavements.

17. Key Words Limestone; Limerock; Resilient Modulus; Moisture Susceptibility; Base Aggregates; Quality Assurance		**18. Distribution Statement**	
19. Security Classification (of this report) Unclassified	**20. Security Classification (of this page)** Unclassified	**21. No. of Pages**	**22. Price** None.

Research Report

EVALUATION OF ALABAMA LIMESTONE SOURCES FOR USE AS PAVEMENT AGGREGATE BASE

Submitted to

The Alabama Department of Transportation

Prepared by

Dr. Benjamin F. Bowers, P.E.
Dr. J. Brian Anderson, P.E.
Dr. Don Guy Biessan

MARCH 2025

DISCLAIMERS

The contents of this report reflect the views of the authors who are responsible for the facts and accuracy of the data presented herein. The contents do not necessarily reflect the official views or policies of Alabama DOT, Auburn University, or the Highway Research Center. This report does not constitute a standard, specification, or regulation. Comments contained in this report related to specific testing equipment and materials should not be considered an endorsement of any commercial product or service; no such endorsement is intended or implied.

NOT INTENDED FOR CONSTRUCTION, BIDDING, OR PERMIT PURPOSES

Dr. Benjamin F. Bowers, PE
Dr. J. Brian Anderson, PE
Research Supervisors

ACKNOWLEDGEMENTS

This project was sponsored by the Alabama Department of Transportation. We greatly appreciate the assistance of the Project Advisory Committee of Mr. Stacey Glass, Mr. Scott George, Mr. Virgil Clifton, and Ms. Kristy Harris, along with Mr. Chance Armstead, Mr. John Jennings, and the staff at ALDOT who provided support and insight throughout this study.

ABSTRACT

In recent years, the number of requests for approval of locally mined limerock in Alabama has increased due to potential economic benefits associated with its use. However, the potential moisture sensitivity of limerock is a concern that has not been fully addressed as it can impact the long-term performance of pavements. The objective of this study was to evaluate the effect of moisture, over a broad spectrum ranging from a very dry state to complete saturation, on the mechanical behavior of crushed limestone and limerock. The second objective is to develop and identify a rapid test method for quality assurance. The resilient modulus of three limestone aggregates and four limerock aggregates were determined at four different moisture contents including 100% saturation. The properties of the base aggregates were also obtained. The results demonstrated that the resilient modulus of limestone and limerock increased significantly with decreasing moisture content when drying from the optimum moisture content. When saturated, limestone and limerock aggregates mostly experienced a reduction in their resilient modulus. A series of statistical and sensitivity analyses of the laboratory test results demonstrated that the fine aggregate content, fines content, fine aggregate angularity, and plastic fines content contribute most to the moisture susceptibility of base aggregates when moisture content exceeds the optimum moisture content. A set of tests was recommended to rapidly obtain these influencing properties, and a threshold chart was developed to assess the moisture susceptibility of unbound base materials. A case study confirmed the validity and reliability of the threshold chart, which can be used during material selection and quality assurance testing in the field or laboratory. This proposed method can help ensure that the unbound base materials selected for construction have the ability to retain their stiffness or recover from the effects of climatic events in a timely and efficient manner. These findings are also valuable for pavement design and construction material selection to achieve more sustainable and climate-resilient pavements.

TABLE OF CONTENTS

1 INTRODUCTION

1.1 OVERVIEW

Alabama is a geologically diverse state, which translates to a geologically diverse roadway network. Many state agencies have a list of approved products that can be used in highway construction to ensure quality materials are used in roadway construction. Included in the approved list of aggregates used in Alabama are gravels, granite, sandstone, limestone, and recently “limerock”, among others (ALDOT 2020). Limestone has been used throughout the Alabama roadway network for many years and is of little concern. However, requests to approve and use a locally mined product known colloquially in Alabama and Florida as limerock have become more frequent. While there are cases where limerock passes required Alabama Department of Transportation (ALDOT) specifications for approval, there can be significant variability depending on when the sample is taken, sometimes resulting in a stone that barely passes or fails the ALDOT specification. There is potentially great benefit to using this stone in roadway construction for economic reasons, however the longer-term performance of a material that seems to have high variability and may potentially fail required ALDOT approval tests is of concern for the long-term performance of the roadway. If inadequate materials are used in roadway construction the road is likely to deteriorate at a faster rate than expected. This may lead to safety concerns or higher long-term maintenance costs.

1.2 BACKGROUND

ALDOT conducts numerous tests as a part of its annual aggregate approval process. These tests help ensure that any aggregate product that a quarry is providing for ALDOT projects will perform satisfactorily. For limestone specifically, the following tests are conducted: unit weight, sieve analysis, T-11 wash test, specific gravity, absorption, soundness, voids, flat and elongated, Los Angeles Abrasion, British Polish Number (BPN), and the total silica content.

Limerock is a colloquial term used throughout Florida, Alabama, and elsewhere for a limestone-type aggregate that is present in these regions. The minerology is like that of limestone and, depending on source, presents similar physical properties to limestone. However, based on ALDOT’s approved aggregates (as of August 4, 2020), the approved limerock sources have much lower specific gravity values and much higher absorption values than a typical limestone. These factors in of themselves do not necessarily indicate that the performance of the aggregate as an aggregate base material in a pavement will not be satisfactory. However, some of the samples taken throughout the year by ALDOT have tended to approach the limits of, or even fail, the required test criteria for an acceptable aggregate base material. Hiltunen et al. (2011) conducted an experiment to characterize aggregate base materials for the Mechanistic Empirical Pavement Design Guide (MEPDG) and concluded that Florida limerock was particularly affected

by moisture. Namely, it was found that the limerock was stronger when below optimum moisture content and that the MEPDG model underpredicted the influence of moisture. This compliments the work of Toros and Hiltunen (2008). However, the modulus testing was not above the optimum moisture content. Considering the potential for aggregate base materials to become saturated (i.e., beyond the optimum) and potentially stay saturated, it would be beneficial to understand what effect saturation has on limerock.

There is a need to (1) understand the impact of moisture on the modulus of limerock compared to other limestone sources throughout Alabama and (2) to develop a rapid test for field acceptance of limerock sources considering the potential variability of the product. Limerock is a product of Alabama and its increased use will presumably help the local Alabama economy and potentially stretch Alabama's funding for roadway projects further. However, it is imperative that ALDOT ensures that it is getting a product that will perform as a pavement base and that will not cause increased roadway maintenance costs.

1.3 RESEARCH OBJECTIVES

Given the needs described above, this project has two primary objectives:

1. Evaluate the consensus properties and the effect of moisture on the resilient modulus of 7 limerock and limestone aggregate sources strategically sampled throughout the state of Alabama.
2. Based on the findings of objectives one, identify a simple rapid test that can be conducted on a sample of limerock or limestone aggregate to determine its suitability as an aggregate base material for highway construction.

2 LITERATURE REVIEW

2.1 LIMESTONE AND LIMEROCK

Limestone is a rock formed by chemical sedimentary processes, such as weathering of other types of rock, precipitation of calcium carbonate from lake or ocean water, and accumulation of once-living organisms. It is mainly composed of calcium carbonate mineral with a chemical composition of CaCO3. It usually also contains low percentages of other minerals such as pyrite and siderite formed by chemical processes or small particles of quartz, feldspar, or even clay minerals transported to sites by streams, currents and wave action (King, 2022). In limestone quarries, two factors that definitely affect the quality of limestone aggregates are the increased amount of small, interconnected pores and clay minerals mixed in the limestone. The main cause that generally increases the volume of pores and the percentage of clay minerals is weathering (Harris and Chowdhury, 2007). In limestone, chemical weathering gradually occurs through a process called carbonation, which is a result of a chemical reaction between rock minerals and carbonic acid. When in contact with carbonic acid, limestone reacts to form a soluble solution called calcium bicarbonate, which can be carried away. The chemical equations shown in Equations 2.1 and 2.2 describe the process (Geo Car., 2022).

$$\text{carbon dioxide } (CO_2) + \text{water } (H_2O) \rightarrow \text{carbonic acid } (H_2CO_3) \quad (2.1)$$

$$\text{calcite } (CaCO_3) + \text{carbonic acid } (H_2CO_3) \rightarrow \text{calcium } (Ca^{2+}) + \text{bicarbonate } (2HCO_{3-}) \quad (2.2)$$

Limestone is a widely used rock in diverse sectors especially in construction where it is usually transformed into crushed stones or aggregates and used in concrete, railroad ballast, drain fields, road base, and other construction uses.

Limerock, according to the Florida Department of Transportation (FDOT) standard specifications for road and bridge construction, is a material consisting of unconsolidated or partly consolidated limestone of marine origin. In the FDOT specifications, limerock is called a rock base for pavement base courses (section 200) while limestone is listed as an example of graded aggregate base (GAB) materials (section 204). The requirements for limerock are different and must conform to section 911 of the specifications, which includes the limerock bearing ratio test requirement (FDOT, 2017). Similarly, the requirements for limerock provided in the ADLOT standard specifications for highway construction also include limerock bearing ratio (LBR) test. In the ALDOT specifications, limerock is listed as a type of soil aggregate materials, which are different from crushed aggregate base materials such as crushed limestone (ALDOT, 2018).

2.2 AGGREGATE PROPERTIES

To properly investigate the quality of aggregates, it is important to determine the aggregate properties (consensus, physical, and mechanical properties). Details concerning the properties considered in this study and their corresponding test methods are described below.

2.2.1 Consensus Properties

Consensus properties are generally the aggregate properties that can be modified during the manufacturing process to satisfy the predetermined consensus source requirements. The consensus properties considered are coarse aggregate angularity, uncompacted void content of fine aggregate, flat and elongated particles, and sand equivalency or plastic fines content. First, coarse aggregate angularity and uncompacted void content are obtained using the test methods described in ASTM D5821 and AASHTO T304, respectively. They inform about the shape, angularity, and texture of the aggregate particles and their ability to interlock in a packed matrix such as a pavement base layer. An appropriate interlocking among particles can increase shear strength and structural stability of the pavement base layer to withstand traffic loads. A pavement base course layer lacking good aggregate particles angularity and surface texture can lead to low stability and pavement distresses such as cracking and rutting (Titi et al., 2018). Second, the flat and elongated particles test performed using the methods in ASTM D4791 helps determine the percentage of coarse aggregate with a maximum to minimum dimension greater than the ratios of 5:1 or 3:1. A high percentage of flat and elongated aggregate particles in pavement base layers is an issue because the particles can break during compaction causing a change in gradation and density (Titi et al., 2018). Third, plastic fines content represents the proportion of clay-like materials in fine aggregate and is determined using the method in AASHTO T176. Aggregates with great amount of clay minerals absorb a lot of water and have an increased number of small pores that weaken their skeletal framework. This can lead to lower strength and more stress softening effect in pavement base layers (Harris and Chowdhury, 2007).

2.2.2 Physical Properties

The physical properties considered are aggregate gradation, specific gravity and absorption, unit weight and void content, Atterberg limits, maximum dry density, and optimum moisture content. First, aggregate gradation or distribution of particle sizes is obtained following the AASHTO T27 procedure and the percentage of particles passing the 0.075-mm sieve can be determined using the washed sieve analysis procedure in AASHTO T11. Aggregate gradation is needed in the determination of almost all other properties. Aggregate particles passing the 4.75-mm sieve are called fine aggregates while the particles retained on the same sieve and above are called coarse aggregates. Fine aggregates have lower permeability compared to coarse

aggregates and some applications such as pavement base layers must have a high permeability for drainage and frost resistance. This is the reason why agencies specify a maximum percentage passing each sieve. In addition, pavement base aggregates with high fines content and improper gradation can create pavement distresses such as fatigue cracking and rutting (Titi et al., 2018). Second, the specific gravity and absorption of fine aggregate and coarse aggregate are determined following AASHTO T84 and T85 specifications, respectively. Specific gravity is the ratio of the density of aggregate to the density of water. For pavement base layers, a high specific gravity can improve stability without the need of increased layer thickness (Titi et al., 2018). Absorption represents the amount of water that can be absorbed by an aggregate into its pore structure. Third, unit weight and void content are determined using procedures in AASHTO T19. Unit weight is the weight of aggregate in a given volume and void is the space between the aggregate particles not occupied by solid minerals. Fourth, the Atterberg limits, liquid limit and plastic limit, are obtained using the test methods in AASHTO T89 and T90, respectively. These limits represent the critical water contents at which the fine-grained soil changes states or conditions. The plasticity of aggregate fine particles greatly influences the strength characteristics of the aggregates (Osouli et al., 2018). Fifth, the maximum dry density and optimum moisture content are obtained by conducting the compaction or Proctor test following AASHTO T180 procedures. Those parameters are crucial in the procedure to determine the resilient modulus of aggregates.

2.2.3 Mechanical Properties

The mechanical properties considered are Los Angeles (L.A.) abrasion or toughness and resilient modulus. First, L.A. Abrasion or aggregate toughness, obtained using ASTM C131, is a measure of the degradation of a coarse aggregate sample after undergoing substantial wear and tear in a rotating drum with steel spheres. Pavement base layers should have aggregates that are tough and hard to resist crushing, degradation and disintegration during construction and under traffic. Weak pavement base aggregates experience degradation under repeated loads, which contributes to fatigue cracking and rutting of the pavement (Titi et al., 2018).

2.3 Resilient Modulus (M_R)

The resilient modulus is a measure of material stiffness and a fundamental mechanical property used to characterize unbound pavement materials and design pavement systems. It is obtained through the application of cyclic dynamic loads on prepared specimens while recording the resulting deformation data. The test procedure is described in AASHTO T307. The resilient modulus is calculated as the ratio of the deviator stress to the recoverable or resilient strain. Deviator stress is the difference between the total axial stress (σ1) and confining stress (σ3) at a point in the pavement system. It is also equal to the applied vertical load divided by the specimen contact area. Recoverable strain (εr) is the strain that is recovered when the applied load is

removed while the plastic strain (εp) is the permanent strain that prevents the distorted body to return to its original shape and size when the applied load is removed. The sum of the plastic strain and the recoverable is called the total strain (εt). Figure 2.1 shows the response of the specimen due to the first cyclic axial loading during the first sequence of the resilient modulus test (Buchanan, 2007).

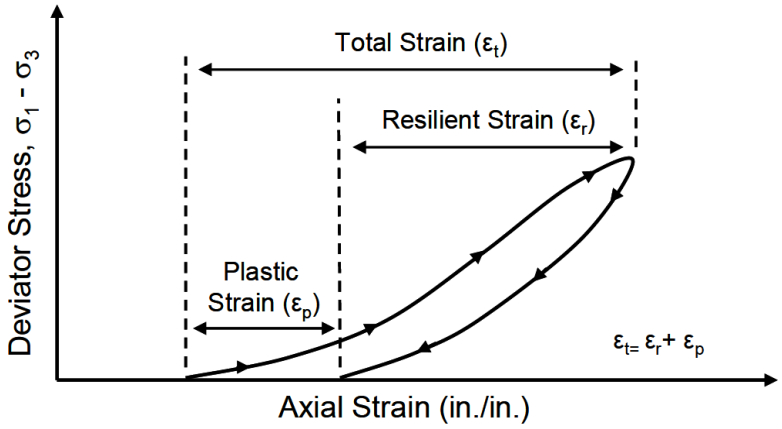

Figure 2.1. Specimen response during axial loading (Buchanan, 2007)

The testing procedure for resilient modulus requires 15 testing sequences, which represent 15 different stress states that can be encountered in the field. A stress state or bulk stress is equal to the sum of deviator stress and three times the confining stress. Figure 2.2 shows an example of a resilient modulus stress state. The stress states are specified for subgrade and base/subbase as shown in Table 2.1. Each sequence is performed by applying 100 loading cycles of the desirable stress state. One cycle has a load period of 0.1 second followed by a 0.9 second rest period. At the end of the test, a graph plotting the bulk stress and the corresponding resilient modulus values is generated.

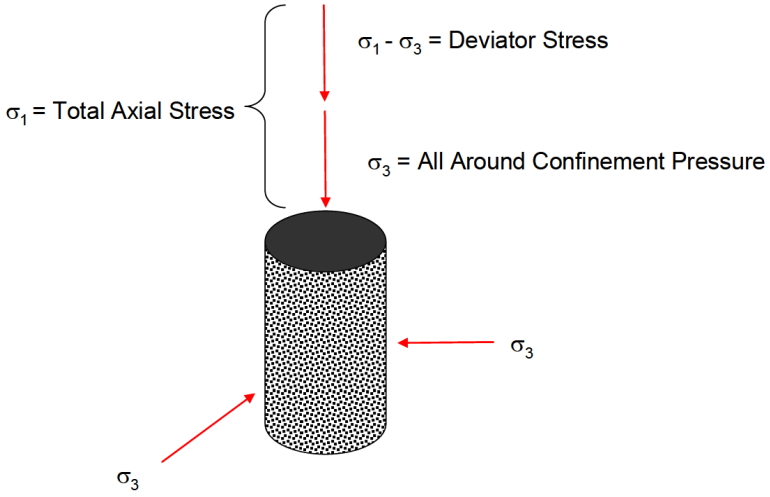

Figure 2.2. Resilient modulus stress state (Buchanan, 2007)

Table 2.1. Test sequences specified for subgrade and base/subbase (AASHTO T307, 2021)

Test Sequence	SUBGRADE			SUBBASE/BASE		
	Confining Pressure (psi)	Deviator (Axial) Stress (psi)	Bulk Stress (psi)	Confining Pressure (psi)	Deviator (Axial) Stress (psi)	Bulk Stress (psi)
0	6	4	22.0	15	15	60.0
1	6	2	20.0	3	3	12.0
2	6	4	22.0	3	6	15.0
3	6	6	24.0	3	9	18.0
4	6	8	26.0	5	5	20.0
5	6	10	28.0	5	10	25.0
6	4	2	14.0	5	15	30.0
7	4	4	16.0	10	10	40.0
8	4	6	18.0	10	20	50.0
9	4	8	20.0	10	30	60.0
10	4	10	22.0	15	10	55.0
11	2	2	8.0	15	15	60.0
12	2	4	10.0	15	30	75.0
13	2	6	12.0	20	15	75.0
14	2	8	14.0	20	20	80.0
15	2	10	16.0	20	40	100.0

2.3.1 Impact of Density of M_R of Base Aggregates

Numerous studies that evaluated the influence of density on MR discovered that specimens compacted at a high density will normally have higher resilient modulus than those compacted at a lower density (Hossain, 1998; Janoo et al., 2004; Buchanan, 2007). However, that influence is dependent on the material type and can be insignificant in some cases (Janoo et al., 2004). Thom and Brown (1987) found in their study that the influence of density on the resilient modulus of crushed-limestone road base was negligible even though denser materials performed better. For them, the change in permanent strain during multicyclic loading is strongly dependent on density. According to Titi et al. (2006), specimens compacted by kneading compaction tend to have lower resilient modulus than those compacted statically. However, compaction has the lowest effect on resilient modulus compared to saturation level and stress state.

2.3.2 Impact of Stress State on M_R of Base Aggregates

Concerning stress state, confining stresses have a more significant effect on resilient modulus than deviator stress especially in granular soils (base/subbase materials) and when there is no excessive plastic deformation caused by that stress (Hossain, 1998; Titi et al., 2006). Usually, resilient modulus of granular soils increases as confining stress increases. An increase in deviator stress creates a strain hardening effect on granular soils because the particles reorient themselves into a denser state which increases the resilient modulus (Titi et al., 2006).

2.3.3 Impact of Gradation, Fines Content, and Plasticity Index on M_R of Base Aggregates

It was found by several researchers that the gradation, the percentage of fines content (% passing No. 200 sieve), and plasticity index have a significant impact on the strength of unbound aggregate base. Even though aggregate base layers rarely have percent fines content exceeding 20%, their aggregate skeleton is greatly influenced by the fines content characteristics (Adhikari and Osouli, 2019).

Salam et al. (2018) used the soaked California bearing ratio (CBR) method to investigate the effects of maximum particle size, dust ratio (DR), fines content (FC), plasticity index (PI), and gradation on the strength properties of crushed limestone aggregates. All the aggregate index properties mentioned above were varied for two different gradations with maximum particle sizes of 1 in. (25 mm) and 2 in. (50 mm). The investigation demonstrated that fines content, maximum particle size, and dust ratio impact the strength of limestone aggregates collectively. The most important influencing properties on aggregate CBR were both gradation and plasticity index. It was discovered that high PI had a significant negative effect on aggregate CBR when more fines content was included in the aggregate matrix. The authors recommended maximum values of 6 for PI and 25% for liquid limit (LL) for limestone aggregate even though most state agencies usually determine their own limits for PI and LL and a few others use the sand equivalency test to evaluate aggregate quality. The authors also proposed a new method for material selection based on their research findings. This method provides strength zones, as shown in Figure 2.3, based on FC, DR, and maximum particle size. However, CBR only represents static behavior of aggregate and in-situ or field stress and strain conditions are not considered.

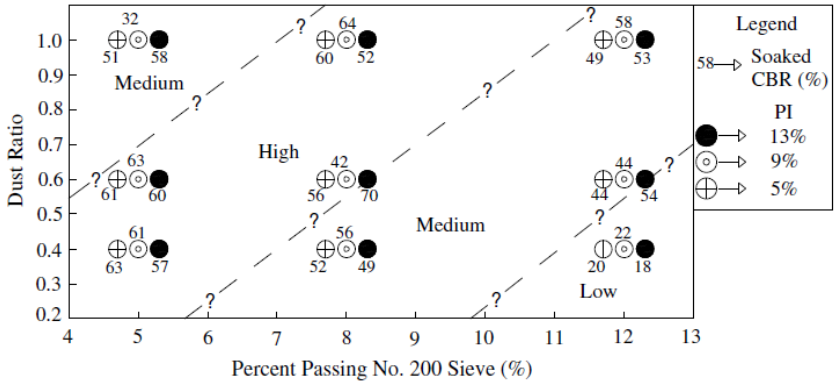

Figure 2.3. Strength zones for gradation with maximum particle size of 1 in. (Salam et al. 2018)

In their study, Adhikari and Osouli (2019) investigated the effect of fines content (from 5% to 12%), plasticity index (from 5% to 9%), and dust ratio (from 0.4 to 1.0) on the cyclic behavior of crushed limestone aggregate base. Dust ratio is the ratio of the percentage of fines content to the percentage of aggregates passing No. 40 sieve. They observed that the resilient modulus (MR)

decreased as the dust ratio increased from 0.4 to 0.6, but the reverse trend was noticed for the dust ratio of 1.0. At low fines content, MR decreased as dust ratio increased and this was due to the increase in void ratio as the number of particles between sieves No. 40 and No. 200 decreased. At high fines content, MR increased as dust ratio increased. In general, resilient modulus decreased slightly with increasing fines content. Resilient modulus was also affected by the plasticity of fines content as MR decreased with respect to increasing plastic index. This is why Yau and Von Quintus (2004) stated that clay content is very important for all soil groups.

Osouli et al. (2021) also analyzed the laboratory cyclic load behavior (resilient modulus) of crushed limestone aggregate as a function of different aggregate properties variations and interactions. The different variables were fines content, plasticity index, dust ratio, gradation and the overall interactions between these properties. At the end, strength zones as shown in Figure 2.4 were proposed for material selection. Zone A represents the materials with resilient modulus of 36 ksi (250 MPa) or more and Zone B represents the materials with resilient modulus below 36 ksi (250 MPa).

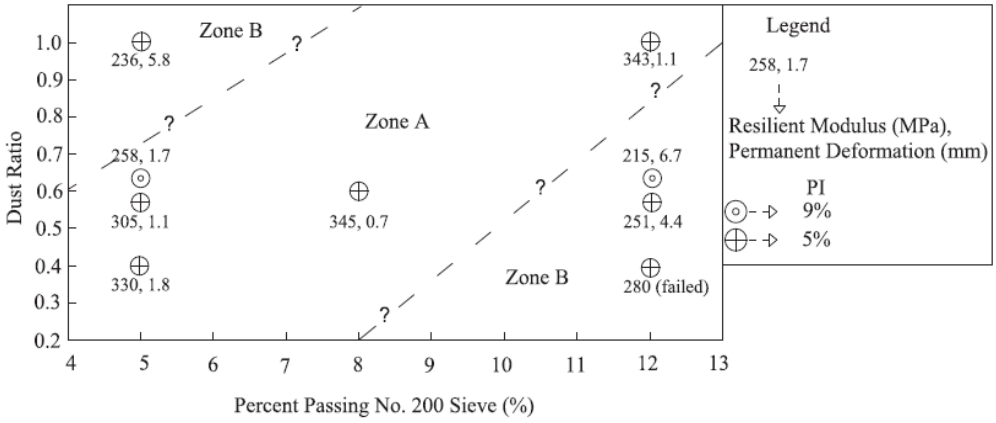

Figure 2.4. Strength zones for gradation with maximum particle size of 1 in. (Osouli et al., 2021)

Mishra et al. (2010) used the Analysis of Variance (ANOVA) approach to analyze the influence of different aggregates properties on the resilient modulus (MR) of unbound aggregates. Fines content (FC) and plasticity index (PI) were the most influencing factors. The samples were prepared at different FC (4%, 8%, 12%, and 16%) and it was noticed that the difference in MR was not significant when FC was increased from 4% to 8%. However, a significant difference in MR was observed at higher FC. The authors also reported that plastic fines can cause stress softening behavior of the aggregates. Hossain (1998) stated that the effect of FC on aggregate MR depends on the aggregate type. Barber (1946) showed that aggregates with more than 5% FC may need time to drain and experience an important strength reduction due to pore pressure development under loading. Thompson (1976) reported that permanent deformation increases

considerably when increasing FC from 3% to 21%. Tamrakar and Nazarian (2016) also reported that the load carrying capacity of aggregates through particle-to-particle contacts is reduced when FC is increased, which modifies the packing density. This leads to a decrease in permeability and an increase in moisture susceptibility. Therefore, base aggregate materials with high FC are not advisable for drainage and frost-protection purposes. To achieve the highest aggregates strength, Gray (1962) proposed 8% as FC maximum limit for aggregates with maximum particle size of 1 in. (25 mm).

2.3.4 Impact of Angularity on M_R of Base Aggregates

Janoo et al. (2004) provided a summary of tests results regarding the impact of aggregate angularity on the resilient modulus (MR) of pavement base/subbase layers. MR tests conducted on large scale samples (12 in. or 300 mmm in diameter) showed that MR of 0% crushed aggregates was higher than MR of 100% crushed aggregates at low bulk stress levels. Base course materials with 0, 25, 50, 75, and 100% crushed aggregates were tested for MR and the results showed that MR had the tendency to decrease with regard to increasing crushed content. One probable reason given for this trend was the slipping at the crushed aggregate interfaces for the reorientation of large particles when confining pressure is lower during loading. However, when the bulk stress increased beyond 46 psi (320 kPa), the trend was reversed as expected and MR increased as crushed content increased. This proved that the impact of angularity on MR becomes important at higher bulk stress when sufficient confinement is applied to hold particles in place.

Other researchers like Mishra et al. (2010) also demonstrated through statistical analyses that aggregate angularity has a significant impact on resilient modulus of unbound aggregates. Allen (1973) and Barksdale and Itani (1989) indicated that angular materials are more resistant to permanent deformation because they have better particle interlock and higher angle of shear resistance between particles compared to rounded materials. Tamrakar and Nazarian (2016) reported that high crushed content contributed to increased MR because the crushed aggregates have more surface contact points, but when fine content was below 10% that effect was minimal. That minimized effect at fine content between 0% and 10% was also observed by Barksdale and Itani (1989). On the contrary, Jorenby and Hicks (1986), Kamal et al. (1993) and Lekarp et al. (2000) reported that there is an increase in MR of well-graded aggregates since the fines replace the voids in the aggregate mix to a certain level.

2.3.5 Impact of Moisture on M_R of Base Aggregates

In the field, the most likely factor to change in granular base layers when climatic variation occurs is moisture content (Hossain, 1998). Ullah and Tanyu (2020) used moisture content reflectometers to monitor the variations of moisture content with seasonal changes in the base

course of 6 flexible pavement sections constructed with the support of the Virginia Department of Transportation (VDOT). The data collected after 10 months showed that seasonal rain events contribute to the changes of base course moisture content although they were initially constructed at optimum moisture content. The moisture content of most granular materials has been found to affect the resilient behavior of the materials in both the laboratory and in-situ conditions (Tamrakar and Nazarian, 2016). The effect of moisture content on the resilient modulus of granular materials is considerable (Hossain, 1998).

Several researchers who previously studied the effect of moisture content (degree of saturation) on the resilient response of granular materials reported that, in general, the resilient modulus decreases as moisture content increases. Haynes and Yoder (1963) found that granular materials deteriorate rapidly and become unstable under repeated loading when the degree of saturation exceeds 80%. Thompson (1976) observed similar trends during repeated load triaxial tests on subgrade soils at different moisture contents. The permanent deformation increased substantially at degree of saturation above 80% and the reason provided was the development of pore water pressure ranging from 0.05 to 0.15 psi for repeated stress between 40 and 60 psi. Kasianchuk (1968) conducted a repeated load triaxial test on a saturated aggregate subbase material under undrained conditions. He concluded that even though the undrained conditions are less likely to occur in a pavement subbase, the results from the test are good indications that the resilient modulus of granular materials will decrease when the pavement structure is saturated. The author recorded a decrease in effective confining pressure and resilient modulus caused by the excess pore water pressure measured. Ksaibati et al. (2000) stated that the modulus values of pavement base layers are greatly reduced by moisture. However, the resilient behavior is not the same for all types of granular base materials.

Thom and Brown (1987) performed numerous repeated load triaxial tests on crushed limestone aggregates at various moisture contents. On one hand, they concluded that permanent deformation increased with no apparent pore pressure being generated upon wetting of the aggregate particles. On the other hand, they concluded that the stiffness was greatly increased due to cementation being created upon subsequent drying out of the limestone aggregate. The influence of suction, which could be present in granular materials, was found to have little effect on stress-strain relationships. They noted that the presence of excessive fines in base aggregates is dangerous as it leads to poor drainage and subsequent saturation. Morales and Pando (2011) investigated the mechanical behavior of crushed limestone aggregates after being submerged for up to 150 days in baths of fresh and salt water. They registered some modest degradation of the mechanical properties of some limestone aggregates. They observed an increase in compressibility of some materials and an increase in mass loss in the LA Abrasion test. They mentioned that geologic genesis, composition and formation type, age, rock quality, degree of weathering, and type and conditions of aggregate processing are factors that can affect

the engineering, durability, and mechanical properties of crushed limestone aggregates. Phommavone and Sangpetngam (2018) evaluated the influence of three different moisture contents on the resilient modulus (MR) of unbound crushed limestone. They noticed a significant increase in MR as moisture content decreased and the materials with fine gradation (60% passing #4 sieve) had slightly higher MR than those with coarse gradation (40% passing #4 sieve).

Limerock is another granular base material commonly used in Florida. Ksaibati et al. (2000) conducted a study on multiple Florida state roads with a goal to evaluate the decrease in moduli of bases and subgrades by cause of the proximity of the water table. All road sections had crushed limerock as base course materials. The modulus values of the layers were backcalculated using the results from the Dynaflect and falling weight deflectometer (FWD) tests performed at different times of the year. The fluctuations of water table depth and water content as well as testing data were collected over a 5-year period. The results from both Dynaflect and FWD evidence the massive negative impact of groundwater table on the modulus of base materials. They concluded that when the moisture content increased by 1%, the layer moduli were reduced by up to 29.41% for FWD and 8.54% for Dynaflect. These results showed that a decrease of pavement base layer modulus may be recorded if the design depths from the finished pavement grade to the water table is reduced. This can shorten the pavement service life and increase maintenance costs. Toros and Hiltunen (2008) investigated the influence of moisture on the stiffness properties of unbound aggregates used for base courses in the state of Florida. Among the five sources chosen for this study, three limerock sources were chosen from Ocala, Newberry, and Miami to represent central, northern, and southern Florida, respectively. The authors reported a dramatic decrease in the small-strain modulus of the materials as moisture increased. Hiltunen et al. (2011) also evaluated the effect of moisture on the effective base Young's Modulus (E) of Florida limerock aggregates. They compacted samples of Miami limerock and Newberry limerock at optimum moisture content (OMC) and left them to dry with no membrane at room temperature. They reported that the effective modulus increased as the moisture content decreased for all limerock materials. Nevertheless, the effective modulus of Miami limerock increased tremendously and at a faster rate with drying in comparison to other limerock. Below OMC, Miami limerock had the highest effective modulus; however, its modulus was the lowest at OMC. The authors suggested that the reduction of moisture content in the limerock materials created suction, which provided significant additional effective confinement and increased nonlinear modulus. They also stated that Miami limerock had the highest increase in small-strain modulus due to suction.

Beyond suction, there are other factors influencing the moisture susceptibility of base aggregates. For Janoo et al. (2004), the variations in gradation and fines content also play a role on the impact of moisture content on the resilient modulus (MR) of base materials. They stated

that there is an increase of MR when moisture content is initially increased; however, the effect reverses, and MR decreases when moisture content reaches a certain level. They explained that this phenomenon is due to the lubrification of the fines in the base course mix and that higher fines content will lead to a more substantial strength loss. Ekblad and Isacsson (2006) evaluated the resilient modulus of the coarse granular granite materials at various saturation levels up to full saturation. It was found that materials with high fines content experienced a significant decrease in resilient modulus whereas the materials with low fine content experienced a minor decrease even at full saturation. According to Teshale et al. (2019), the moisture sensitivity of unbound aggregate base depends on fines content, permeability, and absorption. In their study, Andrei et al. (2009) observed that moisture had less effect on non-plastic base-type materials compared to the plastic ones. They noted that upon drying from optimum moisture content (OMC), the modulus increased two or three times; however, the decrease in resilient modulus upon wetting was insignificant.

2.3.6 Impact of Moisture on Base Aggregates on Pavement Performance

Hossain (1998) investigated the influence of moisture content in granular bases on pavement performance. He performed a structural analysis to evaluate moisture effect on flexible pavement performance. The resilient modulus (MR) of different materials at different moisture contents was calculated using laboratory test data. MR was found to decrease with increasing moisture content. Using a computer program called KENLAYER, the pavement performance was evaluated with a base layer in a three-layer pavement system at different moisture contents. The asphalt concrete surface layer was the most affected by moisture content in the base layer. As moisture content increased, the maximum horizontal tensile stress at the bottom of the layer and the maximum vertical displacement at the top of the layer increased. The vertical stresses at the top of the granular base layer were slightly affected by moisture content. Abu-Rizaiza (1999) collected data on field pavement performances over 11 years and found that fatigue cracking was the predominant distress caused by groundwater rise (GWR). Based on the multilayer elastic theory, Salour and Erlingsson (2014) used FWD deflection data to evaluate pavement responses before and after groundwater rise (GWR). They found that when the groundwater rose up by about 5 ft (1.5 m), the 10 in. thick asphalt pavement experienced a 34% increase in tensile strain at the bottom of the asphalt layer and a 52% increase in compressive strain at the top of the subgrade. Elshaer et al. (2019) analyzed the effect of subsurface water on pavement structural performance using numerical modelling and concluded that full saturation of unbound material layers led to a significant increase in pavement surface deflection and vertical strain. According to Adhikari and Osouli (2019), rutting in the unbound base layer contributes to around 14% of the total pavement rutting. Chen and Wang (2023) reported that groundwater rise is expected to worsen with sea level rise (SLR) and that pavement rutting and cracking develop rapidly when

groundwater rises. This precipitates maintenance, rehabilitation, and reconstruction during the pavement service life.

Using different climatic conditions, Lin and Zhang (2020) numerically simulated the seasonal variations of base course resilient behavior under saturated/unsaturated conditions to evaluate the dynamic performance. Based on the results, they determined that, in the case of a new flexible pavement with a shallow groundwater table, capillary action was the most detrimental factor affecting the base course resilient behavior. During longer duration rainfall events, the degree of saturation of the pavement foundation increases and its resilient modulus decreases. The influence of the capillary action or matric suction could last for 52 days until equilibrium condition is achieved.

2.3.7 Techniques for Peparation of Granular Specimens at Various Moisture Contents

Evaluating the effect of moisture content on the stiffness or strength properties of granular materials have always been challenging for researchers. Different techniques have been used and proposed over the years to prepare granular specimens at various moisture contents up to full saturation and all have their advantages and disadvantages.

Uthus et al. (2005) investigated the effect of moisture on base course samples by compacting the samples at different moisture contents and corresponding dry densities obtained from the moisture/density laboratory compaction curves. The issue with this method is that it is not representative of what happens in an actual pavement structure where additional water due to seasonal variation infiltrates the base layer, which is initially compacted at the optimum moisture content (OMC) and maximum dry density (MDD). Many studies demonstrated (with data from field site) that the moisture content of the base course changes after construction due to water penetration. Therefore, testing the base materials at different water contents and respective densities is a completely different scenario (Ullah and Tanyu, 2020).

To mimic what actually happens in the field, Andrei et al. (2009) initially compacted their unbound materials at OMC/MDD and soaked the specimens in water or allowed them to dry at room temperature to increase and decrease moisture content, respectively. The specimen weights were monitored periodically to estimate the gain or loss of water and determine if the desired moisture content was achieved. Then, membranes were used to seal the specimens for 24 hours before testing to obtain a uniform moisture distribution throughout specimens. Toros and Hiltunen (2008) used a similar method, but for drying, the specimens were kept in plastic cylinder molds and then placed in the oven at 110°F.

Instead of soaking the base materials in water, which can lead to collapsing of the coarse aggregates, Ullah and Tanyu (2020) proposed the injection of additional water to prepare specimens at moisture contents above OMC. They compacted the granular base samples at OMC/MDD and injected additional water, as shown in Figure 2.5, to imitate a field rainfall event

scenario. The injection is done after the specimen is set up on the base of the triaxial cell and the bottom valves of the base plate are closed.

Figure 2.5. Injecting additional water into the specimen compacted at OMC (Ullah and Tanyu, 2020)

Burrage et.al. (2012) proposed a modified triaxial testing procedure that allows the application of matric suction to the unsaturated soils using the axis translation technique for moisture content variations. The axis translation technique, introduced by Hilf (1956), consists of imposing a positive air pressure (ua) and a less positive water pressure (uw) to the sample to achieve the desired matric suction (ua - uw) and respective water content from the soil water characteristic curve (SWCC). Figure 2.6 shows a schematic diagram of the proposed testing system. To use the axis translation technique, most of the standard testing apparatus remained unmodified except the triaxial cell. The base pedestal of the triaxial cell was modified to accommodate the high-air-entry (HAE) disk and reserve a water compartment below the disk for saturation. The role of the HAE consists of separating the air phase and the water phase of the soil so that matric suction is imposed through differential pressures application. A groove was also cut under the disk compartment to allow the flow of water and prevent the flow of air since the disk always needs to be in contact with water to avoid loss of saturation. The customized triaxial base is shown in Figure 2.7. The HAE ceramic disk was previously used in suction measurement by other researchers such as Craciun and Lo, (2010).

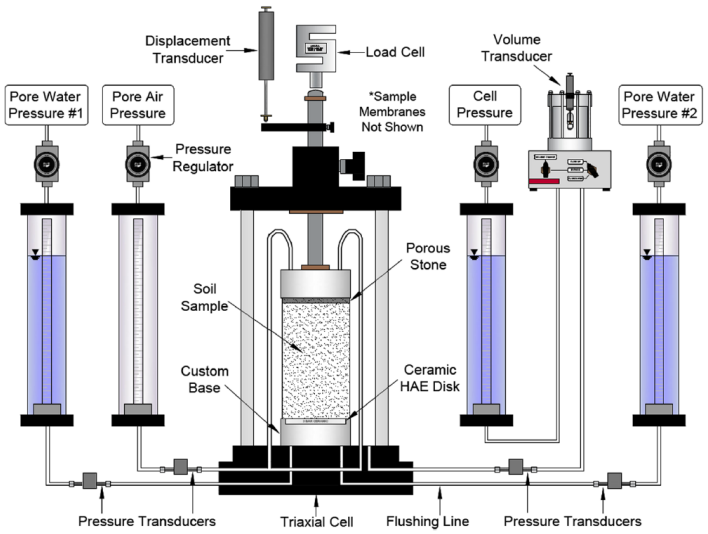

Figure 2.6. Schematic diagram of the modified triaxial apparatus (Burrage et.al., 2012)

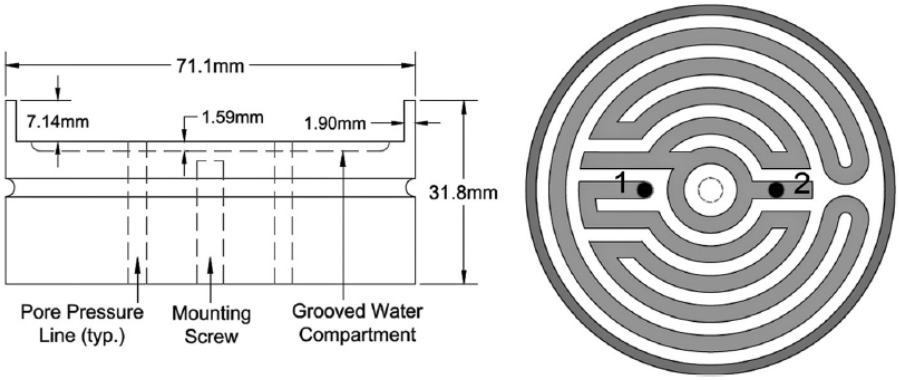

Figure 2.7. Modified triaxial cell base (a) side view, (b) top view showing groove pattern (Burrage et.al., 2012)

The disadvantages of this axis translation technique are: (1) Triaxial cell base needs to be modified or customized; (2) HAE disc is required; (3) The equalization time to achieve desired suction can be very long for a 6 in. by 12 in. sample instead of a Shelby tube size sample like in this study, which even took 2 days to equalize for just a difference of 0.05 psi in suction. This means it will take many days for a larger specimen especially if the gap between the initial suction and final targeted suction is huge; (4) The volume of water exiting the sample is monitored during matric suction application until the targeted suction is reached. However, the initial matric suction needs to be accurately matched with the corresponding initial moisture using an accurate SWCC obtained from tests such as the pressure plate test, etc. This will ensure that the actual targeted moisture content is reached. Furthermore, according to Kumar et al. (2022), there is no great correlation between the axis translation technique and the actual in situ condition in which air pressure is atmospheric and water pressure is negative. The authors proposed the use of the

tensiometer technique to measure suction and allow testing of the soil samples at atmospheric air pressure and negative water pressure at which cavitation can occur. For that, they developed a suction monitoring set up for cyclic triaxial testing of soil as shown in Figure 2.8. The set up includes a high-capacity tensiometer for suction measurement and on-sample displacement transducers mounted at the mid-height of the specimen for volume change measurement. To ensure that the sensing face of the tensiometer makes contact with the soil surface, a circular hole is made in the latex membrane and a rubber grommet is installed through it so that the tensiometer assembly could be pushed inside the hole.

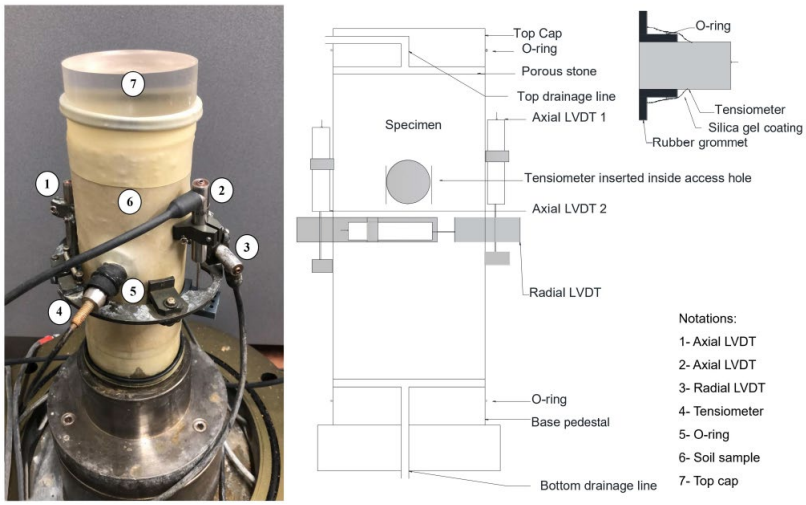

Figure 2.8. Suction monitoring set up for cyclic triaxial testing of soil (Kumar et al., 2022).

For testing at full saturation, it is sometimes difficult to achieve a satisfactory degree of saturation especially for residual soils with high fines content using only high back pressure. While conducting a consolidated undrained test on a residual soil with 40% fines content, Lim et al. (2018) experimented with a technique called the double-vacuuming saturation method to facilitate the saturation process. This method consists of vacuuming the air in both the specimen and the cell chamber simultaneously. The vacuum pressures can be increased incrementally while keeping the difference in pressure constant. This is done before the introduction of de-aired water into the specimen to fill all voids, the application of backpressure, and the Skempton's B test. The authors stated that the duration of the saturation process was shortened by adopting the double-vacuuming method and satisfactory degree of saturation was achieved for the compacted residual soil. One of the issues concerning this method is the lack of literature about the actual procedure steps. Therefore, the use of a simple vacuum saturation process and high back pressure should be used if acceptable B-values are achieved depending on the soil type. For instance, Makhnenko and Labuz (2013) used high back pressure for the saturation of very stiff soils. They followed the procedure suggested by Wissa (1969) to ensure full saturation of the specimens. The procedure consists of determining the Skempton's B coefficient at gradually increasing back pressures while keeping the effective stress approximately constant. An

increasing B-value indicates that the specimen is not yet fully saturated whereas a constant B-value indicates full saturation.

Concerning the evaluation of the degree of saturation using the Skempton Coefficient B, Vernay et al. (2020) performed a parametric study to evaluate the influence of the elastic modulus (E), initial void ratio (e0), and air entry suction (se) of soils on the B-coefficient/Saturation relationship. They found that: (1) the higher elastic modulus is, the higher B-value is for the same degree of saturation and the influence is significant; (2) the higher e0 is, the lower B-value is for the same degree of saturation, but the influence is not significant; and (3) the higher se is, the lower B-value is for the same degree of saturation and the influence is significant. For limestone, Selvadurai and Suvorov (2022) estimated the Skempton coefficient B to range between 0.42 and 0.49.

3 MATERIALS AND METHODS

3.1 MATERIALS

For this study, limestone and limerock samples commonly used in Alabama were gathered from seven quarries, carefully chosen to represent a diverse range of sources across the state, as well as from national and international locations. The selection included three limestone quarries and four limerock quarries. Once collected, the samples were transported and stored at the Advanced Structural Engineering Laboratory (ASEL) in Auburn (Figure 3.1). Table 3.1 provides detailed information about the source locations.

Figure 3.1. Stored limestone and limerock sources at ASEL

Table 3.1. Locations of the limestone and limerock sources

Sources	Material Type	Location
Calera quarry	Limestone	Calera, Alabama (Shelby County)
Tuscumbia quarry		Tuscumbia, Alabama (Colbert County)
Blue Water quarry		Huntsville, Alabama (Madison County)
Brooklyn quarry	Limerock	Andalusia, Alabama (Conecuh County)
JACO quarry		Evergreen, Alabama (Conecuh County)
North Florida quarry		Lamont, Florida (Jefferson County)
Calica quarry		Quintana Roo, Mexico

3.1.1 Aggregate Sources

ALDOT staff collected limestone and limerock aggregate samples and transported them to ASEL. All sampled materials are listed in ALDOT's approved aggregates catalog, which was also used to identify their source locations. As illustrated in Figures 3.2 and 3.3, the limestone sources are in northern and central Alabama, specifically in Calera, Tuscumbia, and Huntsville, which are cities that are distant from large bodies of water. In contrast, the limerock sources are found in cities such as Andalusia, Evergreen, Lamont, and Quintana Roo, all of which are near the Gulf of Mexico. This observation aligns with descriptions in the literature that classify limerock as a marine deposit, suggesting that proximity to large bodies of water may serve as an indicator of limerock formations.

A study by Carpenter et al. (2013) examined the Calica limerock quarry in Quintana Roo, Mexico, due to concerns about potential contamination. The researchers noted that the water table in the quarry was near the surface, with a wet floor and standing water in certain areas. Their findings also identified a heavily weathered upper layer approximately 10 feet (~3 meters) thick, overlaying a more massive zone ranging from 26 to 32 feet (8 to 10 meters) thick, as depicted in Figure 3.4. These findings suggest that the proximity of limerock sources to saltwater contributes to the natural weathering of the rocks.

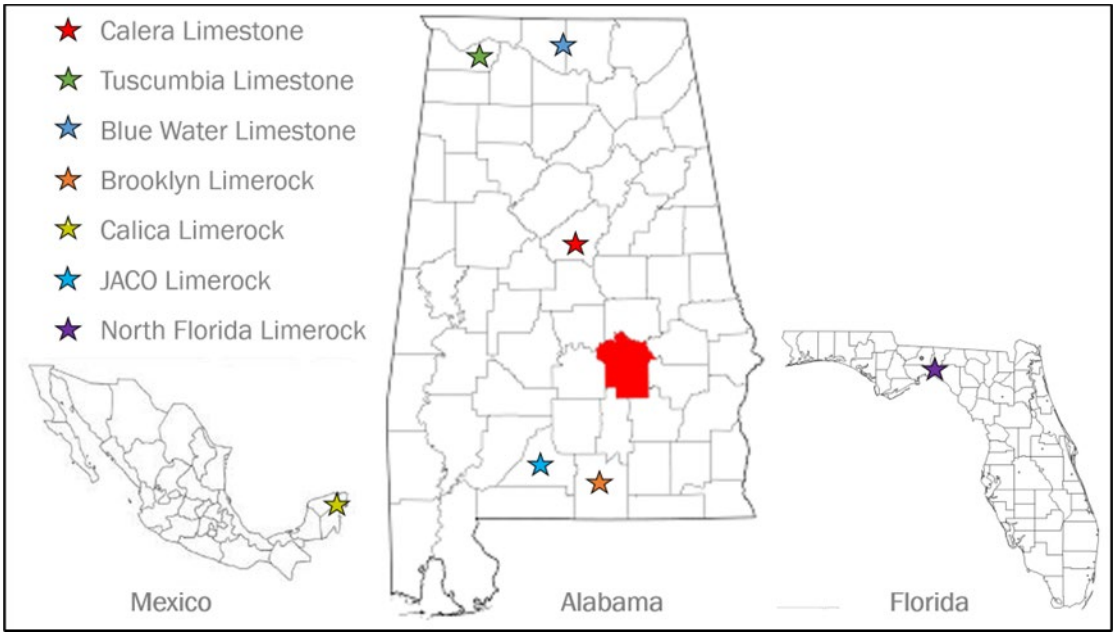

Figure 3.2. Locations of the investigated limestone and limerock sources

Figure 3.3. Large view of location map of the limerock sources (Inner Circle, n.d.)

Figure 3.4. Calica quarry, scale bar in upper left corner (Carpenter et al., 2013)

3.2 AGGREGATE CONSENSUS AND OTHER PROPERTIES

3.2.1 Consensus Properties

The consensus properties were tested using the following test methods:

- Flat and elongated particles - ASTM D4791
- Sand equivalency or plastic fines content - AASHTO T176
- Coarse aggregate angularity - ASTM D5821
- Uncompacted void content of fine aggregate - AASHTO T304

3.2.2 Physical Properties

The limestone and limerock aggregates collected underwent a series of standard laboratory tests to evaluate other important properties,

- Aggregate gradation – AASHTO T27 and AASHTO T11
- Specific gravity and absorption – AASHTO T84 and AASHTO T85
- Unit weight and void content – AASTHO T19
- L.A. Abrasion – ASTM C131
- Atterberg limits – AASHTO T89 and T90
- Moisture-density relationship – AASHTO T180

3.3 RESILIENT MODULUS TESTING

To evaluate the effect of moisture on the mechanical properties of limestone and limerock, the resilient modulus test and the quick shear test were performed on each material at different moisture contents. These two tests help determine the resilient modulus (MR) and the maximum deviator stress (σdmax) at failure or the triaxial shear maximum strength, which are fundamental mechanical properties of pavement base aggregates. The selected moisture contents at which the specimens were prepared and tested are:

- 5% below optimum moisture content or 5BOMC;
- 2.5% below optimum moisture content or 2.5BOMC;
- at optimum moisture content or OMC;
- and at full saturation or SAT.

This helps cover a large spectrum of moisture contents that can occur in the pavement base layer under different environmental conditions.

3.3.1 Test Setup and Data Quality Control

The triaxial pressure cell used in this study to provide air pressure as confining fluid and to contain the specimen meets the AASHTO T307 (2021) requirements for MR testing. The triaxial cell is made of clear acrylic and can accommodate specimen with up to 6 in. (152 mm) diameter as shown in Figure 3.5(a). It has a working pressure of 150 psi (1 MPa) and contains a solid base that provides stability during specimen compaction and testing. The cell has 4 valves (2 top drainage valves and 2 bottom drainage valves) and 2 inlets to provide cell confining pressure (filling and drainage). The confining pressure provided to the triaxial cell during testing was monitored with a Humboldt FlexPanel pressure gauge (Figure 3.5(b)). The triaxial cell also has a linear bearing at the top that allows free movement of the 5/8 in. (15.9 mm)-thick stainless steel piston rod without friction.

(a) (b)

Figure 3.5. (a) Acrylic triaxial cell, (b) Pressure FlexPanel

The loading device used in this study to apply cyclic stresses to specimens during testing is a Universal Testing Machine (UTM), specifically a Materials Test Systems (MTS) Landmark 370 load frame. It is a closed loop high-performance servo hydraulic system created for static and dynamic material testing. It contains a function generator capable of applying a 1-sec duration cycle of haversine-shaped load pulse repeatedly. The load duration was 0.1 sec followed by a rest period of 0.9 sec as recommended by AASHTO T307 (2021) for hydraulic loading devices. The loading machine meets all the AASHTO T307 (2021) requirements for MR testing except the top-loading direction requirement. In this study, the loading device has an actuator built at the bottom of the load frame and cyclic loads are applied bottom-up at the bottom of the triaxial cell as shown in Figure 3.6. The actuator has a maximum force capacity of 22 kips (100 kN) and total dynamic stroke of 6 in. (152 mm). A ¾ in. (19 mm)-thick A36 steel plate was customized and installed on the actuator to allow for bolting of the triaxial cell with a minimum of four bolts as recommended by the Long-Term Pavement Performance (LTPP, 1996) Protocol P463 for base aggregates (Figure 4.3).

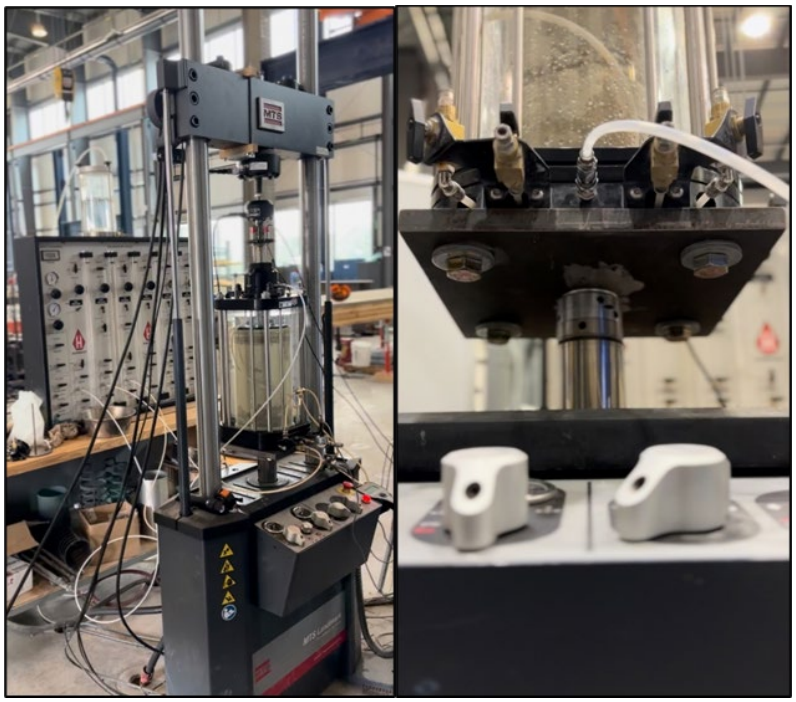

Figure 3.6. MTS Servo hydraulic Bottom-Loading test machine with its customized steel plate during M_R testing

According to AASHTO T307 (2021), the haversine-shaped load pulse should be used for both conditioning and testing. It is necessary to verify that the haversine waveform generated by the system coincides with the response waveform during conditioning and testing. To do this, the operator must display both waveforms and adjust the gains until the two waveforms match closely. In this study, the recommendation was followed during conditioning and testing using MTS Model 793.00 System Software, as shown in Figure 3.7. The proportional, integral, differential, and feed-forward (PIDF) gains were adjusted to ensure that the response waveform (Force 1 in blue) coincides with the system-generated haversine waveform (Force 1 Command in red) (Figure 3.7). Specifically, the applications used for conditioning and testing are MTS Basic TestWare and MTS TestSuite Multipurpose Elite.

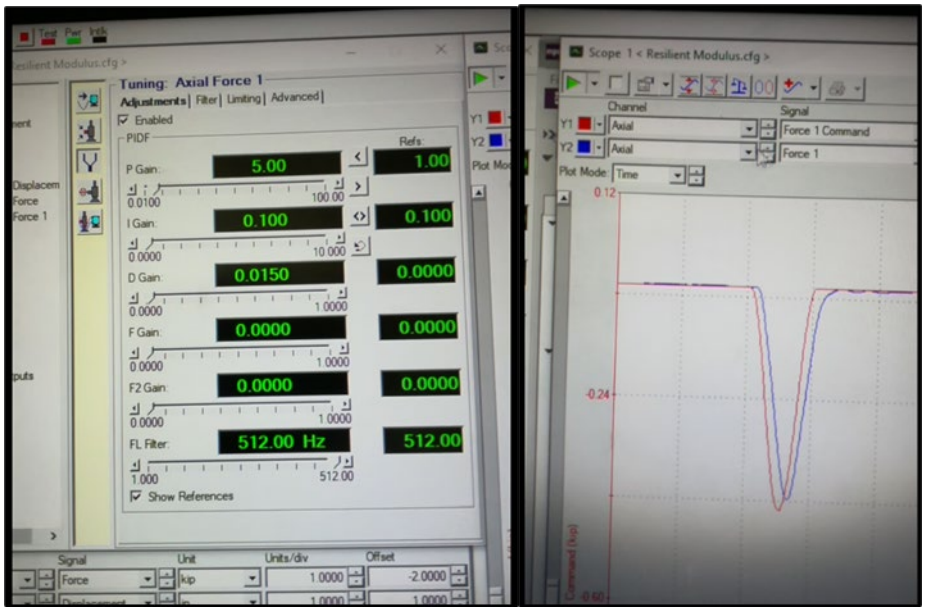

Figure 3.7. PIDF gains adjustment for haversine-shaped load pulse waveforms

The axial load measuring device used in this study was an electronic load cell located between the crosshead of the MTS load frame and the triaxial cell piston rod as shown in Figure 3.8. The load cell has a maximum load capacity of 5 kips (22 kN) and an accuracy of ± 2.5 lb. (± 11 N), which satisfies AAHSTO T307 (2021) requirements for load cells. In accordance with AASHTO T307 (2021) recommendations, the load cell was monitored during MR testing and a calibration check was performed every 50 MR tests using a proving ring from Pine Test Equipment, as shown in Figure 4.5.

Figure 3.8. Load cell calibration with proving ring

The axial deformation measuring devices used in this study were two spring loaded Linear Variable Differential Transformers (LVDTs). They were installed using mounting blocks on opposite sides equidistant from the piston rod and their tips rested on the hard top surface of the

triaxial cell as shown in Figure 3.9(a). The properties of the two LVDTs meet all AAHSTO T307 (2021) minimum requirements for LVDTs as shown in Table 4.1. Both LVDTs were wired separately (Figure 3.9(b)) for independent measurement, calculation purposes, and monitoring of proper alignment during testing. In accordance with AASHTO T307 (2021) recommendations, the LVDTs were monitored during MR testing and calibrated every 50 MR tests using a micrometer, such as shown in Figure 4.6(c).

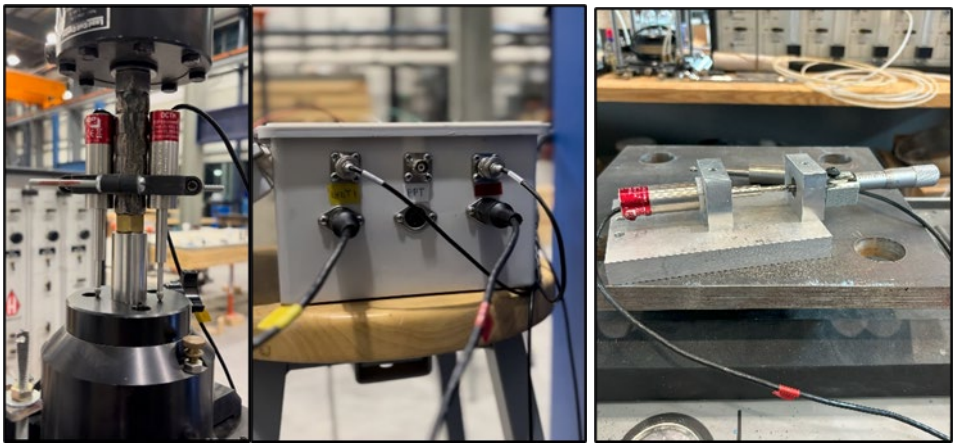

Figure 3.9. (a) two installed LVDTs, (b) wired LVDTs, (c) LVDT calibration with micrometer

Table 3.2. Properties of the two spring-loaded LVDTs

Properties	**Research LVDTs**	**AASHTO T307[1] minimum requirements**
Voltage Units	DC	DC
Range	± 0.3 in (7.5 mm)	± 0.24 in (6 mm)
Linearity	± 0.25% of full scale	± 0.25% of full scale
Repeatability	± 1% of full scale	± 1% of full scale
Minimum Sensitivity	5 mv/v (DC)	2 mv/v (AC) or 5 mv/v (DC)
Version	Spring return	Spring return

The goal of the MR test is to mimic what occurs in the field under loading; however, the non-homogeneity of the specimen can sometimes cause the specimen deformation to be non-uniform through the specimen height. Additionally, errors to MR results can be due to noise introduced to the system during the test (MnDOT, n.d.). Therefore, to eliminate errors and ensure great quality of the data acquired for accurate results, there is a need for data quality control criteria. AASHTO T307 (2021) recommends an acceptable two vertical LVDTs measurement Rv ratio of 1.3 as a quality control criterion. However, it was found based on experience that this criterion does not appropriately address test quality.

To replace the 1.3 ratio criterion, MnDOT (n.d.) developed a set of data quality control criteria based on their testing data. The criteria are Angle of Rotation (AR); Signal-to-Noise ratio

(SNR) and Coefficient of Variation (COV) of the resilient modulus (MnDOT, n.d.). For AR, it is assumed that some rotation of the loading platen may occur while applying force, which can create a bending moment (Figure 3.10) that disturbs the fundamental stress field (Kim et al., 2008). Although AR is a great way to assess uniformity, it requires the use of three internal LVDTs around the specimen and two customized rings to hold the LVDTs, which were not available at time of study. Thus, the use of the AASHTO T307 (2021) recommended Rv ratio was used in this study with only two external LVDTs. Camargo et al. (2012) showed that the difference in MR values between internal and external LVDTs is less significant for unbound materials than for stiff stabilized materials. As for SNR and COV, this study adopted these two criteria because they help evaluate the reliability of the sensors data and the calculated average MR values of the last five cycles of each sequence.

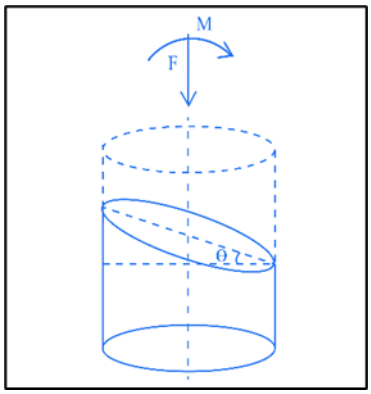

Figure 3.10. The axial force and bending moment imposed by rigid platens that rotate

3.3.2 Specimen Preparation

The materials were prepared according to the AASHTO T307 (2021) procedure for resilient modulus testing of soils and aggregates. This procedure allows specimens to be prepared for testing only at OMC, which is the moisture content at which aggregate base layers are constructed in the field. Therefore, the specimens in this study were first prepared for testing at OMC to achieve consistent density, then were allowed to dry below OMC and were brought to a saturated (SAT) state for testing.

3.3.2.1 Optimum Moisture Content

The materials were sampled from the barrels in which they were stored at ASEL and reduced to test size using the ASTM C702 quartering method. The samples were oven dried at 140°F and any oversize particles (i.e., particles retained on the 1-1/2” sieve) were removed. The mass of water required to achieve OMC was determined and mixed thoroughly with the samples until the moisture was visibly distributed evenly throughout the aggregates. The mixtures were left in sealed containers overnight before compaction the next day. The samples were then compacted

in six layers with a predetermined thickness of 2 in. per layer to achieve at least 95% of the maximum dry density (MDD) obtained from the moisture density relationship curves. The specified dimensions of the specimens are 6 in. in diameter by 12 in. in height. The samples were compacted on the triaxial cell base inside a split mold with an inside diameter of 6 in. and a height of 17 in. using a vibratory compaction hammer (Figure 3.11(a)). After compaction, the split mold was removed and a membrane was installed around the specimen. The inside diameter of the split mold was already known; therefore, the diameter was remeasured following membrane installation to ensure specimens retained their shapes. A bronze porous disc and specimen cap were placed on the top surface of the specimen. A vacuum of 1 psi was applied to check for leaks and the entire assembly including the triaxial cell was installed under the loading device to begin testing (Figure 3.11(b)).

(a) **(b)**

Figure 3.11. (a) Compaction equipment; (b) Prepared specimen under loading device

3.3.2.2 Drying Below OMC

To prepare the specimens for testing at moisture contents below OMC (i.e., 5BOMC and 2.5BOMC), the specimens were first compacted at OMC to achieve the MDD. The specimens were then allowed to dry without membranes at ambient temperature in the laboratory to mimic the natural drying process in the field. Specimen holders fabricated with concrete test cylinders resembling plastic mesh were installed around the specimens with adjustable steel clamps (Figure 3.12(a)) to serve as support and prevent the specimens or large particles from collapsing during the drying process. In this study, the hole size in the fabricated specimen holders was larger than the nominal maximum aggregate sizes (NMAS) of the limestone and limerock aggregates. It was established through preliminary testing that these materials could hold in place

with a low probability of collapsing. Nevertheless, it is best to ensure that the hole size is equal to or less than the NMAS of the aggregates, especially when testing coarser materials with lower cohesion between particles. After securing the specimens, the desired moisture content below OMC was achieved by periodically monitoring the weights of the specimens to estimate water loss (Figure 3.12(b)). Once the targeted moisture was achieved, the membranes were installed and the same post-compaction procedure described previously was followed prior to testing. It is important to note that the specimens were divided into the initial six layers after testing and placed separately in the oven for moisture content determination (Figure 3.12(c)). This was done to verify that uniform moisture distribution throughout the specimens was obtained. The moisture content was relatively consistent as shown in the example in Figure 3.12(c) for Calica limerock at 2.5BOMC. Another alternative to room temperature drying was oven drying, which was not adopted in this study due to the risks of damage associated with handling and moving specimens away from the triaxial cell base. For study repeatability, the actual OMCs are provided in Table 3.9 and the targeted moisture contents below OMC are 2.5BOMC and 5BOMC. The targeted moisture content of the laboratory-compacted specimen for base aggregates must not vary by more than ±1% as recommended by AASHTO T307.

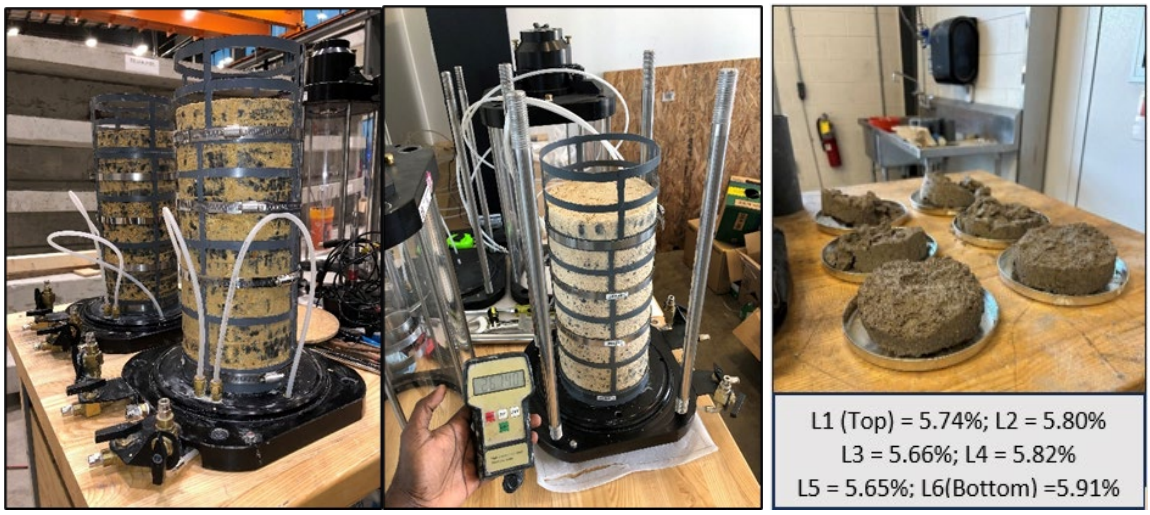

Figure 3.12. (a) Drying process; (b) Specimen's weight monitoring; and (c) Post-test moisture content determination (Calica limerock example at 2.5BOMC))

3.3.3.3 Saturation

First, the same specimen preparation procedure at OMC was followed until the assembly was installed under the loading device. The triaxial cell was then closed and filled with water to 95% of its volume. A confining stress of 5 psi was applied, and the specimen was vacuum saturated by alternately vacuuming the top and venting the base of the specimen to allow water to be pulled

through and let air escape. A back-pressure saturation was performed on the specimens by initially increasing the cell pressure to 55 psi and the pore pressure to 50 psi. The vacuum saturation and back-pressure saturation of the specimens were carried out using a vacuum pump, a pressure Flex Panel, and a de-aired tank (Figures 3.13(a) and 3.13(b)).

The Skempton's B-coefficient was then determined, and the procedure suggested by previous researchers such as Wissa (1969) was followed to ensure complete saturation of the specimens before starting the test. The procedure consists of gradually increasing the back pressures while keeping the effective stress constant and determining the Skempton's B-coefficient. The specimen is considered fully saturated if the B-coefficient remains constant and not yet saturated if the B-coefficient increases with increasing back pressures. After full saturation was reached, the back pressures were maintained to ensure the specimen remained saturated throughout the testing process. It is important to clarify that the term "saturated" typically refers to 100% saturation. However, it's possible to be between 95% and 98% saturation with significantly lower B-values. The B-coefficients of the limestone and limerock materials are presented in Figure 5.3(c). These reflect the highest saturation level achievable under the given testing conditions. A parametric study showed that the relationship between B-coefficient and saturation is significantly influenced by the air entry suction (se) and the elastic modulus (E) of the material and slightly influenced by the initial void ratio (e0) (Vernay et al., 2020). For the same degree of saturation, a higher se and a higher e0 result in a lower B-coefficient, and a higher E results in a higher B-coefficient. This explains the variation in B-coefficients presented in Figure 6(c). The materials with higher e0 and se and lower E had lower B-coefficients at saturation. The e0 values were calculated and the se values were obtained from the soil water characteristic curves of the materials. The initial elastic modulus (E0) values were estimated from the stress-strain curves resulting from the quick shear testing at OMC of the materials. All specimens were considered fully saturated after their B-coefficients remained constant with increasing back pressures after several days. The specimens were placed in the oven at the end of testing for moisture content determination. The moisture content obtained at saturation after testing was not very precise because some external water from the drainage hoses entered the membranes during specimen removal. This is why the saturation moisture content is not reported. However, it's important to note that this does not change the fact that the specimens were tested near 100% saturation ($S \approx 1$).

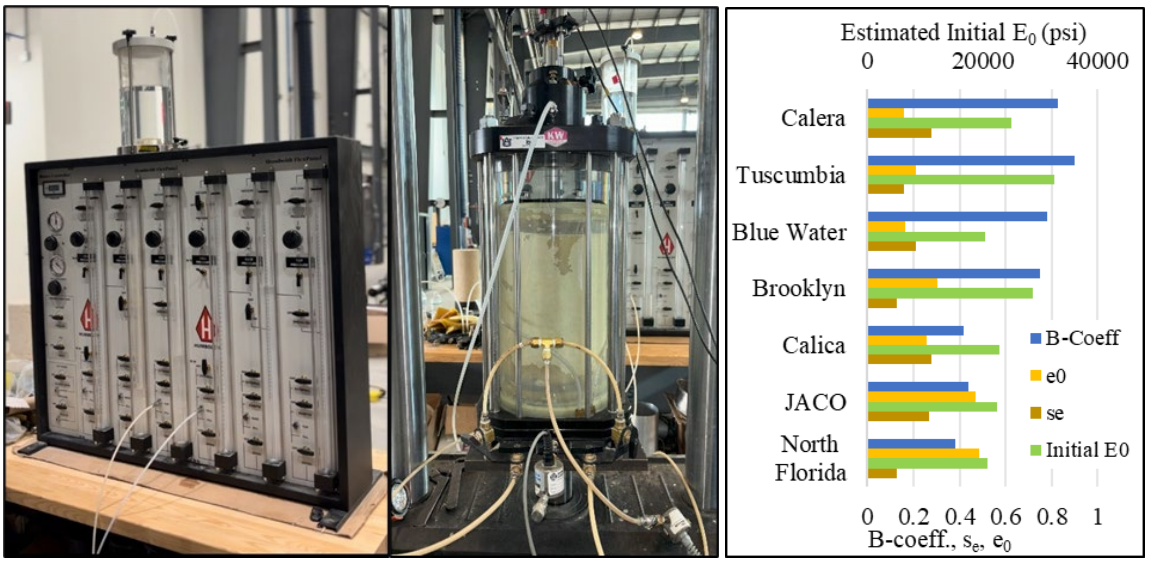

(a) (b) (c)

Figure 3.13. (a) Pressure Flex Panel and de-aired tank; (b) Specimen in saturation process; (c) Average Skempton's B-coefficients of saturated limestone and limerock aggregates

3.3.3 Procedure

Following the AASHTO T307 (2021) protocol, the resilient modulus tests were conducted on limestone and limerock specimens prepared at different moisture contents, namely 5BOMC, 2.5BOMC, OMC, and SAT. The tests were performed under drained conditions at and below OMC and under undrained conditions at saturation as specified in AASHTO T307. For unsaturated base aggregates, the MR can be reliably assessed by assuming that the pore air and pore water are in drained conditions. This eliminates the need for controlled pore-air pressure testing, as unsaturated aggregates may exhibit a more complex behavior during consolidation than when saturated. At saturation, base materials, particularly those with higher fines content, can accumulate excess pore water pressure due to reduced permeability in the field, particularly because they are very dense (compacted) and the loading condition can occur faster than the materials can drain, representing undrained conditions that closely mimic flooding scenarios. Three replicates were tested at each moisture content to ensure repeatability and the coefficient of variation (COV) of intra-laboratory results was calculated (maximum limit = 30%). At each moisture level, the specimens underwent 15 sequences of load applications representing 15 different stress states, as specified by the AASHTO T307 protocol to establish stress sensitivity of the material. A servo-hydraulic universal testing machine (UTM) was used to apply the dynamic loads (Figure 5.4(a)). Each sequence consisted of applying a confining pressure and 100 cycles of a specified dynamic deviator stress to the specimens and measuring the vertical deformations. A loading cycle lasts 1 second including 0.1 seconds of loading followed by 0.9 seconds of rest

period. A sequence of 1000 load repetitions considered as specimen conditioning was carried out prior to testing to eliminate the effects of initial loading imperfections. During testing, the signals from all sensors were verified to be noise-free and the vertical deformation ratio (Rv) described in the testing protocol was monitored to ensure data accuracy. At the end of the test, the recorded loads and deformations were reduced to obtain the corresponding stresses and strains (Figure 3.14(b)). The resilient modulus at each stress state was determined as the ratio of the average deviator stress to the average resilient strain of the last five cycles. At each moisture content, the COV of the MR obtained at each test sequence using the three replicates was calculated and the average COV across the 15 test sequences was determined to verify repeatability.

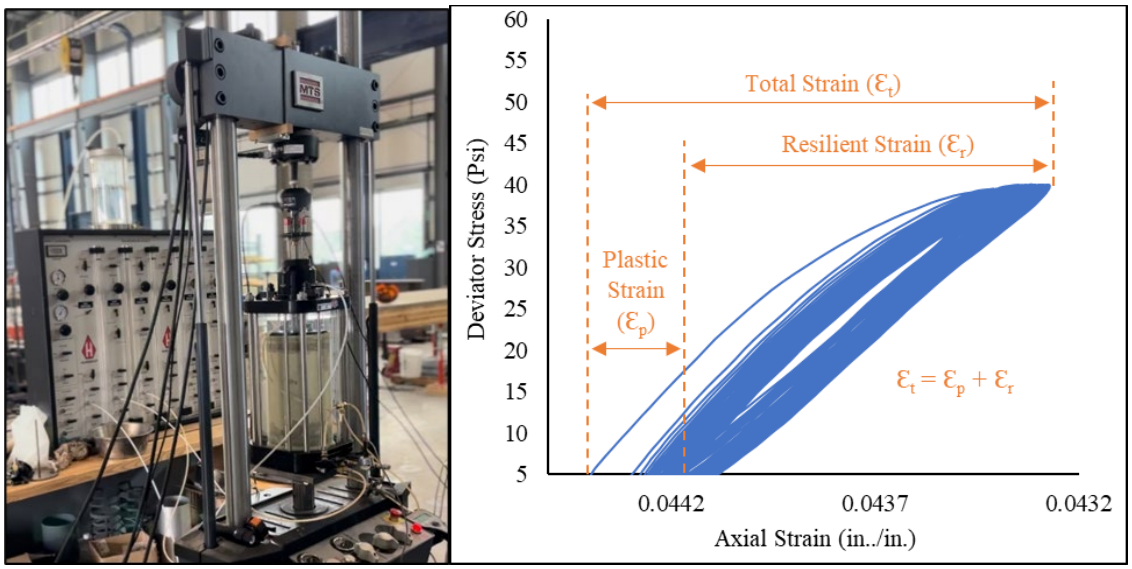

(a) **(b)**

Figure 3.14. (a) Specimen in servo-hydraulic UTM; (b) Example of a test sequence reduced data

3.3.4 Significance Testing

Statistical Significance

Multiple one-sided hypothesis t-tests (unpaired) were conducted with a 95% confidence level to determine whether the average MR at each sequence for each material obtained at 5 or 2.5BOMC and SAT was statistically greater and less, respectively, than the MR obtained at OMC. The population parameter ( ) represents average MR. The Hypotheses were:

$$H_1: U_{(2.5BOMCor5BOMC)} > U_OMC; H_0: U_{(2.5BOMCor5BOMC)} \leq U_OMC$$

$$H_1: U_SAT < U_OMC; H_0: U_SAT \geq U_OMC$$

When the obtained p-values were lower than the significance level of 0.05 the null hypotheses ( ) were rejected and the alternative hypotheses ( ) were accepted as statistically significant with a 95% confidence.

Practical Significance

In this study, a change in aggregate base MR is considered practically significant if the resulting change in thickness of the asphalt concrete (AC) layer during design is greater than 0.5 in. Because layer thicknesses are rounded to the nearest 0.5 inches in the design process, any increase beyond this threshold is likely significant enough to impact constructability and cost. As a result, a minimum design thickness difference of 0.5 in. was selected to establish practical significance. A sensitivity analysis consisting of designing a simple 2-layer asphalt pavement with an aggregate base layer was conducted. Two traffic levels were considered: 3,700,000 ESALs for low traffic volume roads (e.g. arterial road) and 44,600,000 ESALs for high traffic roads (e.g. interstate). All other inputs were obtained from ALDOT design standards (ALDOT, 1990) and the design was performed following the AASHTO 1993 design methodology (AASHTO, 1993). The analysis demonstrated that a minimum change of 4,000 psi in base aggregate MR results in a 0.5 in. change in AC layer thickness, particularly under higher traffic loads as shown in Figure 3.15. As a result, a change in MR greater than or equal to 4,000 psi is considered practically significant in this study. Details regarding the sensitivity analysis can be found in Appendix B.

It is important to note that the words “significant” and “insignificant” are used in this paper only when the significance was proven both statistically and practically.

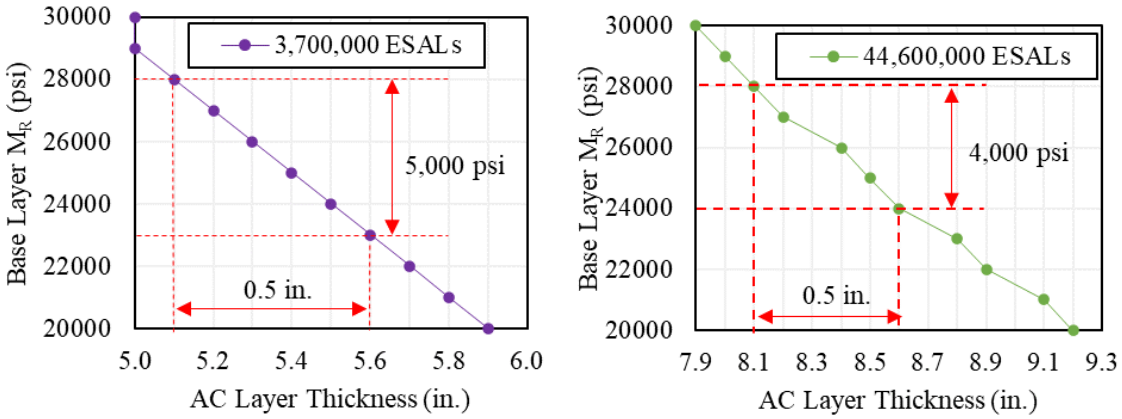

Figure 3.15. Sensitivity analysis to determine the practical significance of M_R change

4 CONSENSUS PROPERTIES AND RESILIENT MODULUS TEST RESULTS

4.1 CONSENSUS PROPERTIES

The results of these tests are presented in Table 4.1, with ALDOT specification limits provided in the last row, and visually represented in Figure 4.1.

Table 4.1. Consensus Properties of Limestone and Limerock samples

Source	Flat and Elongated (%) 3:1	5:1	Sand Equivalent Value (%)	% of particles with 1 or more fractured faces	% of particles with 2 or more fractured faces	Uncompacted Voids (%)
Calera	2.5	0.2	63	100	100	43
Tuscumbia	8.5	1.2	58	100	100	42
Blue Water	5.7	0.6	38	100	100	46
Brooklyn	0.6	0.0	39	100	100	55
Calica	0.1	0.0	45	100	100	42
JACO	/	/	30	100	100	61
North Florida	3.7	0.2	21	100	100	62
Specifications	Max. 20	10		Min. 80	Min. 80	

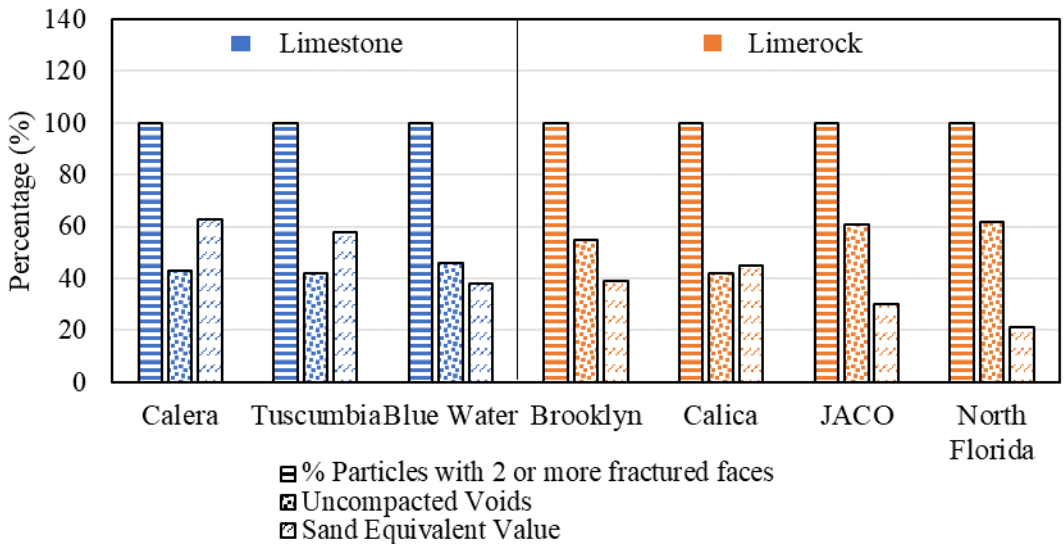

Figure 4.1. Consensus properties of limestone and limerock aggregates

4.1.1 Coarse Aggregate Angularity (ASTM D5821)

The limestone and limerock aggregates have 100% of particles with two or more fractured faces, exceeding ALDOT's minimum requirement of 80%. This suggests that the coarse particles of both aggregate types possess great shape, texture, and angularity, which contribute to strong particle interlock within the matrix and enhance resistance to permanent deformation.

4.1.2 Uncompacted Void Content (AASHTO T304)

The test was conducted twice on two separate samples from each aggregate source to ensure reliable results. The results indicate that most limerock aggregates, particularly those from Brooklyn, JACO, and North Florida, have a higher uncompacted void content (above 50%) compared to limestone aggregates, which generally fall below 50%. The only exception among the limerock sources was Calica, where the fine aggregates exhibited an uncompacted void content below 50%. This shows that, in general, limerock fine aggregates tend to have higher angularity than limestone fine aggregates. However, since Calica deviates from this trend, the conclusion is not definitive.

4.1.3 Flat and Elongated Particles (ASTM D4791)

All limestone and limerock sources met ALDOT's flat and elongated particle requirements for both the 3:1 and 5:1 ratios, with exceptionally low percentages. This indicates that the particle sizes are unlikely to undergo significant changes during compaction due to the minimal presence of flat or elongated particles.

4.1.4 Sand Equivalency (AASHTO T176)

The test was conducted three times on each aggregate sample to ensure high-quality results. Among the limestone aggregates, only those from Calera and Tuscumbia had sand equivalency (SE) values exceeding 50%, indicating a lower content of clay-like materials (below 50%). In contrast, all limerock aggregates and the Blue Water limestone aggregates had SE values below 50%, meaning their clay-like material content was higher than 50%. While it might seem that limestone generally contains lower clay-like minerals than limerock, the exception of Blue Water limestone suggests that this is not always true. In this study, the percentage of clay-like material in the aggregates is referred to as Plastic Fines Content (PFC), calculated by subtracting the SE value from 100%. PFC serves as an indicator of plasticity, as materials with higher clay mineral content exhibit higher PFC and lower SE values. Aggregates with significant amounts of clay minerals tend to absorb more water and contain a greater number of small pores, which weaken their skeletal framework. This can result in reduced strength and increased stress softening effects in pavement base layers.

4.2 PHYSICAL AND OTHER PROPERTIES

4.2.1 Washed Sieve Analysis and Sieve Analysis (AASHTO T11 - T27)

The washing process was used to determine the fines content of each aggregate material at the Auburn University geotechnical lab. As shown in Figure 4.2, limerock aggregates mostly have higher fines content than limestone aggregates. JACO and North Florida limerock have particularly high fines content, exceeding 20%. In Florida, the minimum required fines content for most limerock base courses is 35% (Ko, 2005), which is greater than the fines content observed in JACO and North Florida limerock.

The sieve analysis test was conducted to determine the particle sizes of each aggregate material, with the results presented in Figures 4.3 to 4.4 and Table 4.3. The gradation curves for the limestone sources fall within the minimum and maximum limits established by ALDOT. However, two limerock sources, Brooklyn and North Florida, slightly fall outside these boundaries between the 1” and #8 sieve sizes. Despite this, all limestone and limerock aggregates are classified as well-graded due to their high coefficients of uniformity (Cu) (see Table 4.3), with no significant differences observed between the two aggregate types. It is worth highlighting that the JACO limerock samples collected and brought to ASEL contained large cobble-sized rocks, as illustrated in Figure 4.5. According to Ko (2005), the maximum allowable particle size for most limerock base courses in Florida is 3 inches, which is still smaller than some of the cobble-sized rocks found in the JACO limerock sample.

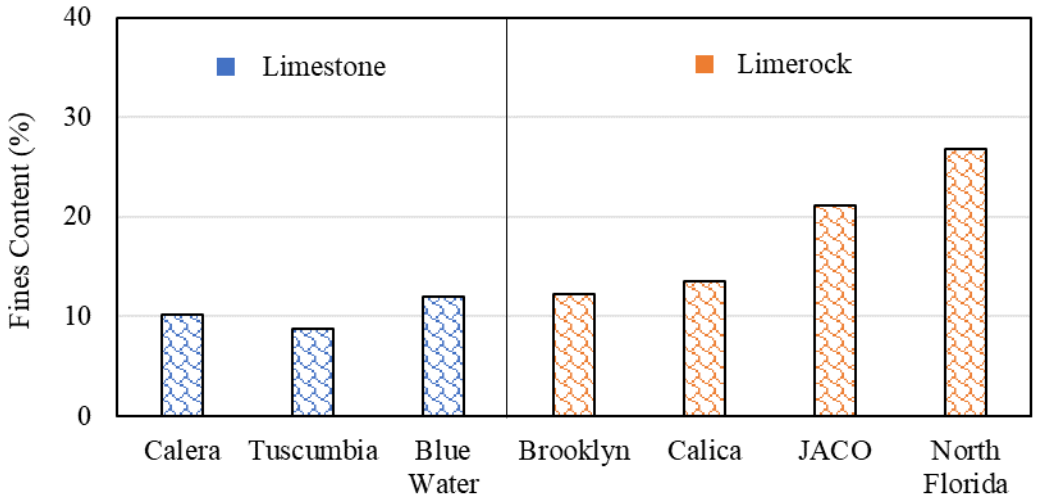

Figure 4.2. Fines contents of limestone and limerock aggregates

Table 4.2. Particle size distribution or gradation

Source	**Calera**	**Tuscumbia**	**Blue Water**	**Brooklyn**	**Calica**	**JACO**	**North Florida**
Aggregate Type	Limestone			Limerock			
Sieve size N° (mm)		Cumulative % Passing					
2” (50)	100	100	100	100	100	100	100
1-1/2” (37.5)	99	100	100	100	100	96	100
1” (25)	93	93	96	92	98	89	83
3/4” (19)	86	83	87	79	91	83	72
1/2” (12.5)	76	68	73	60	79	75	60
3/8” (9.5)	72	60	66	52	71	70	54
#4 (4.75)	61	42	55	40	61	60	42
#8 (2.36)	43	32	45	33	52	54	37
#16 (1.18)	28	24	34	29	42	49	35
#30 (0.6)	21	18	26	25	33	44	34
#50 (0.3)	16	14	19	21	23	36	33
#100 (0.15)	12	11	15	16	16	25	31
#200 (0.075)	10	9	12	12	13	21	27

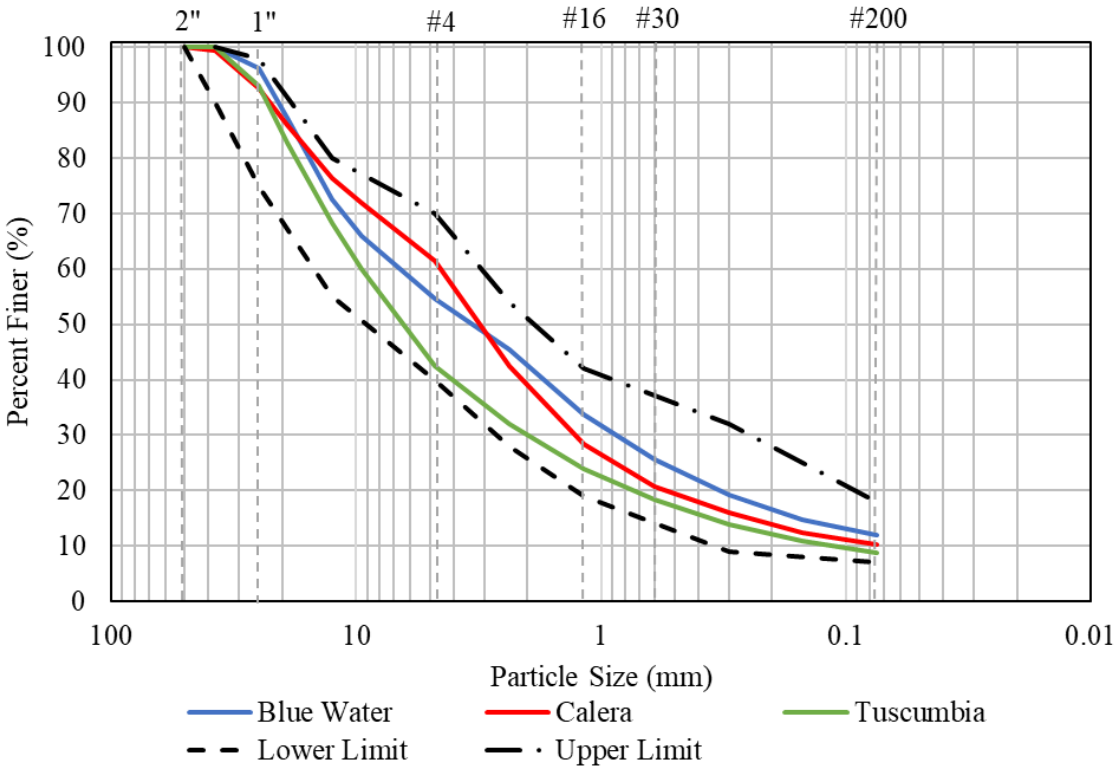

Figure 4.3. Particle size distribution curves of limestone sources

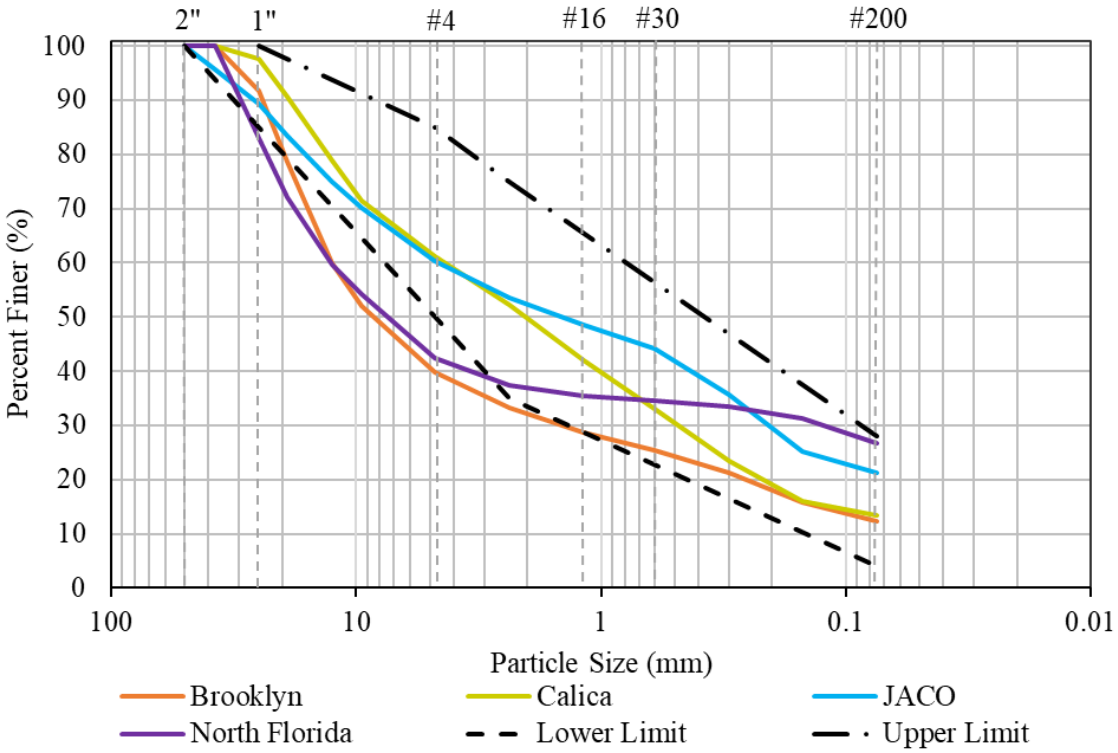

Figure 4.4. Particle size distribution curves of limerock sources

Table 4.3. AASHTO classification of limestone and limerock aggregates

	D_{60}	D_{30}	D_{10}	C_u	C_c	AASHTO Class.
Calera	4.5	1.5	0.075	60	6.2	A-1-a
Tuscumbia	9.5	2.0	0.145	66	2.9	A-1-a
Blue Water	6.5	0.9	0.03	217	4.2	A-1-a
Brooklyn	12.5	1.6	0.05	250	4.1	A-1-a
Calica	4.5	0.5	0.02	225	2.8	A-1-a
JACO	4.8	0.2	0.007	679	1.5	A-1-b
North Florida	12.5	0.1	0.008	1563	0.2	A-1-b

Figure 4.5. JACO limerock cobbles

4.2.2 Specific Gravity and Absorption (AASHTO T84-T85)

At NCAT, these tests were conducted to measure the specific gravity and water absorption of both coarse and fine aggregates for each material. The findings, detailed in Tables 4.4 and 4.5, revealed that the coarse aggregates of limerock sources have notably lower specific gravity and greater water absorption compared to those of limestone sources. In contrast, the fine aggregates of both limestone and limerock displayed comparable specific gravity and absorption values. Additionally, weighted averages for specific gravity and absorption were computed following standard specifications and are shown in Table 4.6. The limerock sources, in general, displayed lower specific gravity and higher absorption than limestone sources. A visual representation of these results is provided in Figures 3.16 and 3.17.

Table 4.4. Specific gravity and absorption of the coarse aggregates of limestone and limerock materials

	Bulk Specific Gravity	Bulk Specific Gravity (SSD)	Apparent Specific Gravity	Absorption (%)
Calera	2.729	2.740	2.759	0.4
Tuscumbia	2.583	2.625	2.697	1.6
Blue Waters	2.673	2.698	2.740	0.9
Brooklyn	2.114	2.280	2.535	7.8
Calica	2.168	2.292	2.475	5.7
JACO	1.835	2.110	2.532	15.0
North Florida	1.848	2.128	2.566	15.1

Table 4.5. Specific gravity and absorption of the fine aggregates of limestone and limerock materials

	Bulk Specific Gravity	Bulk Specific Gravity (SSD)	Apparent Specific Gravity	Absorption (%)
Calera	2.595	2.654	2.759	2.3
Tuscumbia	2.454	2.549	2.712	3.9
Blue Waters	2.527	2.600	2.728	2.9
Brooklyn	2.582	2.600	2.630	0.7
Calica	2.372	2.474	2.640	4.3
JACO	2.536	2.571	2.629	1.4
North Florida	2.626	2.651	2.692	0.9

Table 4.6. Specific gravity and absorption of limestone and limerock coarse and fine aggregates

	Bulk Specific Gravity	Bulk Specific Gravity (SSD)	Apparent Specific Gravity	Absorption (%)
Calera	2.645	2.687	2.759	0.8
Tuscumbia	2.526	2.592	2.703	2.2
Blue Waters	2.590	2.643	2.733	1.5
Brooklyn	2.280	2.398	2.572	1.6
Calica	2.288	2.400	2.574	4.8
JACO	2.200	2.365	2.589	2.2
North Florida	2.111	2.320	2.618	2.0

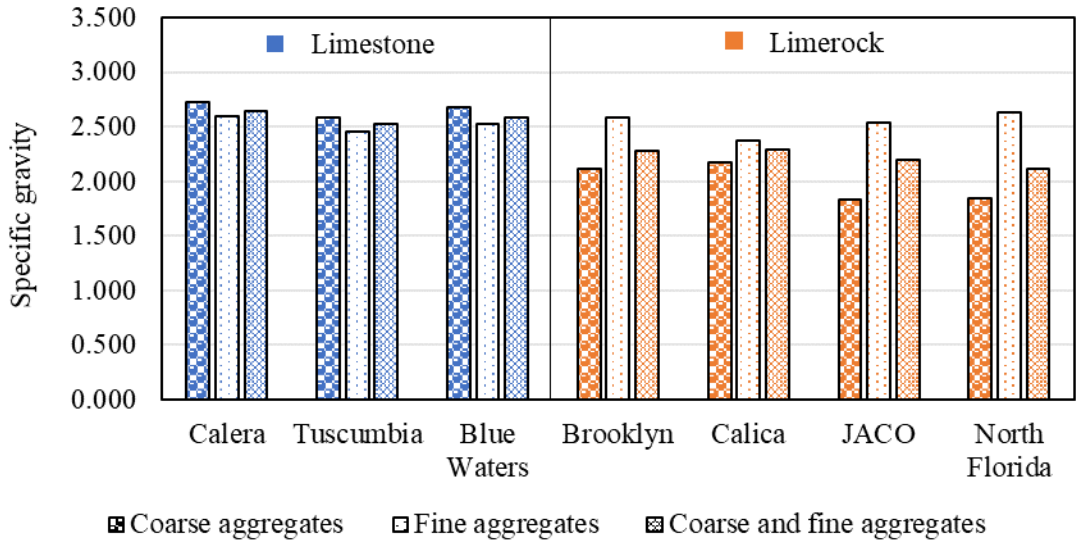

Figure 4.6. Bulk specific gravity of the limestone and limerock aggregates

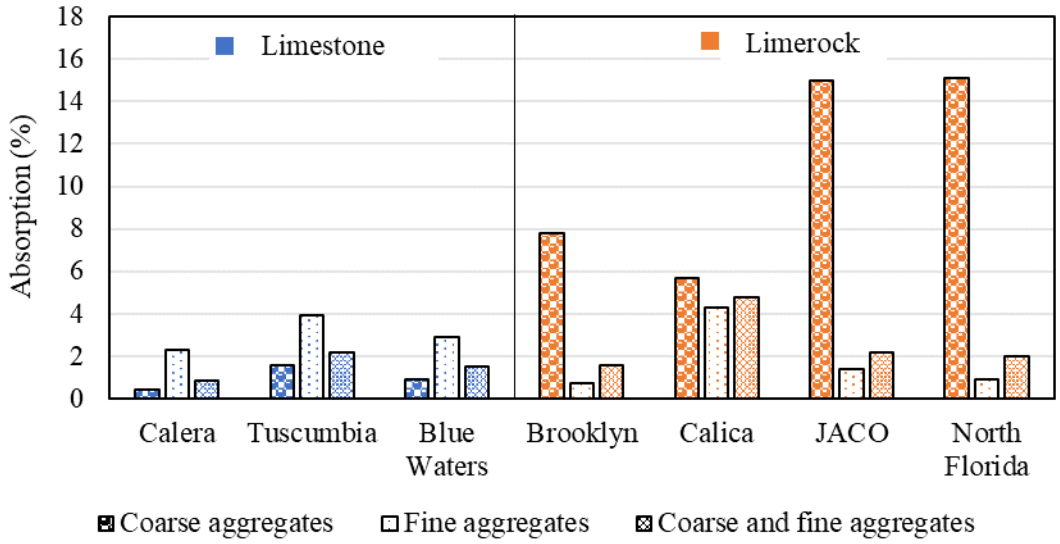

Figure 4.7. Absorption of the limestone and limerock aggregates

4.2.3 Unit weight, L.A. Abrasion, and Atterberg limits (AASHTO T19); (ASTM C131); (AASHTO T89-T90)

The unit weight and L.A. abrasion values for all materials were obtained. The results are shown in Table 4.7 and Figure 4.8. The limestone sources had higher unit weights and lower L.A. abrasion than the limerock sources. Determining the plasticity index (PI) for both limerock and limestone materials proved difficult using the Atterberg limits tests, as the materials often collapsed at lower

moisture contents during the liquid limit test. Consequently, the PI results were considered inconclusive. As an alternative, Plastic Fines Content (PFC), a dependable indicator of the quantity and plasticity of aggregate fines, was used to assess plasticity.

Table 4.7. Unit weight, L.A. abrasion, and PI of limestone and limerock sources

Source	Unit Weight (pcf)	L.A. Abrasion (%)
Calera	122	27
Tuscumbia	116	38
Blue Water	127	26
Brooklyn	99	42
Calica	111	39
JACO	90	55
North Florida	86	61

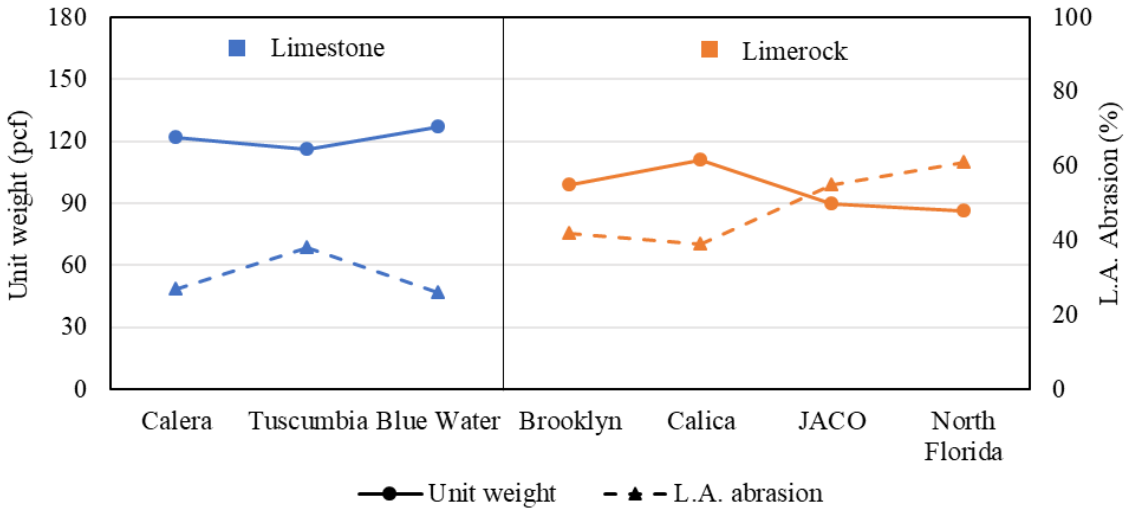

Figure 4.8. Unit weight and L.A. abrasion of the limestone and limerock aggregates

4.2.4 Moisture – density relationship (AASHTO T180)

Initially, the moisture-density relationships for all limestone and limerock aggregates were determined using the AASHTO modified proctor procedure (T180). However, for some materials, the oversized particles retained on the ¾ in. sieve, which were removed before testing as per the procedure, accounted for up to 30% of the total weight. This led to significant corrections for moisture and dry density to account for the oversized particles, especially due to their moisture content and specific gravity estimates. Consequently, an alternative compaction control method

was employed, utilizing a vibratory compaction hammer and a split mold with a 6 in. (152 mm) inside diameter and 15 in. (381 mm) height. The materials were compacted in six layers using consistent compaction efforts, similar to those used in preparing specimens for resilient modulus testing. The final optimum moisture contents and maximum dry densities of the limestone and limerock aggregates are shown in Table 4.8 and Figure 4.9. The limestone sources have higher maximum dry densities and lower optimum moisture contents compared to the limerock sources.

Table 4.8. Moisture-density relationships of limestone and limerock sources

Source	Max. Dry Density (pcf)	Optimum Moisture Content W_{opt} (%)
Calera	150	4.7
Tuscumbia	141.8	5.5
Blue Water	147.6	5.2
Brooklyn	123.8	10.4
Calica	128	8
JACO	112.2	16
North Florida	111.7	16.7

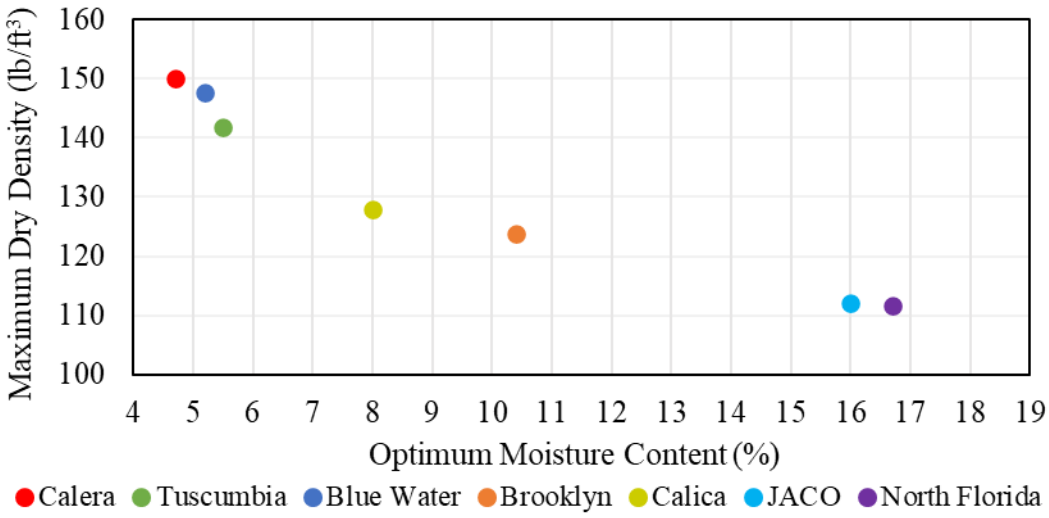

Figure 4.9. Moisture density relations of limestone and limerock sources

4.3 RESILIENT MODULUS TEST RESULTS

The results obtained from the resilient modulus test were the MR values at each of the 15 stress states imposed to the specimens during testing. These MR values and their corresponding stress states were plotted and used in a regression analysis to determine the MR k-parameters of each

material. The detailed results of all the MR tests, including all graphs, are presented in Appendix A. The regression analysis was based on the mechanistic-empirical pavement design guideline (MEPDG) MR prediction model shown in Equation 4.1 (AASHTO, 2020):

$$M_{R=k_{1P_a}}(\theta/P_a)^{(k_2)}[(\tau_{oct}/P_a)+1]^{(k_3)} \qquad (4.1)$$

where, = bulk stress, Pa = atmospheric pressure, = octahedral shear stress = , and k1, k2, k3 = material specific regression coefficients. The MR parameters k1, k2, and k3 were determined for all limestone and limerock materials at every moisture content in this study. They are used in pavement design to help predict MR at different stress states and are great indications of material response to applied stresses. The coefficients k1 and k2 are normally positive because k1 is proportional to the elastic modulus of the material and k2 indicates the increase in MR with bulk stress. The coefficient k3 is the exponent of the shear stress term in Equation 4.1. It can be positive or negative depending on the material response to increasing deviator stress at constant confining pressures. A positive k3 coefficient is an indication of stress hardening likely due to the air voids reduction and aggregate reorientation created at higher stress magnitudes, increasing friction between aggregate particles. A negative k3 coefficient is an indication of stress softening meaning that the material weakens and decreases in stiffness as shear stress increases, which is typically seen.

4.3.1 Limestone Aggregates

The final test results of all limestone aggregates, including MR k-coefficients, R2 from regression analysis, and average coefficients of variation (COV) are presented in Table 4.9. The calculated average intra-laboratory COVs were below the maximum limit of 30% at all moisture levels for all limestone aggregates, demonstrating satisfactory repeatability. Figure 5.6 shows an example graph plotting the MR values and corresponding stress states for the three replicates at all moisture levels. Figure 5.6 is the graph obtained for Calera limestone and the graphs of all the other materials can be found in Appendix A. As shown in Figure 4.10, the resilient modulus of the Calera limestone increased with bulk stresses at all moisture levels. This behavior was the same for all limestone aggregates in this study and is indicated by all k2 coefficients being positive. At constant confining pressures, MR of the Calera limestone increased with increasing deviator stress at moisture levels 5BOMC and OMC, which is indicated by the positive k3 coefficients and visible in Figure 4.10. Contrarily, a slight stress softening behavior was observed at 2.5BOMC and SAT and is indicated by the negative k3 coefficients. The k-coefficients of all limestone aggregates indicating their stress sensitivity during MR testing at each moisture content are presented in Table 4.9.

The bulk stress observed in the field at mid-depth of a base layer varies between 20 and 40 psi in most highway structures (Rada and Witczak, 1981; Ullah and Tanyu, 2020). The bulk stress of 30 psi (i.e., 5 psi confining pressure and 15 psi deviator stress) has been recommended

for determining aggregate base MR values by the National Cooperative Highway Research Program (NCHRP) Research Digest 285 (NCHRP, 2004). This is equivalent to the bulk stress at sequence 6 during MR testing, therefore the average MR values at sequence 6 were used to evaluate the effect of moisture. Figure 4.11 shows the average sequence 6 MR for each limestone aggregate at all moisture contents. At OMC, the MR values of all limestone aggregates were slightly greater than the default design MR of 30,000 psi recommended for limestone in the Alabama flexible pavement design guide (ALDOT, 1990). As shown in Figure 5.7, the MR of all limestone aggregates increased significantly upon drying from OMC to 2.5BOMC and slightly increased from 2.5BOMC to 5BOMC for two limestone aggregates, Blue Water limestone and Calera limestone. This increase in MR with decreasing moisture content was likely due to cementation of the limestone aggregates during the drying process and the possible presence of increased suction, respectively improving the bonding between aggregate particles and providing additional confinement. This behavior matched well with previous research results, even though the drying method was different. The only exception recorded in the behavior below OMC was the decrease in MR of Tuscumbia limestone from 2.5BOMC to 5BOMC. This could be due to the very dry state of the particles at 5BOMC, lack of sufficient lubricant, and cracking in increased air voids causing greater deformations.

At saturation, a decrease in MR for all limestone aggregates was expected, however diverse behaviors were observed among the materials. As shown in Figure 4.11, MR slightly decreased by 1,734 psi for Tuscumbia limestone and slightly increased by 1,066 psi for Calera limestone from OMC to SAT, which are insignificant changes. The only significant change observed at saturation was the decrease in MR of 5,923 psi for Blue Water limestone. This significant decrease in MR can be explained by the higher plastic fines content (PFC = 62%) and slightly higher fines content (FC = 12%) that Blue Water limestone has compared to Tuscumbia limestone (PFC = 42%, FC = 9%) and Calera limestone (PFC = 37%, FC = 10%). The presence of high clay-like-minerals in the fines of Blue Water limestone caused higher excess pore pressure to develop under loading, decreasing effective confining pressure, increasing deformation susceptibility, creating stress softening behavior of the aggregates, and resulting in significant stiffness reduction.

Table 4.9. k-parameters and coefficients of variation for all limestone aggregates

Sources	Properties	Moisture Content			
		5BOMC	2.5BOMC	OMC	SAT
Calera	k_1	3702	3118	1685	1938
	k_2	0.31	0.32	0.40	0.54
	k_3	0.05	-0.03	0.02	-0.50
	R^2	0.99	0.98	0.99	0.97
	cov	3%	5%	8%	2%
Tuscumbia	k_1	3300	3734	1982	2024
	k_2	0.22	0.33	0.39	0.56
	k_3	-0.04	-0.17	0.01	-0.49
	R^2	0.71	0.95	0.97	0.97
	cov	7%	5%	8%	7%
Blue Water	k_1	3564	2758	1737	1496
	k_2	0.29	0.29	0.39	0.53
	k_3	-0.04	0.18	-0.13	-0.48
	R^2	0.98	0.97	0.88	0.96
	cov	5%	17%	8%	3%

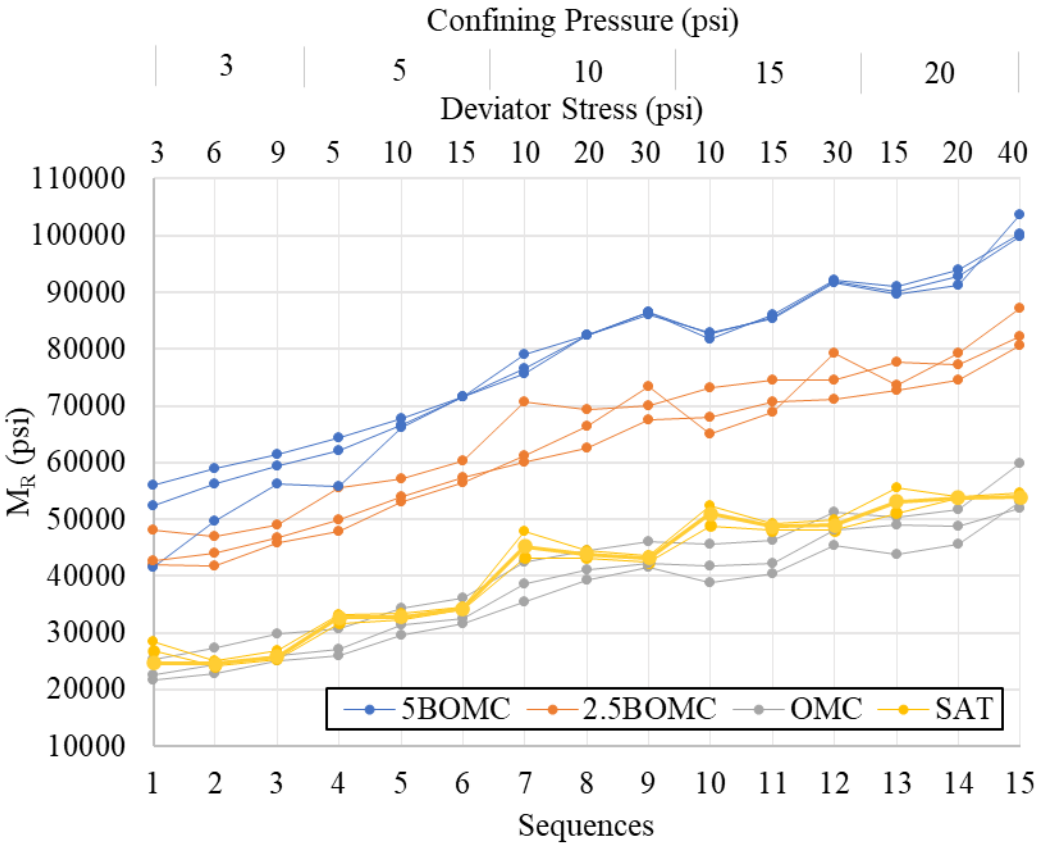

Figure 4.10. Example of final M_R test results for Calera limestone

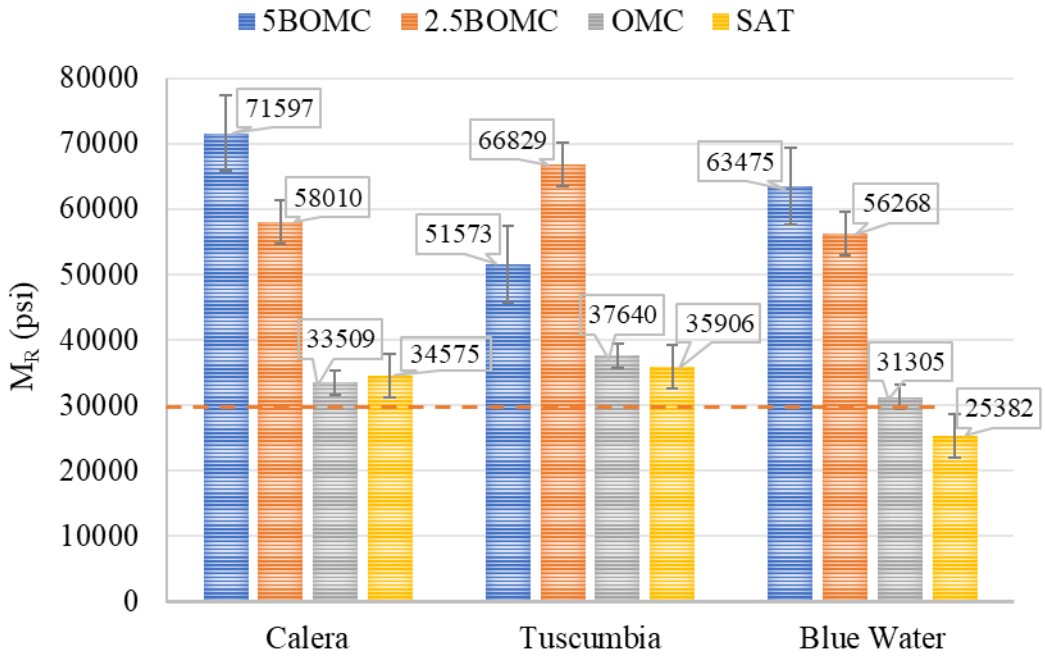

Figure 4.11. Summary of M_R values for all limestone aggregates at sequence 6

4.3.2 Limerock Aggregates

For all limerock aggregates, the MR k-coefficients, R2 values from regression analysis, and the average intra-laboratory COV at each moisture level are presented in Table 4.10. All COVs were less than the maximum limit of 30% at all moisture levels, which provides evidence of satisfactory repeatability. Figure 4.12 shows an example graph plotting the MR values and corresponding stress states at the end of testing for North Florida limerock. The graphs of all the other base materials can be found in Appendix A. As shown in Figure 4.12, the MR of North Florida limerock increased with bulk stresses at all moisture levels. Every other limerock aggregate in this study had a similar response to increased bulk stress as indicated by the positive k2 coefficients in Table 5.3. At constant confining pressures, North Florida limerock demonstrated stress softening behavior as MR decreased with increasing deviator stress at all moisture levels. This behavior can be seen in Figure 5.8 and is supported by the negative k3 coefficients in Table 4.10. The responses of all limerock aggregates to applied stresses during testing can be interpreted using their k-coefficients presented in Table 4.10.

The average sequence 6 MR values obtained at all moisture contents for each limerock aggregate are shown in Figure 4.13. The MR values at OMC for all limerock aggregates were greater than 30,000 psi, the ALDOT recommended default design MR for limestone. The MR values at OMC for both limerock and limestone aggregates are very comparable ranging between 30,000 and 40,000 psi. Similar to limestone aggregates, the MR of all limerock aggregates increased significantly with decreasing moisture content from OMC to 2.5BOMC and also to 5BOMC. The reason for this increase in MR may be the enhanced hardening and binding reaction of the aggregates caused by the chemical reaction of cementitious limerock minerals during the drying process. Additionally, the reduction of moisture content may have created suction leading to increased stiffness.

At saturation, a decrease in MR for all limerock aggregates was expected, however various behaviors similar to those of limestone aggregates were observed. As shown in Figure 4.13, MR decreased slightly by 1,539 psi for Brooklyn limerock and increased slightly by 1,020 psi for Calica limerock from OMC to SAT, representing insignificant changes (<4,000 psi). The significant changes observed at saturation were the decrease in MR of 9,628 psi for JACO limerock and the decrease in MR of 10,686 psi for North Florida limerock. The MR of JACO and North Florida limerocks decreased significantly at saturation because they have a much higher fines content (FC = 21% and 27%) and plastic fines content (PFC = 70% and 79%), respectively, than those of Brooklyn (PFC = 61%, FC = 12%) and Calica (PFC = 55%, FC = 13%) limerocks. Even though the fines contents of these limerock aggregates met the specification requirements for limerock, they can be extremely detrimental to the stiffness of the materials. The combination of high fines content with high clay-like-minerals content created higher excess pore pressure development under loading, resulting in a decrease in effective confining pressure, stress

softening behavior, and a significant reduction in stiffness. It is important to note that the Brooklyn limerock had the same fines content and plastic fines contents as the Blue Water limestone, however its MR did not decrease significantly upon saturation as the MR did for Blue Water limestone. This was possibly because Blue Water limestone is finer with 55% of the overall particles passing sieve #4 (4.75 mm), while Brooklyn limerock contains 40%. This is supported by several researchers, notably Hubler et al. (2022), who showed that gradation significantly influences pore pressure generation, with finer particles leading to a rapid increase in pore pressure in gravelly soils.

Table 4.10. k-parameters and coefficients of variation for all limerock aggregates

Sources	Properties	Moisture Content			
		5BOMC	2.5BOMC	OMC	SAT
Brooklyn	k_1	3394	2214	1555	2017
	k_2	0.47	0.45	0.41	0.61
	k_3	-0.35	0.09	0.28	-0.68
	R^2	0.89	0.99	0.99	0.96
	cov	7%	5%	9%	7%
Calica	k_1	5613	2529	1556	1744
	k_2	0.28	0.43	0.42	0.48
	k_3	-0.54	-0.16	0.07	-0.25
	R^2	0.68	0.99	0.99	0.98
	cov	2%	5%	6%	4%
JACO	k_1	3404	2635	1696	1458
	k_2	0.44	0.38	0.61	0.51
	k_3	-0.36	-0.13	-0.34	-0.38
	R^2	0.91	0.98	0.98	0.93
	cov	10%	12%	8%	11%
North Florida	k_1	2631	2651	1938	1542
	k_2	0.52	0.39	0.52	0.71
	k_3	-0.60	-0.55	-0.52	-1.19
	R^2	0.96	0.93	0.98	0.90
	cov	14%	6%	6%	6%

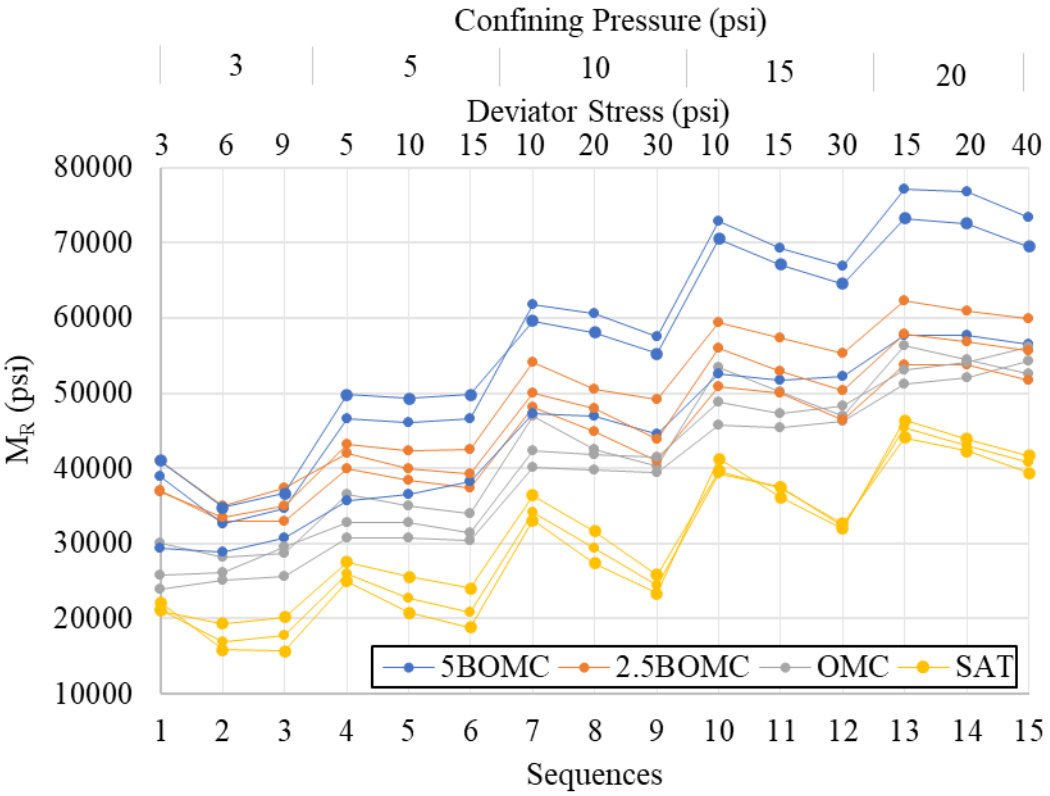

Figure 4.12. Example of final M_R test results for North Florida limerock

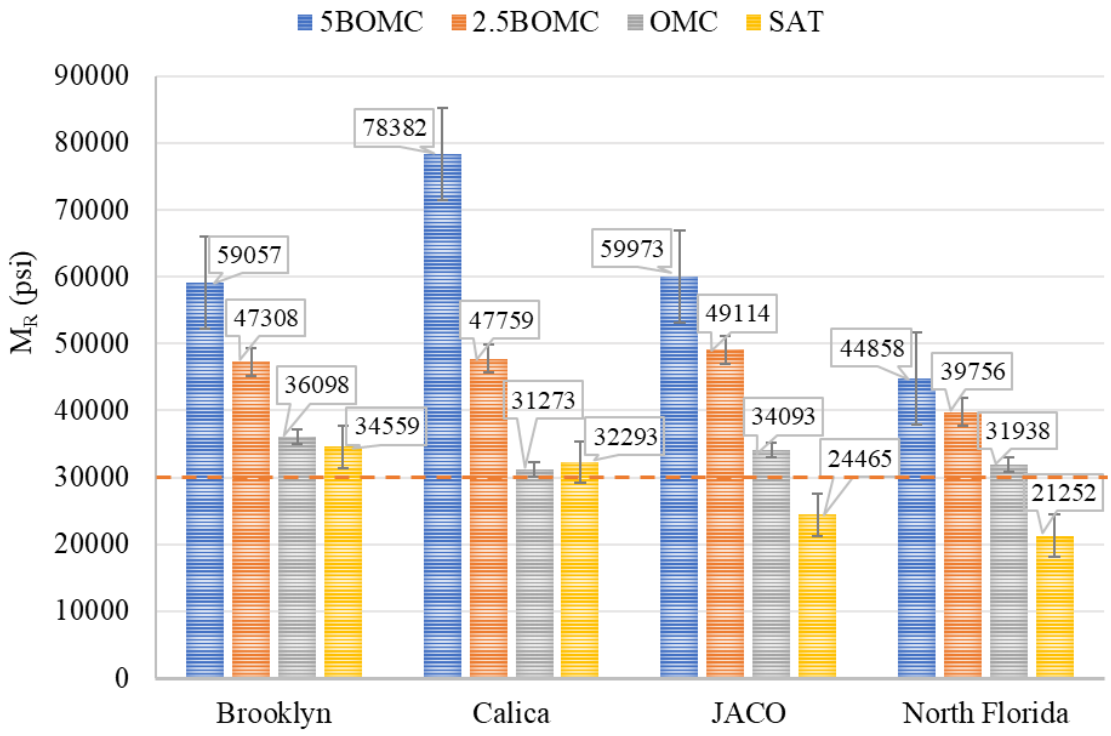

Figure 4.13. Summary of M_R values for all limerock aggregates at sequence 6

Overall, these MR results showed that moisture had a significant effect on the resilient modulus of limestone and limerock aggregates. Fines content, clay-like-minerals content or plastic fines content, and percent passing sieve #4 are the most influencing factors suggested. Further study should be conducted using statistical and practical methods to clearly identify all influencing factors among the aggregate properties. These results also showed that although limerock materials often do not meet specification requirements for an acceptable aggregate base, they can have similar mechanical behavior to limestone materials and demonstrate satisfactory performance.

4.4 FINDINGS

- At optimum moisture content (OMC), the resilient modulus of limestone and limerock are similar, ranging between 30,000 psi and 40,000 psi, while the triaxial shear maximum strength of limerock is slightly lower than that of limestone.
- A sensitivity study revealed that a change in MR of 4,000 psi or more is deemed practically significant for base aggregates.
- The resilient modulus and maximum strength of limestone and limerock increase significantly with decreasing moisture content. This mechanical behavior was attributed to the cementing of the aggregates when drying and the suction created by the reduction in moisture content providing additional confinement. The only exceptions were the decrease in MR for one limestone material and the decrease in maximum strength of a limerock material, both at 5BOMC. The suggested reasons were the weakening of these not well graded aggregate structures at very low moisture levels.
- At saturation, the resilient modulus decreases significantly for limestone and limerock aggregates having a higher content of at least two of the following three aggregate properties: (1) fines (percent passing #200 sieve), (2) fine aggregates (percent passing #4 sieve), and (3) clay-like materials or plastic fines. Limestone and limerock aggregates, not meeting the above criteria, do not experience any significant decrease in MR and may even become slightly stiffer. The importance of the moisture effect above OMC therefore depends strongly on certain aggregate properties.

5 PROPOSED RAPID ACCEPTANCE TEST

5.1 STATISTICAL ANALYSIS OF LABORATORY TESTS

To identify the aggregate properties that influence the moisture susceptibility of the pavement base aggregates and evaluate the level of impact, several regression analyses and a sensitivity analysis were conducted using all laboratory tests results. First, a pre-selection of aggregate properties capable of affecting the MR of base aggregates was done based on the findings of the literature review. The pre-selected properties include: plastic fines content (PFC), fine aggregate angularity (FAA), maximum dry density (MDD), %particles passing the #4 sieve or fine aggregate content (FAC), %particles passing the #200 sieve or fines content (FC), and absorption (Abs.). Before conducting the analyses, the correlation or collinearity between the pre-selected properties was investigated. Figure 5.1 presents the results of the investigation where a higher R2 equates to a higher correlation between the properties concerned. It was found that, except for Abs. and FAC, the pre-selected properties exhibited multicollinearity, meaning that they are highly correlated to two or more other properties.

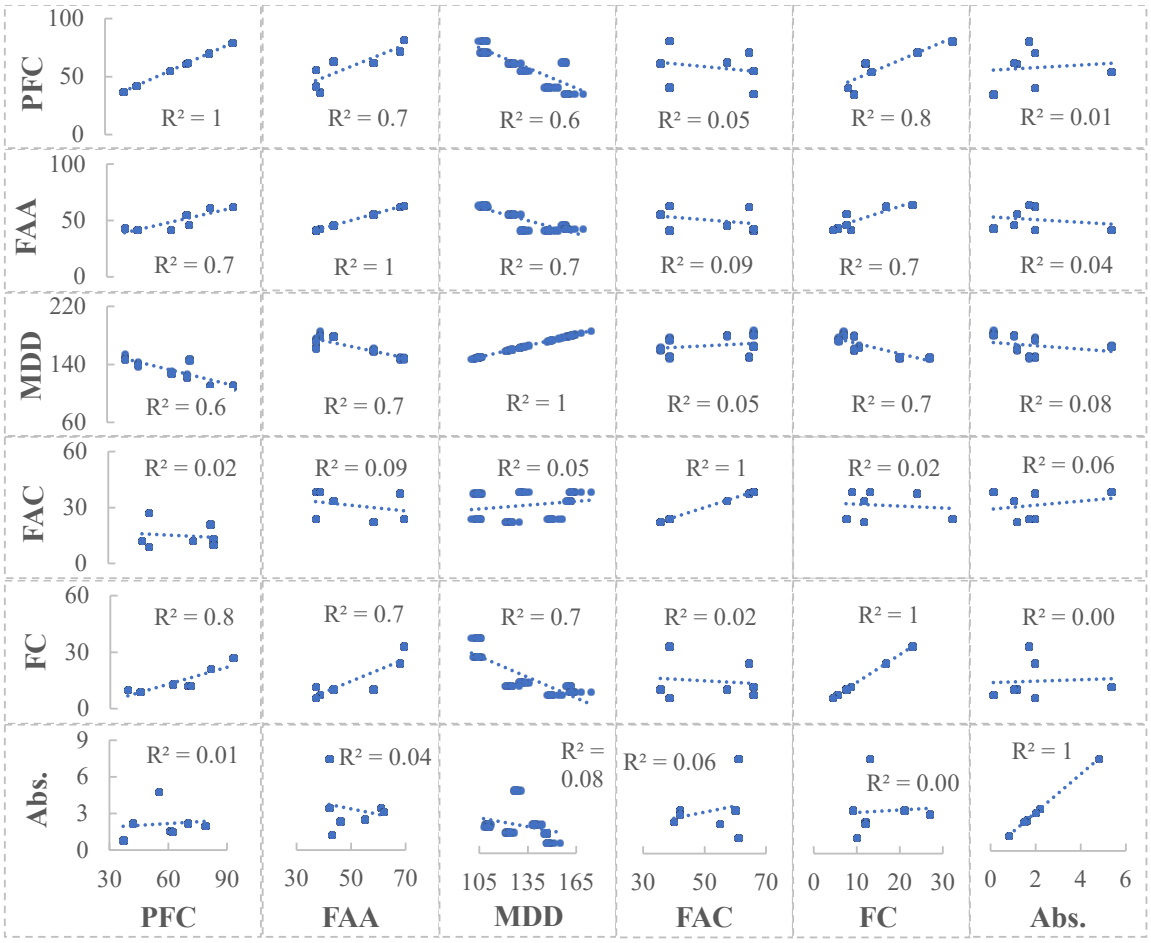

Figure 5.1. Correlations between the pre-selected aggregate properties

5.1.1 Sensitivity Analysis

Knowing that the pre-selected aggregate properties affect the change in MR due to increasing moisture, the objective of the sensitivity analysis was to determine which of these properties influence the moisture susceptibility (i.e., the decrease in MR with increasing moisture content). By identifying key aggregate properties, appropriate rapid screening tests may be selected or developed for the quality assurance (QA) of these materials. The sensitivity analysis consisted of predicting MR using the regression models previously obtained for each aggregate property and increasing the value of each property by 1% to assess whether its influence is positive or negative. In other words, for every unit increase in the independent variable (aggregate property), in what direction and by what amount the dependent variable (MR) will change from 5BOMC to SAT, 5BOMC to OMC, and OMC to SAT. The regression models of Abs. were still used in this analysis despite their unreliability due to higher P-values of the coefficients. This was done because the effect of Abs. on the change in MR has been proven, but the magnitude of the resulting MR values was ignored and only the negative or positive influence was assessed.

The results of the sensitivity analysis are presented in Figures 5.2(a), 5.2(b), and 5.2(c), for moisture content intervals 5BOMC to SAT, 5BOMC to OMC, and OMC to SAT, respectively. It is observed in Figure 5.2(a) that only three properties among the six pre-selected properties contribute to the decrease of MR from 5BOMC to SAT. The influencing properties include FC, PFC, and FAA. In Figure 5.2(b), the same influencing properties FC, PFC, and FAA influence the moisture susceptibility of base aggregates from 5BOMC to OMC. However, it can be seen in Figure 5.2(c) that FAC joined the list of influencing factors making FC, PFC, FAA and FAC the four properties influencing the moisture susceptibility of base aggregates from OMC to SAT.

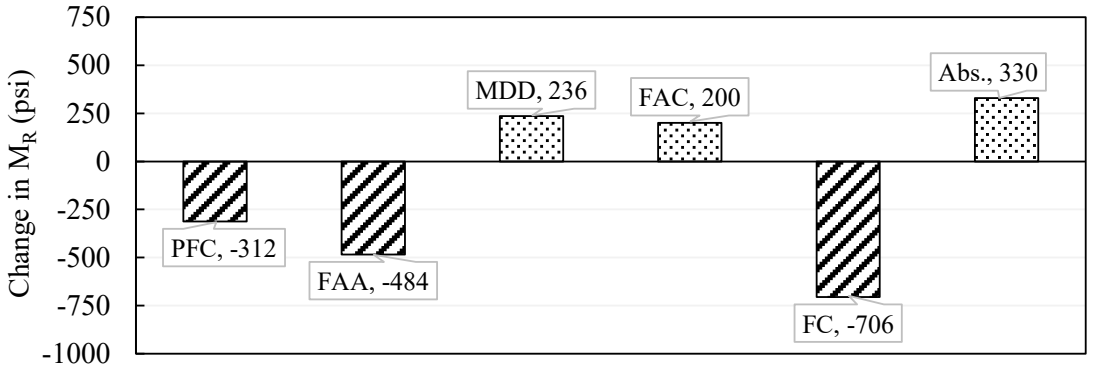

(a)

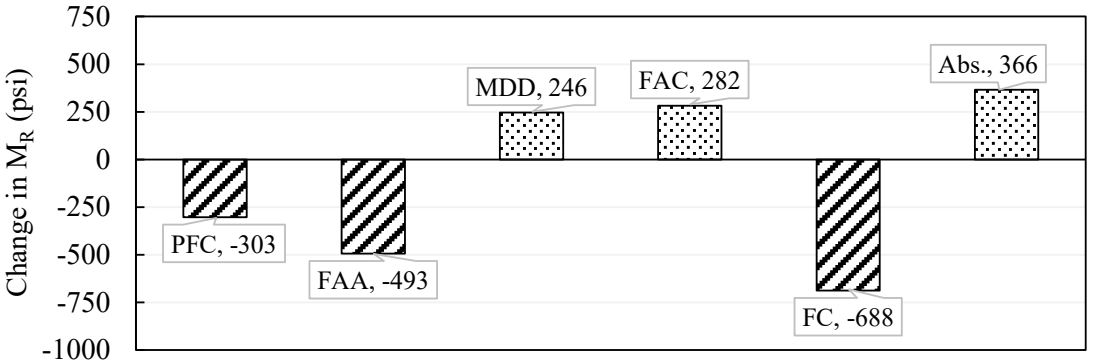

(b)

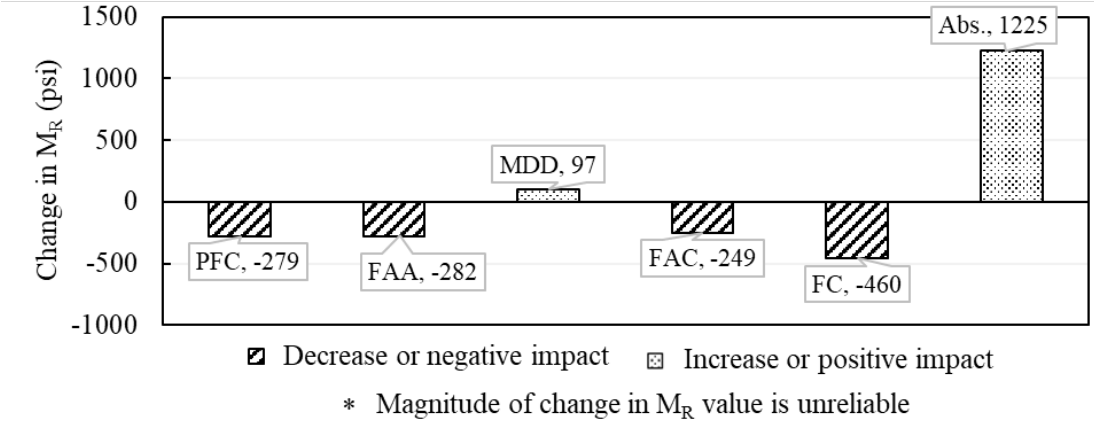

(c)

Figure 5.2. Influence of aggregate properties on the change in M_R (a) from 5BOMC to SAT, (b) from 5BOMC to OMC, and (c) from OMC to SAT

5.1.2 Multiple Regression Analysis (OMC to SAT)

According to the resilient modulus tests performed in this study, pavement base aggregates particularly lime-based crushed stones constructed at OMC in the field will increase in stiffness upon drying and most likely decrease in stiffness when they are saturated. This makes base aggregate saturation the most concerning moisture scenario in the field. Therefore, a multiple regression analysis was performed to determine a regression model that can help predict the moisture susceptibility of base aggregates from OMC to SAT. Since FC, PFC, and FAA are highly correlated, they are considered as collinear independent predictors and only one of them could be used in a multiple regression analysis. Thus, the multicollinearity was eliminated by removing FC and FAA, and choosing only PFC to accompany FAC for the analysis. PFC was chosen because an increase of PFC means an increase of FC and FAA whereas an increase of FC or FAA does not necessarily mean an increase of the remaining two properties. Additionally, FC and FAA are regularly used by agencies to evaluate the quality of base aggregates and have established thresholds, while PFC from the sand equivalent test is often less regulated for base aggregates. The multiple regression analysis was performed only for the moisture interval OMC to SAT with MR as the dummy dependent variable and PFC and FAC as the two independent variables.

The results of the multiple regression analysis are presented in Table 5.1. The adjusted R2 which is important when analyzing a multiple regression, was 0.70. The regression model resulting from this analysis is presented in Equation 5.1. The significance F of this regression model and the p-values of the coefficients of the PFC and FAC variables were all below the significance threshold of 0.05. These results demonstrated that the obtained regression model is reliable and can help predict the MR of base aggregates at saturation. As Equation 5.1 shows, PFC contributes to 62% (i.e., 253.8 / (253.8+154.1)) of the decrease in MR caused by the two properties and FAC contributes to 38% (i.e., 154.1 / (253.8+154.1)). Thus, a new variable was determined combining 62% of PFC and 38% of FAC for each of the seven base aggregates to compare their moisture susceptibility. Figure 5.3 shows the new variables of the base aggregates, except for Calica and Calera which were not moisture susceptible from OMC to SAT. It can be seen in Figure 5.3 that the moisture susceptibility ranking of the materials obtained using the new variables corresponds to the ranking previously obtained using the MS ratios from OMC to SAT.

$$M_{R\,SAT}(psi) = 57519.5 - 253.8\,(PFC) - 154.1(FAC) - 5902.1 \qquad (5.1)$$

where, PFC = plastic fines content (%) and FAC = fine aggregate content or % particles passing the #4 sieve (%).

Table 5.1. Summary of multiple regression analysis results

Moisture Level	Variables	Coefficients	Standard Error	p-value	Adjusted R^2	Significance F
OMC to SAT	Intercept	57519.5	4284.0	3.3E-13	0.7	5.5E-07
	PFC	- 253.8	50.5	3.1E-05		
	FAC	- 154.1	76.3	0.05		
	SAT = 1	- 5902.1	1198.9	4.1E-05		

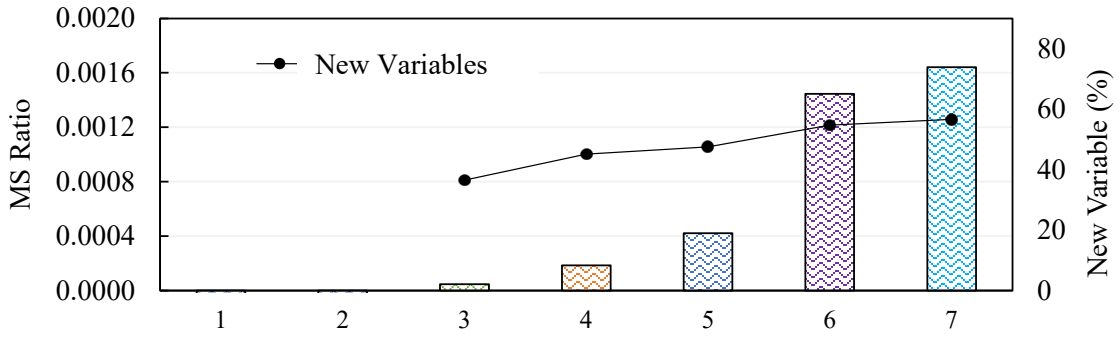

Figure 5.3. Moisture susceptibility comparison of the base aggregates from OMC to SAT

5.1.3 Recommended Thresholds for Quality Assurance Tests

The results of the laboratory tests and the statistical analyses were used to determine the aggregate properties influencing the moisture susceptibility of pavement base aggregates from OMC to SAT. In this section, certain tests are recommended to rapidly determine these properties in the field or laboratory and thresholds for these properties were determined for quality assurance.

As moisture content increases from OMC to SAT, the MR of every base aggregate is expected to change. As demonstrated by the sensitivity analysis in Chapter 3, a change in aggregate base MR of 4,000 psi for high traffic roads and 5,000 psi for low traffic roads is judged practically significant. Therefore, a base material with a minimum change in MR of 4,000 psi is considered highly moisture susceptible in this study. The changes in MR from OMC to SAT for the seven base aggregates in this study are shown in Figure 5.4. Only three base aggregates, namely Blue Water limestone, North Florida limerock, and JACO limerock showed a significant decrease in MR from OMC to SAT during laboratory testing.

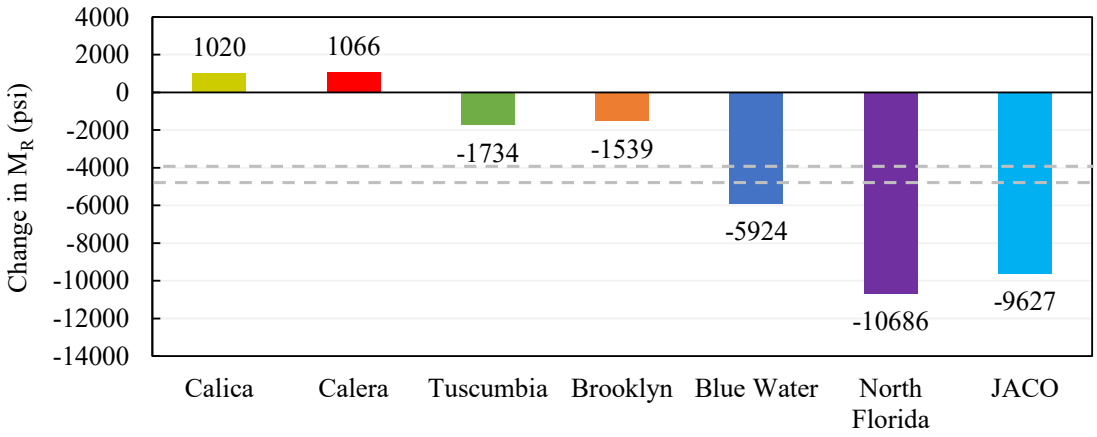

Figure 5.4. Changes in M_R from OMC to SAT for all seven aggregate base materials

From OMC to SAT, the properties influencing the moisture susceptibility of base aggregates are FC, PFC, FAA and FAC. Since PFC is also an excellent indicator of FC and FAA, PFC and FAC are the two critical properties for which thresholds were sought. To determine the thresholds, a sensitivity analysis was performed using the regression model in Equation 5.1 obtained from the multiple regression analysis. The following steps were taken:

- The M_R values of the seven base aggregates obtained from laboratory testing at OMC were averaged to be $M_{R\ OMC}$ = 33,700 psi.
- In the regression model, the value of FAC was increased from 0% to 100% in 1% increments.
- At each 1% increment of FAC, the value of PFC was varied in the regression model until the difference between the predicted $M_{R\ SAT}$ and $M_{R\ OMC}$ equaled the targeted decrease in M_R at which moisture susceptibility is considered high. This targeted decrease in M_R was 4,000 psi for high traffic roads and 5,000 psi for low traffic roads.

As a result, a graph plotting FAC versus PFC as presented in Figure 5.5 was obtained to represent the thresholds for PFC and FAC. As shown in Figure 5.5, the limit for PFC decreases as the value of FAC increases. The solid line is the limit for low traffic roads while the dashed line is the limit for high traffic roads. Figure 5.5 shows three zones of moisture susceptibility. The first zone, colored red, is the “High Moisture Susceptibility Zone”. In this zone, the decrease in M_R from OMC to SAT is greater than or equal to 4,000 psi for high traffic and 5,000 psi for low traffic and the material is considered highly moisture susceptible at saturation. The second light green colored zone is the “Low Moisture Susceptibility Zone”. The decrease in M_R from OMC to SAT is not significant in this zone, however not all percentages of FAC are acceptable for pavement base aggregates. Generally, state transportation agencies require a specific range for FAC to ensure high quality base aggregates. For ALDOT, the value of FAC should only vary between 40 – 70% for limestone aggregates and 50 – 85% for limerock aggregates. Therefore, the third zone in Figure 5.5 is the “Recommended Zone” for quality assurance where FAC varies between 40 –

85%. Before using the threshold chart in Figure 6.8, it is also important to ensure that the base material meets the specification requirements for FC and FAA as they also contribute to moisture susceptibility from OMC to SAT.

The threshold chart can be used to evaluate the moisture susceptibility of base aggregates at saturation. Therefore, to achieve more sustainable and climate-resilient pavements, the following tests and recommendations can be used in the laboratory or field for material selection before construction or for quality assurance testing during construction:

1. Determine the FC of the material by performing the aggregate washing test (AASHTO T11). Ensure that FC meets the agency specification requirements. If agency requirements do not exist, use the grading requirements for base aggregates in AASHTO M147. For ALDOT, the acceptable range of FC is 7 – 18% for limestone and 4 – 28% for limerock.
2. Determine the FAA of the material by performing the uncompacted void content test (AASHTO T304). Make sure FAA meets the agency specification requirements.
3. Determine the FAC of the material by performing the sieve analysis test (AASHTO T27). Ensure that FAC falls in the range required by the agency specification. If agency specifications do not exist, use the required range for base aggregates in AASHTO M147. In the threshold chart (Figure 5.5), use that range as the x-axis boundaries of the Recommended Zone. For ALDOT, the acceptable range of FAC is 40 – 70% for limestone and 50 – 85% for limerock.
4. Determine the PFC of the material by performing the sand equivalent test (AASHTO T176). Depending on the projected traffic level, determine the threshold for PFC using the threshold chart or the trendline equations in Figure 5.5. Materials whose PFC falls within the Recommended Zone are the least susceptible to moisture at saturation.

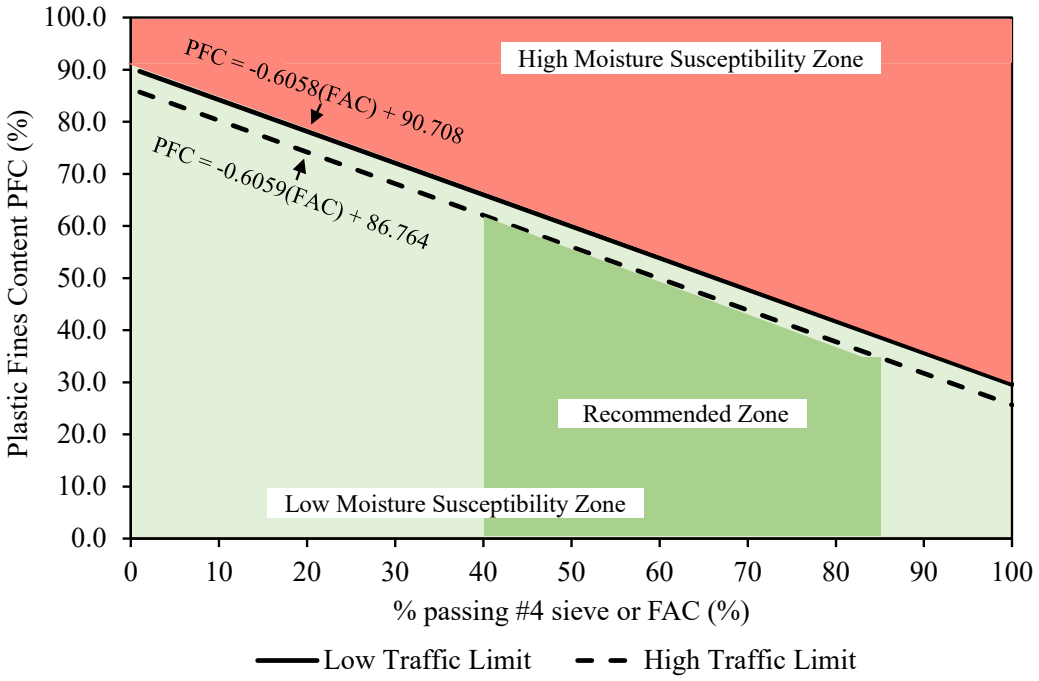

Figure 5.5. Threshold chart representing the quality assurance limits for moisture susceptibility evaluation at saturation

The aforementioned recommendations were followed using the properties of the seven base aggregates in this study. All the materials were plotted in the threshold chart as shown in Figure 5.6. It can be seen that Brooklyn limerock, Tuscumbia limestone, and Calera limestone fell within the recommended zone, meaning that the change in their MR at saturation is insignificant. This is consistent with the laboratory test results shown previously in Figure 5.4. Calica limerock was approximately on the threshold line for high traffic limit in Figure 5.6 although the laboratory results in Figure 5.4 showed that the change in MR is practically insignificant. This slight inconsistency is understandable since other factors such as the mineral compositions of the materials, which can also affect moisture susceptibility, were not considered in this study. Moreover, in Figure 5.6, Blue Water limestone, JACO limerock, and North Florida limerock fell in the high moisture susceptibility zone, which means that the change in their MR at saturation is practically significant. This is also consistent with the laboratory test results shown in Figure 5.4, where their MR decreased beyond 5,000 psi from OMC to SAT.

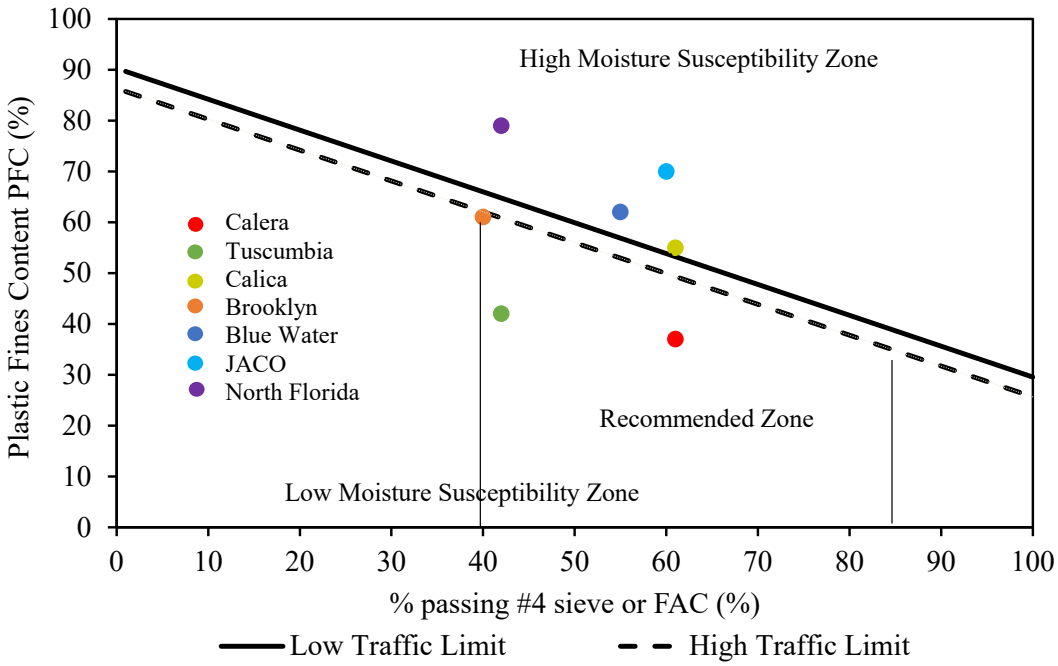

Figure 5.6. Threshold chart with the seven base aggregates of this study

5.2 CASE STUDY

The objective of the case study was to investigate the viability of the threshold chart. Two base aggregates with similar gradations and angularity, but with significantly different plastic fines contents, were selected among the seven materials tested in this study. Both Calera limestone and Blue Water limestone are limestone aggregates with FC of 10% and 12%, FAC of 61% and 55%, and FAA of 43% and 46%, respectively. However, Calera limestone has a PFC of 37% and Blue Water limestone has a PFC of 62%. It was demonstrated previously that Blue Water limestone has a high moisture susceptibility at saturation while Calera limestone has a low moisture susceptibility from OMC to SAT. According to the threshold chart using the high traffic limit equation, the value of PFC for Blue Water limestone must be less than 53% to be considered a base material with low moisture susceptibility at saturation. Thus, the case study consisted of replacing the fines (%passing #200 sieve) of Blue Water limestone with the fines of Calera limestone, and determining whether or not the reduction of PFC would reduce the moisture susceptibility of Blue Water limestone at saturation. Figure 5.7(a) shows the gradations of the Calera limestone, the original Blue Water limestone, and the New Blue Water limestone containing the fines of Calera limestone. The sand equivalent test was performed on New Blue Water limestone and the PFC obtained was 45%, which is less than 53%. The moisture density relationship did not considerably change for New Blue Water limestone, as shown in Figure 5.7(b).

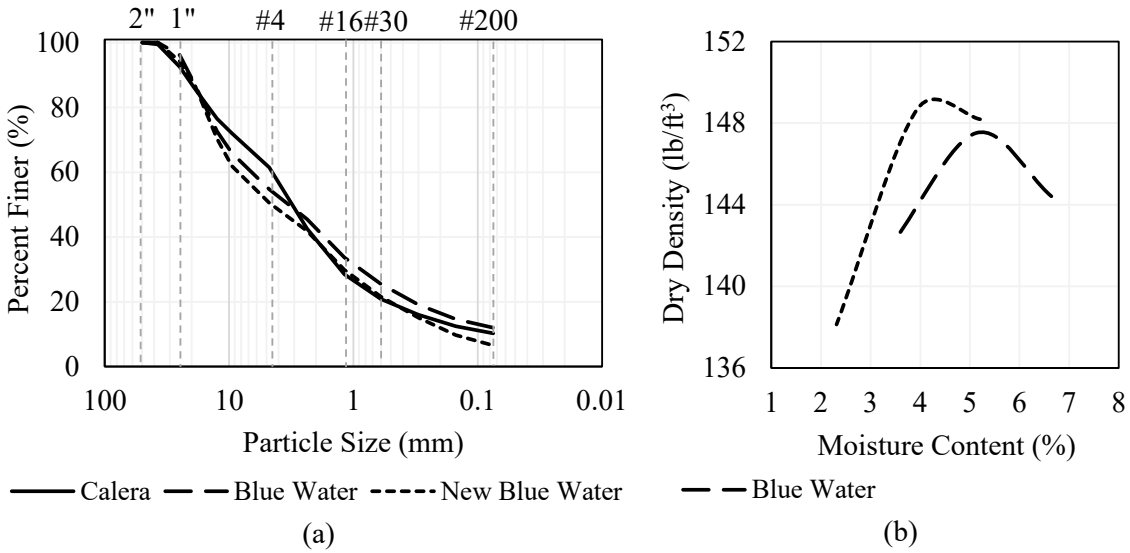

Figure 5.7. Case study (a) Gradations (b) Moisture density relationships

To practically evaluate the moisture susceptibility of New Blue Water limestone, resilient modulus tests were performed at OMC and at SAT. At each moisture content, two specimens were prepared and tested to ensure repeatability. The results are shown in Figures 5.8 and 5.9. At OMC, the MR of the New Blue Water limestone was slightly greater than the MR of the original Blue Water limestone over the 15 test sequences. At SAT, the MR of the New Blue Water limestone was significantly greater than the MR of the original Blue Water over the 15 test sequences. The final average MR value at each moisture content was obtained at the bulk stress of 30 psi and the change in MR from OMC to SAT was assessed. The results of the case study are summarized in Figure 5.10. By decreasing the PFC, the Blue Water limestone moved from the high moisture susceptibility zone to the recommended zone in the threshold chart, as shown in Figure 5.10(a). This was confirmed in practice by the resilient modulus test results shown in Figure 5.10(b), as the decrease in MR from OMC to SAT was reduced from 5,924 psi to 3,397 psi, which is less than 4,000 psi. The case study demonstrated that the threshold chart is a viable tool for quality assurance and can help investigate the moisture susceptibility of pavement base aggregates at saturation.

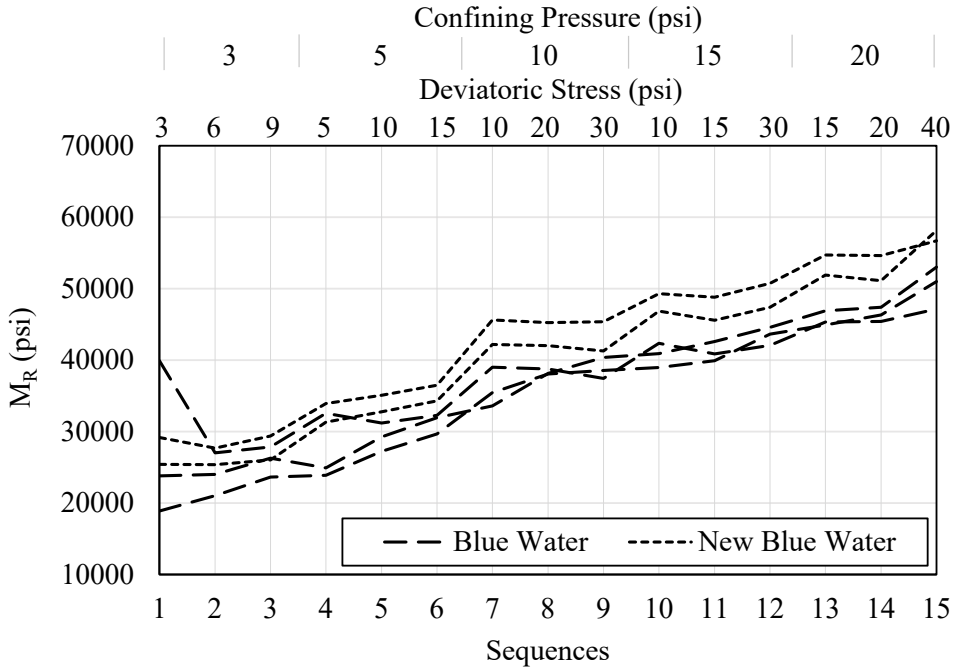

Figure 5.8. Case study - Summary of M_R test results at OMC

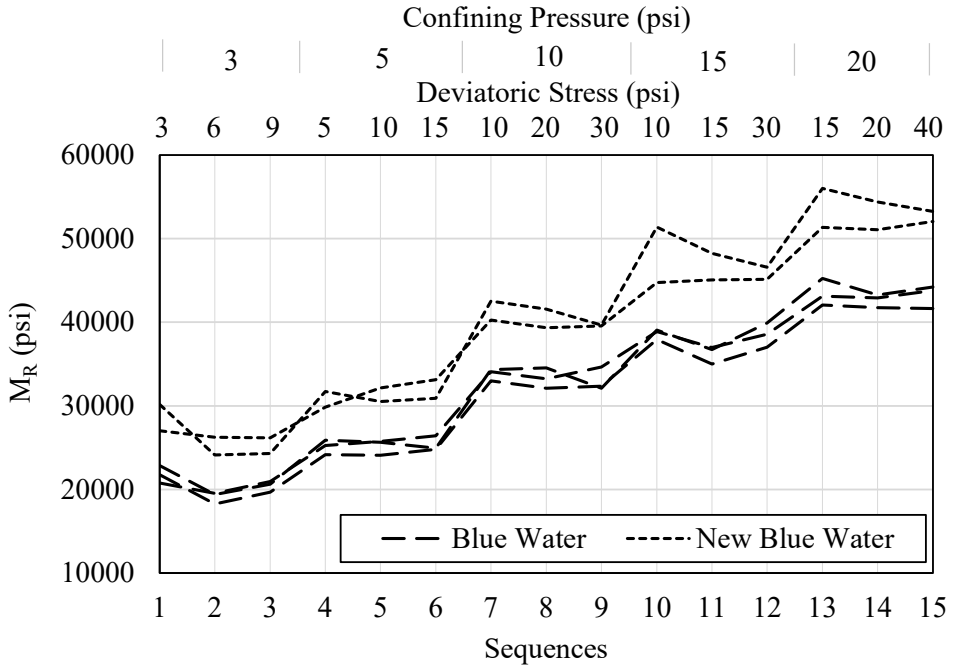

Figure 5.9 Case study - Summary of M_R test results at SAT

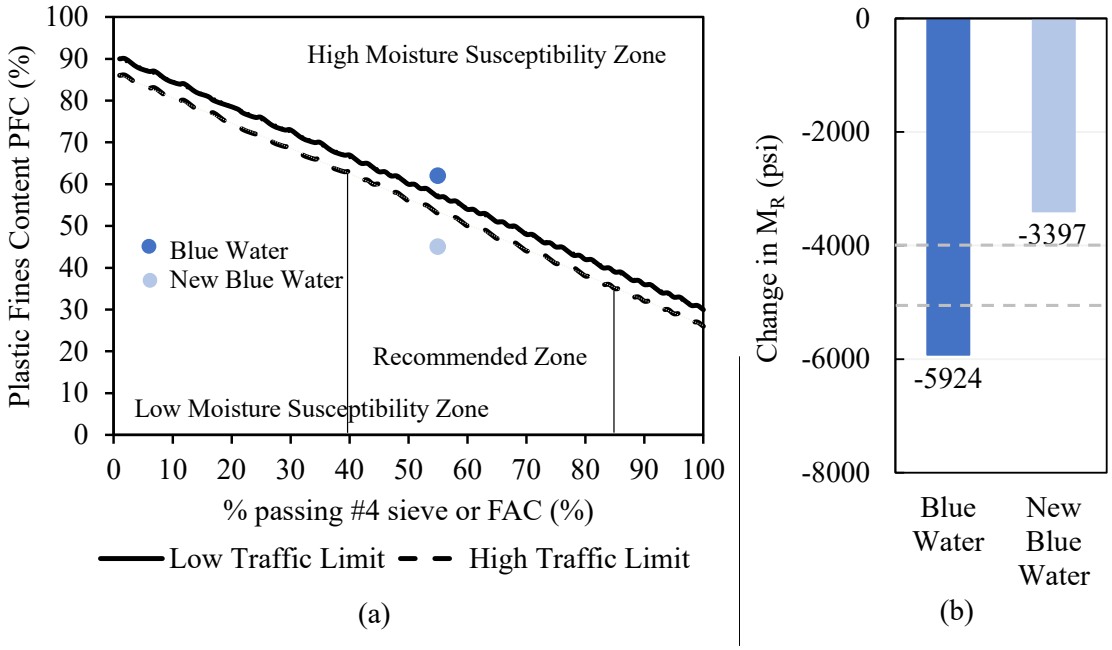

Figure 5.10. Case study (a) Threshold chart, (b) Decrease in M_R from OMC to SAT

5.2.1 Findings:

- The resilient modulus tests established that all seven materials were susceptible to moisture from 5BOMC to SAT, however their moisture susceptibility from 5BOMC to OMC differed from that of OMC to SAT.
- The results of the analyses showed that fines content (FC), plastic fines content (PFC), and fine aggregate angularity (FAA) were the influencing factors from 5BOMC to SAT and from 5BOMC to OMC. However, from OMC to SAT, the fine aggregate content (FAC) becomes an influencing factor and joins the three other factors.
- A case study demonstrated that the threshold chart is a viable, valid, and reliable tool that can help investigate the moisture susceptibility at saturation of unbound pavement base materials.

6 CONCLUSIONS, RECOMMENDATIONS, AND IMPLEMENTATION

6.1 CONCLUSIONS AND RECOMMENDATIONS

Moisture has a significant impact on the mechanical properties of *both* limestone and limerock. At OMC, while limestone and limerock exhibit similar MR, limerock generally has a slightly lower triaxial shear maximum strength (σdmax at failure) than limestone. Both limestone and limerock exhibit a significant increase in MR and ultimate strength as moisture content decreases. This behavior is attributed to the cementing effect of the aggregates as they dry and the additional confinement provided by the suction created at reduced moisture content. At saturation, the MR of limestone and limerock decreases significantly only when the base material has a higher content of at least two of the following properties: fines (percent passing No. 200 sieve), fine aggregates (percent passing No. 4 sieve), and plastic fines. Thus, the impact of moisture beyond the OMC strongly depends on specific properties of the aggregates.

The moisture susceptibility of the studied unbound base materials varies considerably depending on whether the moisture content is below, above, or at saturation relative to the OMC. When the moisture content is below the OMC, the aggregate properties most influential on moisture susceptibility are fines content (FC), plastic fines content (PFC), and fine aggregate angularity (FAA). At saturation, the key properties affecting moisture susceptibility include FC, PFC, FAA, and fine aggregate content (FAC). A threshold chart was developed to assess the moisture susceptibility of pavement base aggregates at saturation is both valid and reliable by simply plotting a given aggregates percent passing the No. 4 sieve versus the plastic fines content.

6.1.1 Recommendations

The following recommendations are resulting from this research effort:

- *Recommendation 1:* Limerock *may* be considered for use as an aggregate base in Alabama given the lab testing results and the fact that some currently accepted limestones appear to be *more* moisture susceptible than some of the sampled limerock.
- *Recommendation 2:* It is recommended that field experiments be conducted in a low-lying, flood prone and/or high ground water table region with limerock and limestone to investigate the in situ impacts of saturation to validate the laboratory experiment.
- *Recommendation 3:* ALDOT is recommended to consider adopting the developed threshold chart for acceptance of limerock and limestone aggregate base. This chart can be used by an engineer or inspector to determine whether or not an aggregate sample in the field is acceptable.

6.2 IMPLEMENTATION PLAN

The research team will support the Materials and Tests Bureau to draft appropriate guidance for the adoption of the threshold chart, if ALDOT determines it is appropriate. The research team will also investigate the feasibility of field instrumented sites with appropriate ALDOT personnel to further validate the findings of this study.

REFERENCES

AASHTO (Association of State Highway and Transportation Officials). 1993. Guide for Design of Pavement Structures. Washington, D.C.

AASHTO. 2020. “Mechanistic-Empirical Pavement Design Guide: A Manual of Practice”. American Association of State Highway and Transportation Officials. Washington, DC.

AASHTO T11. 2020. “Standard Method of Test for Materials Finer Than 75-µm (No. 200) Sieve in Mineral Aggregates by Washing”. American Association of State Highway and Transportation Officials. Washington, D.C.

AASHTO T180. 2020. “Standard Method of Test for Moisture–Density Relations of Soils Using a 4.54-kg (10-lb) Rammer and a 457-mm (18-in.) Drop”. American Association of State Highway and Transportation Officials. Washington, D.C.

AASHTO T19. 2014. “Standard Method of Test for Bulk Density (“Unit Weight”) and Voids in Aggregate”. American Association of State Highway and Transportation Officials. Washington, D.C.

AASHTO T27. 1995. “Sieve Analysis of Fine and Coarse Aggregates”. American Association of State Highway and Transportation Officials. Washington, D.C.

AASHTO T304. 1995. “Uncompacted Void Content of Fine Aggregate”. American Association of State Highway and Transportation Officials. Washington, D.C.

AASHTO T307. 2021. “Determining the Resilient Modulus of Soils and Aggregate Materials”. American Association of State Highway and Transportation Officials. Washington, D.C.

AASHTO T84. 1995. “Specific Gravity and Absorption of Fine Aggregate”. American Association of State Highway and Transportation Officials. Washington, D.C.

AASHTO T85. 1995. “Specific Gravity and Absorption of Coarse Aggregate”. American Association of State Highway and Transportation Officials. Washington, D.C.

AASHTO T89. 2022. “Standard Method of Test for Determining the Liquid Limit of Soils”. American Association of State Highway and Transportation Officials. Washington, D.C.

AASHTO T90. 2020. “Standard Method of Test for Determining the Plastic Limit and Plasticity Index of Soils”. American Association of State Highway and Transportation Officials. Washington, D.C.

Abu-Rizaiza, O.S. 1999. “Threats from Groundwater Table Rise in Urban Areas in Developing Countries”. Water Int.; 24(1):46–52.

Adhikari, P., and Osouli, A. 2019. “Cyclic Triaxial Tests on Crushed Limestone for Base Layers”. In Proc., 8th Int. Conf. ASCE Geo-Congress: Geotechnical Materials, Modeling, and Testing GSP 310. Pennsylvania: Geo-Institute of ASCE.

Alabama Department of Transportation (ALDOT). 1990. “Holman Report: Guidelines for Flexible Pavement Design in Alabama”.

Alabama Department of Transportation (ALDOT). 2018. “Standard Specifications for Highway Construction”. https://www.dot.state.al.us/publications/Construction/pdf/Specifications/2018/StandardSpecificationsCompleteBook.pdf

Allen, J. 1973. “The Effect of Non-constant Lateral Pressures of the Resilient Response of Granular Materials”. Ph.D. Thesis, University of Illinois at Urbana-Champaign, Urbana, IL.

Andrei, D., Witczak, M.W., and Houston, W.N. 2009. “Resilient Modulus Predictive Model for Unbound Pavement Materials”. International Foundation Congress and Equipment Expo.

ASTM C131. 2006. “Standard Test Method for Resistance to Degradation of Small-Size Coarse Aggregate by Abrasion and Impact in the Los Angeles Machine”. American Association of State Highway and Transportation Officials. Washington, D.C.

ASTM C670. 2015. “Standard Practice for Preparing Precision and Bias Statements for Test Methods for Construction Materials”. American Association of State Highway and Transportation Officials. Washington, D.C. http://doi.org/10.1520/C0670-15

ASTM D4791. 2019. “Standard Test Method for Flat Particles, Elongated Particles, or Flat and Elongated Particles in Coarse Aggregate”. American Association of State Highway and Transportation Officials. Washington, D.C.

ASTM D5821. 2017. “Standard Test Method for Determining the Percentage of Fractured Particles in Coarse Aggregate”. American Association of State Highway and Transportation Officials. Washington, D.C.

Barber, E. S. 1946. “Application of Triaxial Compression Test Results on the Calculation of Flexible Pavement Thickness”. Proceedings, 26th Annual Meeting of the Highway Research Board, Washington D.C., pp.26-39.

Barksdale, R.D. and Itani, S.Y. 1989. “Influence of Aggregate Shape on Base Behavior”. Transportation Research Record 1227, TRB, National Research Council, Washington, D.C., pp. 173-182

Buchanan, S. 2007. “Resilient Modulus: What, Why, and How?”. Vulcan Materials Company.

Burrage, R. E., Anderson, J. B., Pando, M. A., Ogunro, V. O., and Cottingham, M. A. 2012. “A Cost Effective Triaxial Test Method for Unsaturated Soils”. Geotechnical Testing Journal, Vol. 35, No. 1.

Camargo F., Benson, C., and Edil, T. 2012. “An Assessment of Resilient Modulus Testing: Internal and External Deflection Measurements”. Geotechnical Testing Journal, Vol. 35, No. 6. ASTM International, West Conshohocken, PA. http://doi.org/10.1520/GTJ20120077

Carpenter, P.J., Adams, R.F., and Lenczewski, M. 2013. “Ground-Penetrating Radar, Resistivity and Spontaneous Potential Investigations of a Contaminated Aquifer Near Cancún, Mexico”. 3th Sinkhole Conference Nckri Symposium 2.

Cary, C., and Zapata, C. 2011. “Resilient modulus for unsaturated unbound materials”. Road Mater. Pavement Des., 12(3), 615–638.

Chen, X., and Wang, H. 2023. “Impact of Sea Level Rise on Asphalt Pavement Responses Considering Seasonal Groundwater and Moisture Gradient in Subgrade”. Transportation Geotechnics.

Cherian, C., N. J. Kollannur, S. Bandipally, and D. N. Arnepalli. 2018. “Calcium Adsorption on Clays: Effects of Mineralogy, Pore Fluid Chemistry and Temperature”. Applied Clay Science 160, 282–289.

Chowdhury, S.M.R.M. 2021. “Evaluation of Resilient Modulus Constitutive Equations for Unbound Coarse Materials”. Construction and Building Materials Vol. 296, 123688.

Craciun, O., and Lo, S.R. 2010. “Matric Suction Measurement in Stress Path Cyclic Triaxial Testing of Unbound Granular Base Materials”. Geotechnical Testing Journal, Vol. 33, N1.

Ekblad, J., and Isacsson, U. 2006. “Influence of Water on Resilient Properties of Coarse Granular Materials”. Road Materials and Pavement Design, 7(3), 369–404.

Elshaer, M., Ghayoomi, M., and Daniel, J.S. 2019. “Impact of Subsurface Water on Structural Performance of Inundated Flexible Pavements”. International Journal of Pavement Engineering; 20(8): 947–57.

Florida Department of Environmental Protection. Florida Geological Survey. https://floridadep.gov/fgs. Accessed in 2023.

Florida Department of Transportation (FDOT). 2017. “Standard Specifications for Road and Bridge Construction”. https://www.fdot.gov/docs/defaultsource/programmanagement/Implemented/SpecBooks/July2017/Files/717eBook.pdf

Fredlund, D.G., Bergan, A.T., and Wong, P.K. 1977. “Relation Between Resilient Modulus and Stress Research Conditions for Cohesive Subgrade Soils”. Transportation Research Record. 642, Transportation Research Board, Washington, D.C., 73–81.

Fredlund, D.G., and Xing, A. 1994. “Equation for Soil Water Characteristic Curve”. Canadian Geotechnical Journal, 31(3), 521–532.

Geo Car. /Social Studies. Weathering. https://gpres.weebly.com/weathering.html. Accessed in August 2022.

Geological Survey of Alabama (GSA). “Geologic Investigations Program”. https://www.gsa.state.al.us/gsa/geologic/hazards/sinkholes. Accessed in 2023.

Gray, J. E. 1962. “Characteristics of Graded Base Course Aggregates Determined by Triaxial Tests”. National Crushed Stone Association, Washington, DC.

Groeger, J.L., Rada, G.R., and Lopez, A. 2003. “AASHTO T307 - Background and Discussion”. Resilient Modulus Testing for Pavement Components, ASTM STP 1437, G.N.

Gu, F., H. Sahin, X. Luo, R. Luo, and R. L. Lytton. 2014. “Estimation of Resilient Modulus of Unbound Aggregates Using Performance-Related Base Course Properties”. Journal of Materials in Civil Engineering.

Han, Z., and S. K. Vanapalli. 2014. “Prediction of the variation of the resilient modulus with respect to the soil suction for three granular materials using three methods”. Presented at GeoShanghai Int. Conf. on Geotech. Eng., Shanghai, China.

Harris, J. P., and Chowdhury, A. 2007. “Tests to Identify Poor Quality Coarse Limestone Aggregates and Acceptable Limits for such Aggregates in Bituminous Mixes”. Federal Highway Administration. FHWA/TX-05/0-4523-2.

Haynes, J. H., and Yoder, E. J. 1963. “Effects of Repeated Loading on Gravel and Crushed Stone Base Material Used in the AASHTO Road Test”. Highway Research Record 39, Highway Research Board, Washington, D.C., 82–86.

Heath, A.C., Pestana, J.M., Harvey, J.T., and Bejerano, M.O. 2004. “Normalizing Behavior of Unsaturated Granular Pavement Materials”. J. Geotech. GeoEnv. Eng., ASCE.

Hilf, J.W. 1956. “An Investigation of Pore Water Pressure in Compacted Cohesive Soils”. Technical Memorandum 654, U.S. Dept. of Interior, Bureau of Reclamation, Denver, CO.

Hiltunen, D.R., Roque, R., and Ayithi, A. 2011. “Final Report: Base Course Resilient Modulus for the Mechanistic Empirical Pavement Design Guide”. University of Florida, Florida Department of Transportation Research Center.

Hossain, M. 1998. “Influence of Moisture Content in Granular Bases on Pavement Performance”. Master’s Thesis. Texas Tech University.

Hubler, J. F., A. Athanasopoulos-Zekkos, and D. Zekkos. 2022. “Pore Pressure Generation of Gravelly Soils in Constant Volume Cyclic Simple Shear”. Journal of Geotechnical and Geoenvironmental Engineering, ASCE, ISSN 1090-0241., 2022. DOI:10.1061/(ASCE)GT.1943-5606.0002928.

Inner Circle. n.d. “US Map - Color, Classic Text”. Great Big Canvas. https://www.greatbigcanvas.com/view/us-map-color-classic-text,2530062/. Accessed in 2023.

Janoo, V., Bayer Jr., J.J., and Benda, C.C. 2004. “Effect of Aggregate Angularity on Base Material Properties”. Journal of Materials in Civil Engineering. 16(6). ASCE. https://doi.org/10.1061/(ASCE)0899-1561(2004)16:6(614)

Jorenby, B.N., and Hicks, R.G. 1986. “Base Course Contamination Limits”. Transportation Research Record, (1095), 86–101.

Kamal, M.A., Dawson, A.R., Farouki, O.T., Hughes, D., and Sha’at, A.A. 1993. “Field and Laboratory Evaluation of the Mechanical Behavior of Unbound Granular Materials in Pavements”. Transportation Research Record, (1406), 88–97.

Kasianchuk, D. A. 1968. “Fatigue Considerations in the Design of Asphalt Concrete Pavements”. Ph.D. Thesis, University of Califomia, Berkley, CA.

Khosravifar, S., Z. Afsharikia, and C. W. 2015. Schwartz. “Evaluation of Resilient Modulus Prediction Models for Cohesive and Noncohesive Soils”. Airfield and Highway Pavements. ASCE.

Kim, W., Labuz, J., Chadbourn, B., and Loken, M. 2008. “Uniformity of Deformation in Element Testing”. Geotechnical Testing Journal, Vol. 31, No. 3, ASTM International, West Conshohocken, PA. http://doi.org/10.1520/GTJ100722

King, H. M. 2022. “Limestone - What is Limestone and How is it Used?” Geology News and Information. Accessed in August 2022.

Ko, J. 2005. “Evaluating Limerock-Base Thick Lift”. Master’s Thesis. University of Florida.

Ksaibati, K., Armaghani, J., and Fisher, J. 2000. “Effect of Moisture on Modulus Values of Base and Subgrade Materials”. Transportation Research Record, Journal of the Transportation Research Board, 1716(1), 20-29. https://doi.org/10.3141/1716-03.

Kumar, A., Azizi, A., and Toll, D. G. 2022. “Application of Suction Monitoring for Cyclic Triaxial Testing of Compacted Soils”. American Society of Civil Engineers: J. Geotech. Geoenviron. Eng. 148(4): 04022009.

Lekarp, F., Isacsson, U., and Dawson, A. 2000. “State of the Art. I: Resilient Response of Unbound Aggregates”. Journal of Transportation Engineering, 126(1), 66–75.

Liang, R.Y., Rabab’ah, S., and Khasawneh, M. 2008. “Predicting Moisture-Dependent Resilient Modulus of Cohesive Soils Using Soil Suction Concept”. Journal of Transportation Eng., 10.1061/(ASCE)0733-947X (2008)134:1(34), 34–40.

Lim, J.X., Chong, S.Y., Tanaka, Y., and Lee, M.L. 2018. “Anisotropically Consolidated Undrained Compression Test on Residual Soil”. EDP Sciences. E3S Web Conf. Volume 65.

Lin, C., and Zhang, X. 2020. “Numerical Simulation of Seasonal Variations of Base Course Resilient Modulus in Pavement Structures in Nonfrost Regions”. Journal of Transportation Engineering, Part B: Pavements, 146(3): 04020038.

“Long-Term Pavement Performance (LTPP) Protocol P46: Resilient Modulus of Unbound Granular Base/Subbase Materials and Subgrade Soils”. 1996. U.S. Department of Transportation – Federal Highway Administration.

Lytton, R.L. 1995. “Foundations and pavements on unsaturated soils”. Proceedings of the first International Conference on Unsaturated Soils, unsat'95, Paris, France. Volume 3.

Makhnenko, R.Y., and Labuz, J.F. 2013. “Saturation of Porous Rock and Measurement of the B Coefficient”. 47th US Rock Mechanics / Geomechanics Symposium. American Rock Mechanics Association.

Minnesota Department of Transportation. n.d. “MnDOT Resilient Modulus (MR) Testing Protocol and Data Quality Control Criteria”.

https://web.archive.org/web/20240515195800/https://www.dot.state.mn.us/mnroad/modulus-protocol.html. Accessed 07/2023.

Mishra, D., Tutumluer, E., and Xiao, Y. 2010. “Particle Shape, Type and Amount of Fines, and Moisture Affecting Resilient Modulus Behavior of Unbound Aggregates”. In Proc., GeoShanghai International Conference. Paving Materials and Pavement Analysis. https://doi.org/10.1061/41104(377)34.

Mitchell, J.K., and Soga, K. 2005. “Fundamentals of Soil Behavior”. John Wiley & Sons, Inc., Hoboken, New Jersey. 3rd Edition.

Morales, A.C., and Pando, M.A. 2011. “Moisture Effects on Two Crushed Limestone Aggregates”. Geo-Frontiers. ASCE.

Morvan, M., Vernay, M., and Breul, P. 2016. “Study of the Variation of B with Sr”. E3S Web of Conferences 9, 10003.

National Cooperative Highway Research Program (NCHRP). 2004a. “Guide for Mechanistic Empirical Design of New and Rehabilitated Pavement Structures, Chapter 3: Environmental Effects”. Final Report 1-37A. Champaign, IL.

National Cooperative Highway Research Program (NCHRP). 2004b. “Research Results Digest – Number 285: Laboratory Determination of Resilient Modulus for Flexible Pavement Design”. National Academies of Sciences, Engineering, and Medicine.

Osouli, A., Adhikari, P., Tutumluer, E., and Shoup, H. 2021. “Fines Content, Plasticity Index and Dust Ratio Influencing the Modulus and Permanent Deformation Behavior of Aggregates”. Transportation Geotechnics, Volume 30. https://doi.org/10.1016/j.trgeo.2021.100630.

Osouli, A., Tutumluer, E., and Vaughn, B. 2018. “Plasticity Requirements of Aggregates Used in Pavement Base and Subbase Courses”. Illinois Center for Transportation Series No. 18018.

Phommavone, C., and Sangpetngam, B. 2018. “Influences of Moisture Content on Resilient Modulus of Unbound Crushed Limestone”. Engineering Journal, Volume 22 Issue 4. https://doi.org/10.4186/ej.2018.22.4.39.

Rada, G., and M. W. Witczak. 1981. “Comprehensive Evaluation of Laboratory Resilient Moduli Results for Granular Material”. Transportation Research Record: Journal of the Transportation Research Board, No. 810. pp. 23-33.

Salam, S., Osouli, A., and Tutumluer, E. 2018. “Crushed Limestone Aggregate Strength Influenced by Gradation, Fines Content, and Dust Ratio”. Journal of Transportation Engineering, Part B: Pavements, © ASCE, ISSN 2573-5438. https://doi.org/10.1061/JPEODX.0000032.

Salour, F., and Erlingsson, S. 2014. “Impact of Groundwater Level on the Mechanical Response of a Flexible Pavement Structure: A Case Study at the Torpsbruk Test Section along

County Road 126 Using Falling Weight Deflectometer". Report No. 808A. Swedish National Road and Transport Research Institute (VTI), Linkoping.

Seed, H.B., Mitry, F.G., Monismith, C.L., and Chan, C.K. 1967. "Prediction of Pavement Deflection from Laboratory Repeated Load Tests". NCHRP Rep. No. 35, Washington, D.C.

Selvadurai, A.P.S., and Suvorov, A.P. 2022. "Poroelastic Properties of Rocks with a Comparison of Theoretical Estimates and Typical Experimental Results". Scientific Reports 12, 10975.

Samuel Ginn College of Engineering (SGCE). "NOAA awards Auburn team $1.5M to research resilient transportation infrastructure". https://eng.auburn.edu/news/2021/09/auburn-noaa-resilient-infrastructure-grant. Accessed in 2024.

Sousa, B.J.O., and Vasconcelos, J.G. 2024. GSSHA Modeling Applied to a Coastal Roadway in Alabama. In Proc., ASCE World Environmental and Water Resources Congress. https://doi.org/10.1061/9780784485477.063

Steele, G. W., Anderson, D. A., and Antle, C. E. 1994. "Round 1 Type 1 Unbound Granular Base Course Proficiency Sample Program". Strategic Highway Research Program SHRP-P-692. National Research Council. Washington, DC.

Tamrakar, P., and Nazarian, S. 2016. Final Report: "Impact of Gradation and Moisture Content on Stiffness Parameters of Base Materials". University of Texas at El Paso. Texas Department of Transportation.

Teshale, E.Z., Shongtao, D., and Walubita, L.F. 2019. "Evaluation of Unbound Aggregate Base Layers Using Moisture Monitoring Data". Transportation Research Board, 98th Annual Meeting. MnDOT.

Thom, N.H., and Brown, S.F. 1987. "Effect of Moisture on The Structural Performance of a Crushed-Limestone Road Base". Transportation Research Record, Journal of the Transportation Research Board, 1121, 50-56.

Thompson, M. R. 1976. "Final Report: Resilient Properties of Subgrade Soils". Civil Engineering Studies, Series; 160, University of Illinois, Urbana-Champaign, EL.

Titi, H. H., Elias, M. B., and Helwany, S. 2006. "Determination of Typical Resilient Modulus Values for Selected Soils in Wisconsin". Wisconsin Highway Research Program.

Titi, H. H., Tabatabai, H., and Faheem, A. 2018. "Evaluation of the Long-Term Degradation and Strength Characteristics of In-situ Wisconsin Virgin Base Aggregates under HMA Pavements". WisDOT Technical Report WHRP 0092-15-06.

Toros, U., and Hiltunen, D. 2008. "Effects of Moisture and Time on Stiffness of Unbound Aggregate Base Coarse Materials". Transportation Research Record, Journal of the Transportation Research Board, No. 2059, pp. 41-51. Washington, D.C.

Ullah, S., and Tanyu, B.F. 2020. "Effect of Variation in Moisture Content on the Mechanical Properties of Base Course Constructed with RAP-VA Blends". Geo-Congress. ASCE.

United States Geological Survey (USGS). “National Geologic Map Database”. https://ngmdb.usgs.gov/mapview/?center=-97,39.6&zoom=4. Accessed in 2022.

United States Geological Survey (USGS). “The North America Tapestry of Time and Terrain”. Geologic Investigations Series I-2781. https://pubs.usgs.gov/imap/i2781/ Accessed in 2023.

Uthus, L., Hoff, I., and Horvli, I. 2005. “A Study on the Influence of Water and Fines on the Deformation Properties of Unbound Aggregates”. In Proceedings, 7th Internacional Conf. on the Bearing Capacity of Roads, Railways and Airfields, Trondheim (Norway).

Vernay, M., Morvan, M., and Breul, P. 2020. “Evaluation of the Degree of Saturation Using Skempton Coefficient B”. Geomechanics and Geoengineering, 15:2, 79-89.

Wissa, A.E. 1969. “Pore Pressure Measurements in Saturated Stiff Soils”. Journal of Soil Mechanics and Foundations. Division, ASCE. 95:1063-1073.

Witczak, M., and Uzan, J. 1988. “The Universal Airport Design System, Report I of IV”. Granular Material Characterization. Rep. to Department of Civil Engineering, Univ. of Maryland, College Park, Md.

Yau, A., and Von Quintus, H.L. 2004. “Predicting Elastic Response Characteristics of Unbound Materials and Soils”. Journal of the Transportation Research Board. pp. 47–56.

Zapata, C. E. 1999. “Uncertainty in Soil-Water Characteristic Curve and Impacts on Unsaturated Shear Strength Predictions”. Ph.D. dissertation, Arizona State Univ., Tempe, Ariz.

Appendix A

A.1 For Calera limestone

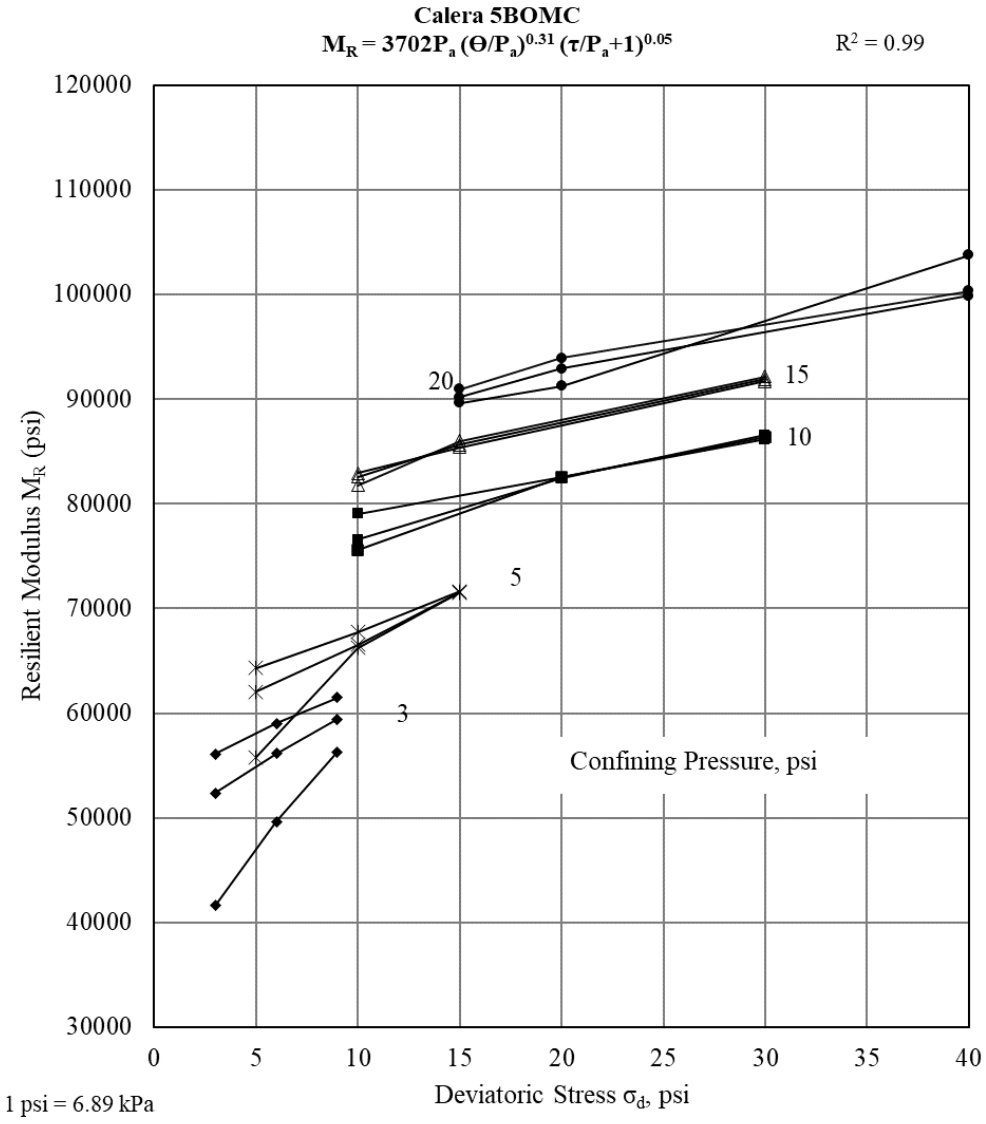

Figure A.1. 1. Detailed M_R test results at 5BOMC for Calera limestone

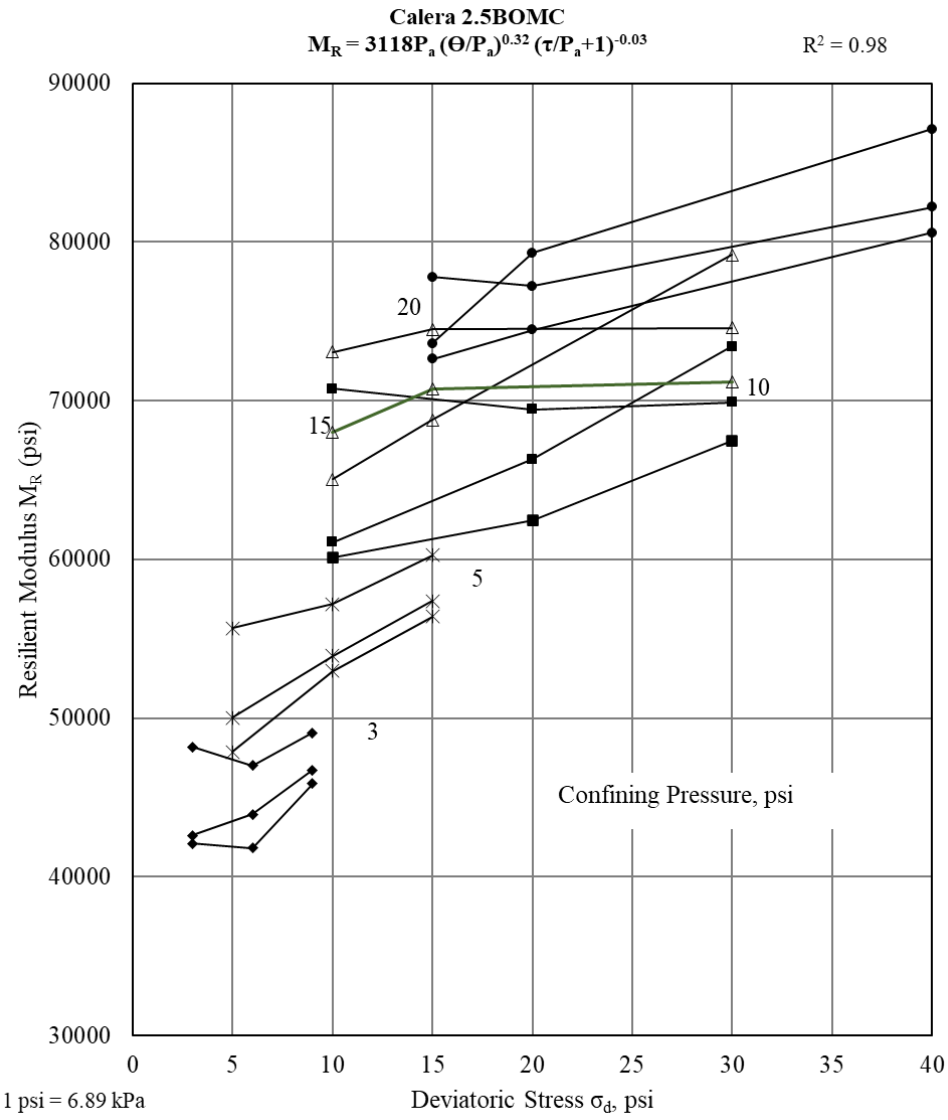

Figure A.1. 2. Detailed M_R test results at 2.5BOMC for Calera limestone

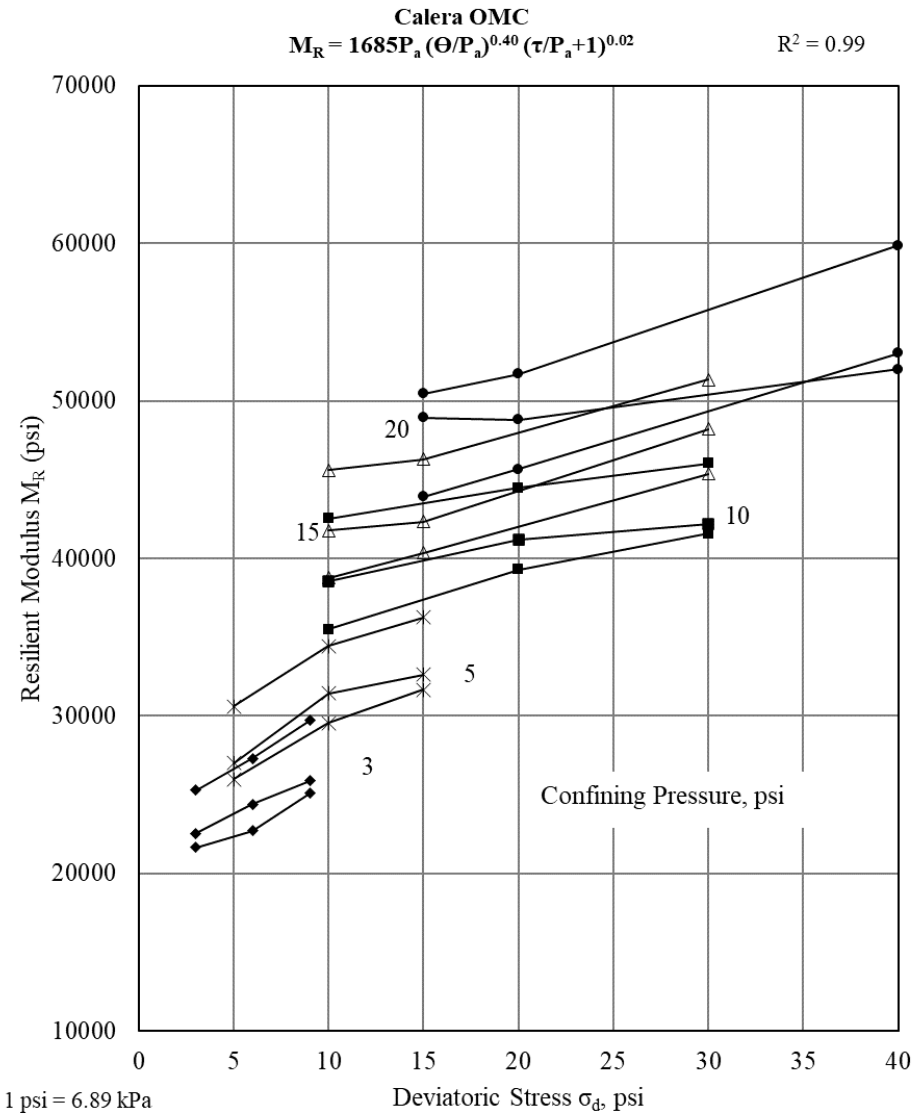

Figure A.1. 3. Detailed M_R test results at OMC for Calera limestone

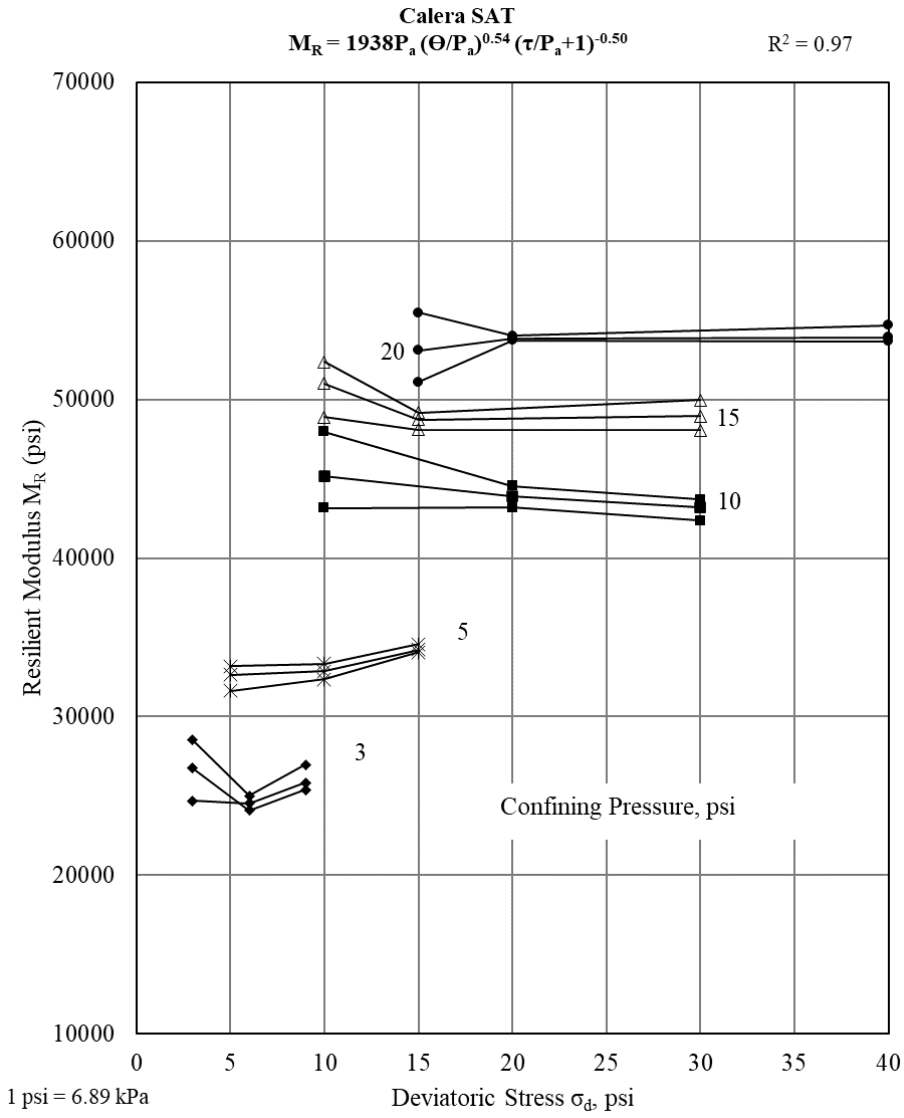

Figure A.1. 4. Detailed M_R test results at SAT for Calera limestone

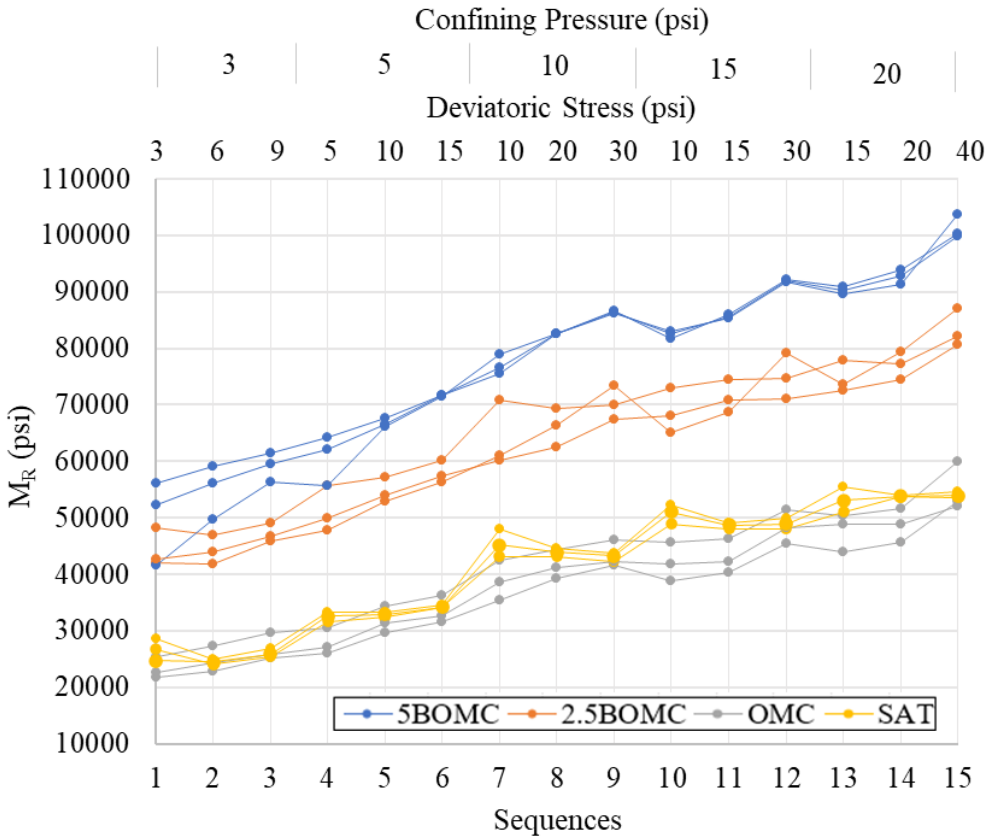

Figure A.1. 5. Final M_R test results for Calera limestone

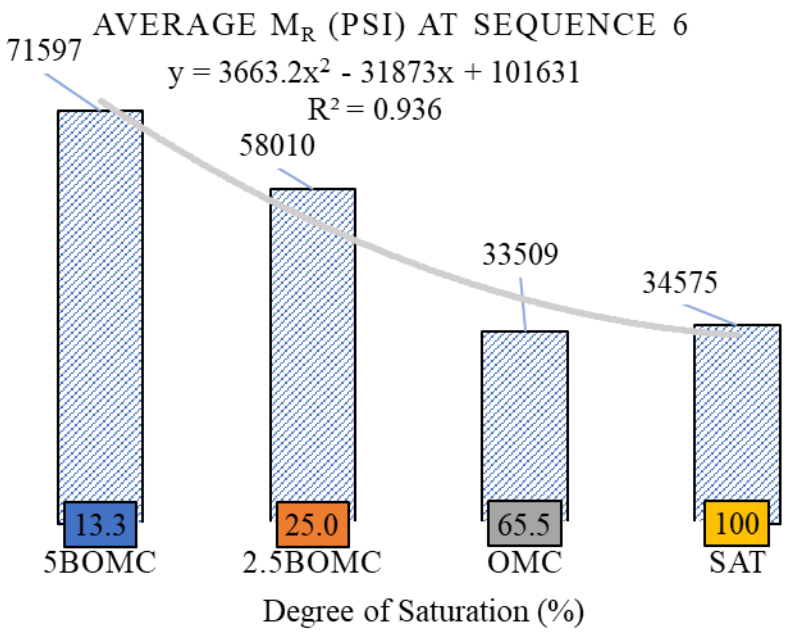

Figure A.1. 6. Final triaxial shear maximum strengths for Calera limestone

A.2 For Tuscumbia limestone

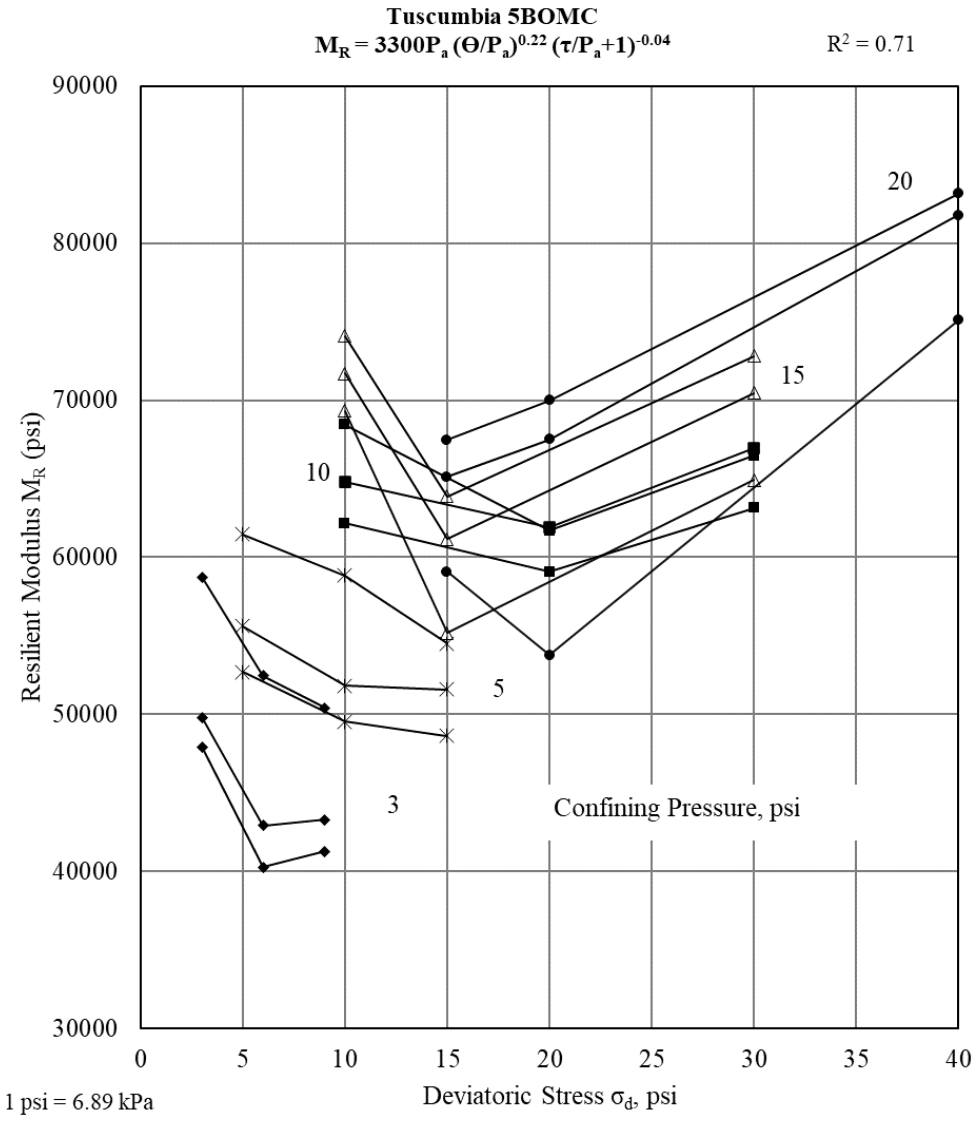

Figure A.2. 1. Detailed M_R test results at 5BOMC for Tuscumbia limestone

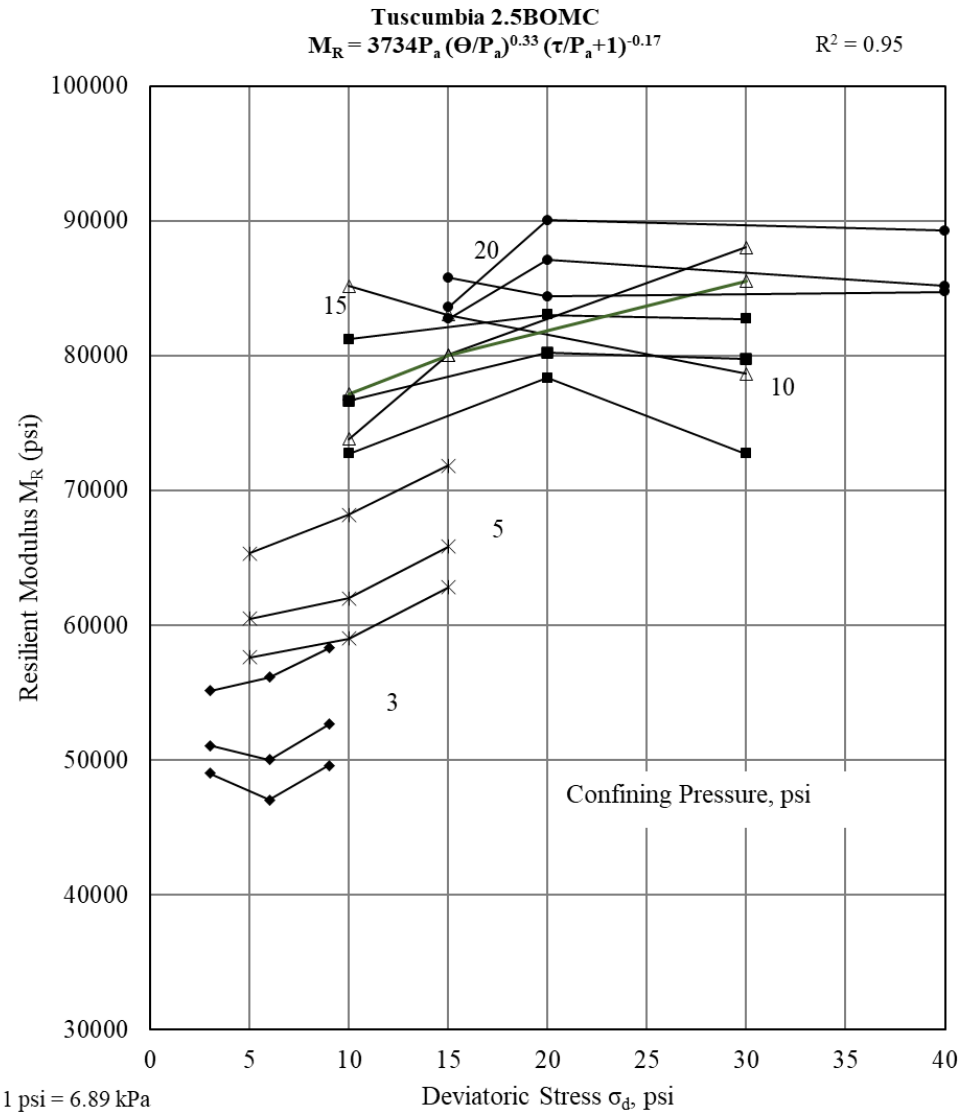

Figure A.2. 2. Detailed M_R test results at 2.5BOMC for Tuscumbia limestone

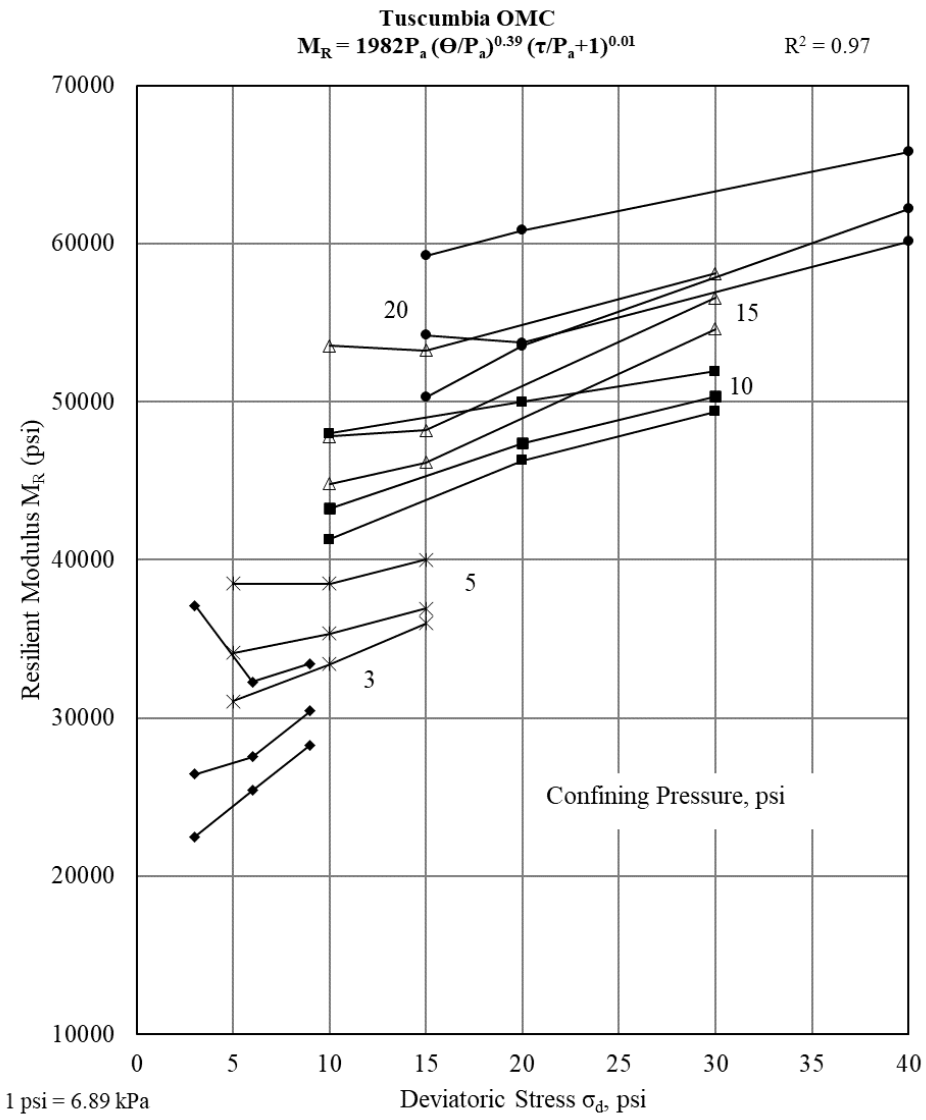

Figure A.2. 3. Detailed M_R test results at OMC for Tuscumbia limestone

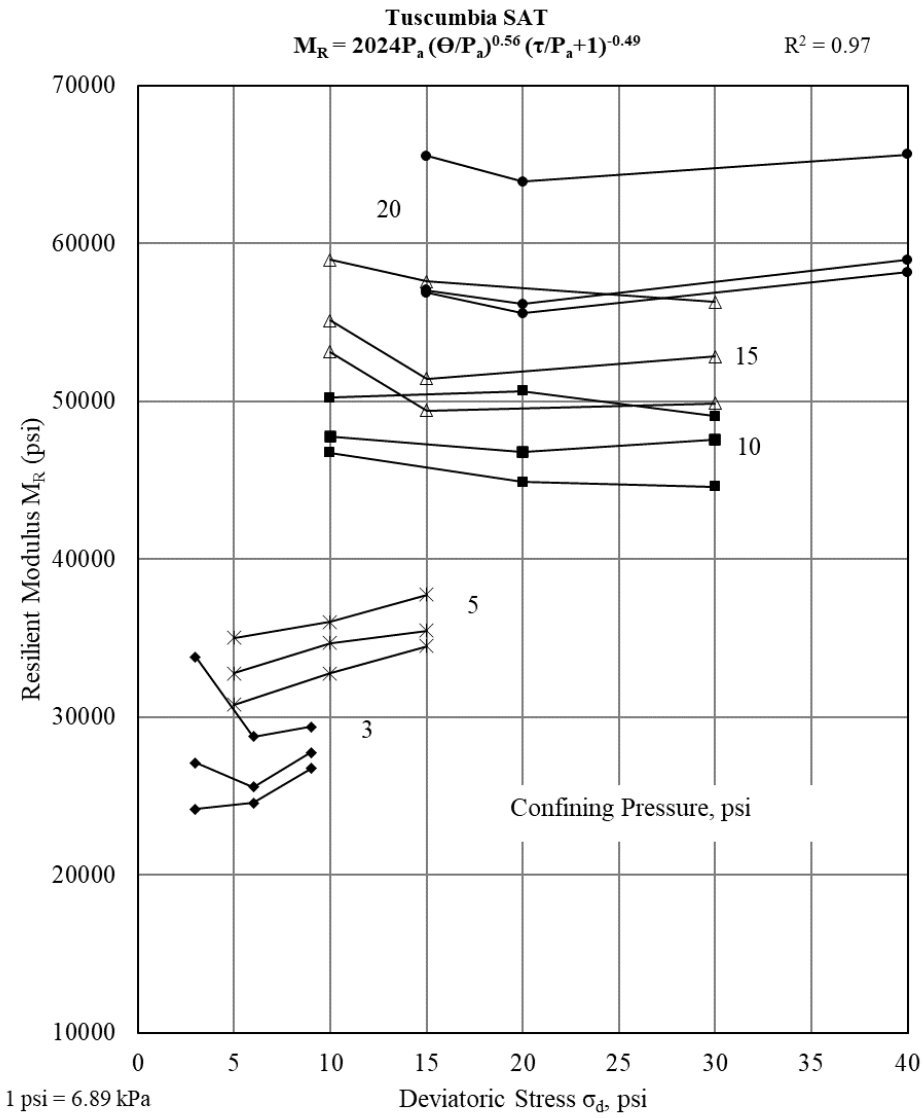

Figure A.2. 4. Detailed M_R test results at SAT for Tuscumbia limestone

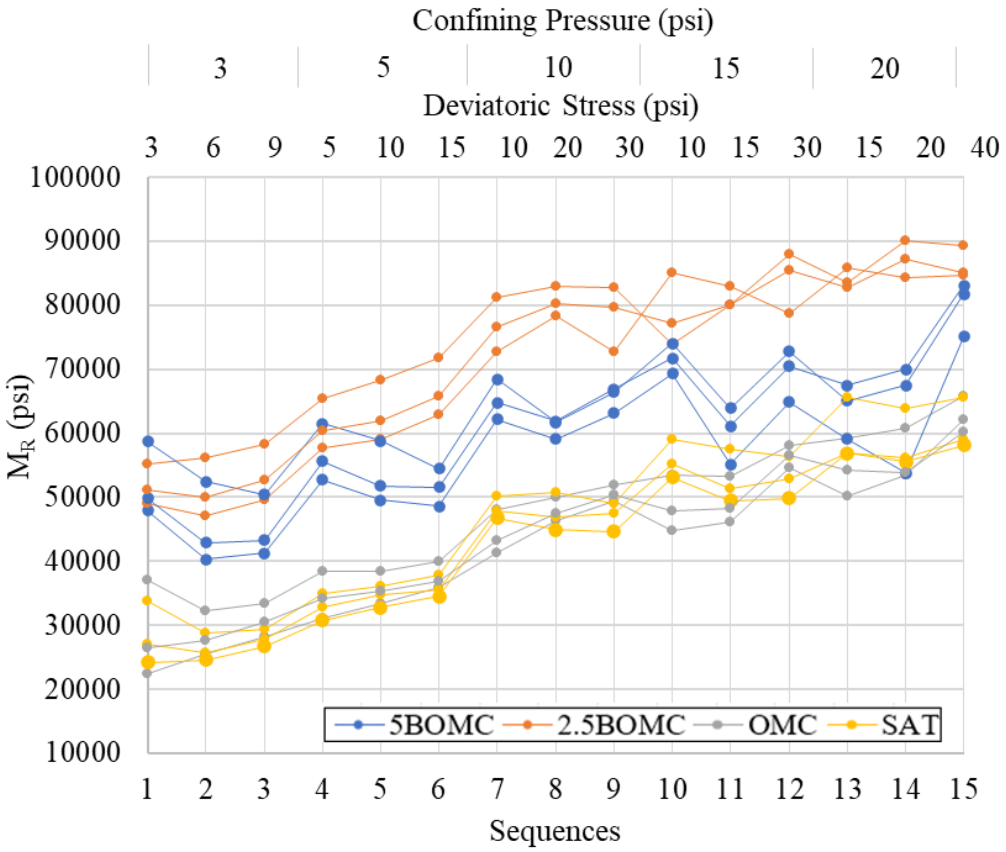

Figure A.2. 5. Final M_R test results for Tuscumbia limestone

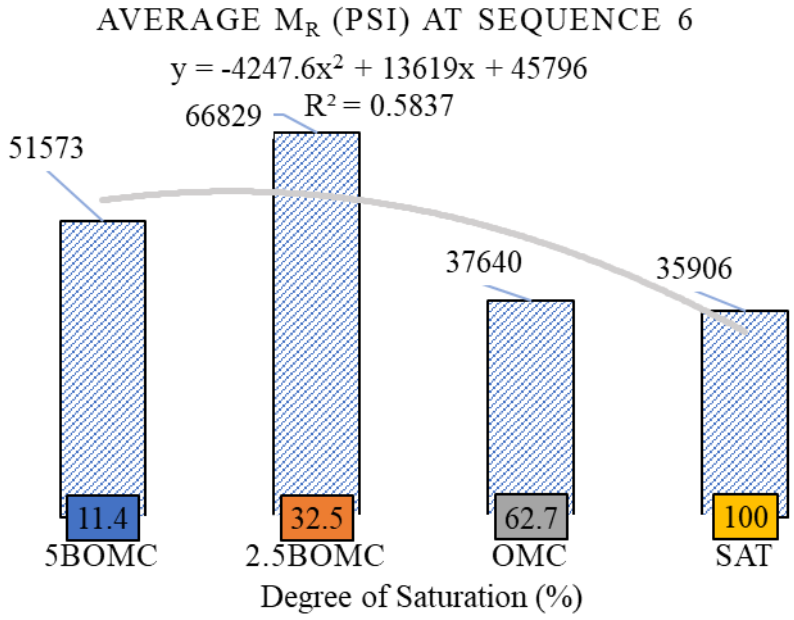

Figure A.2. 6. Final triaxial shear maximum strengths for Tuscumbia limestone

A.3 For Blue Water limestone

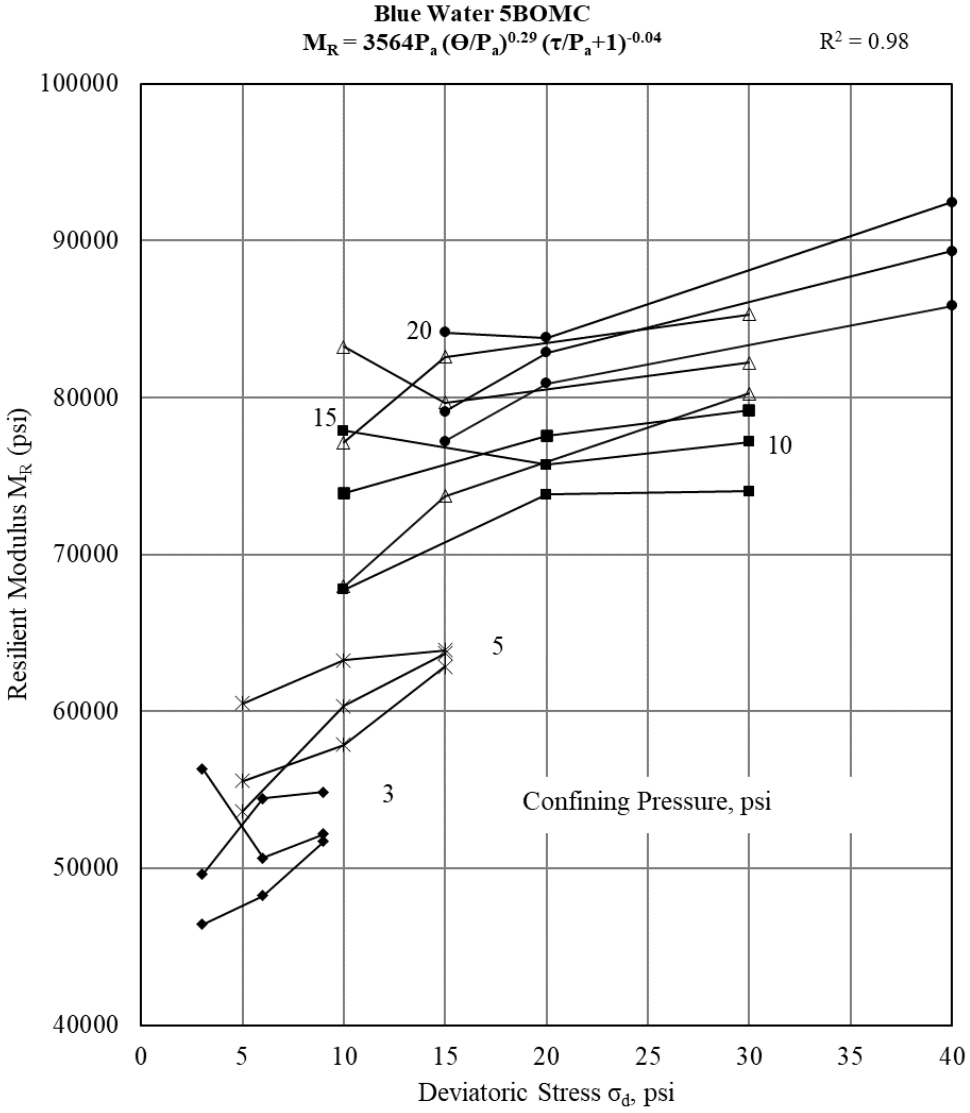

Figure A.3. 1. Detailed M_R test results at 5BOMC for Blue Water limestone

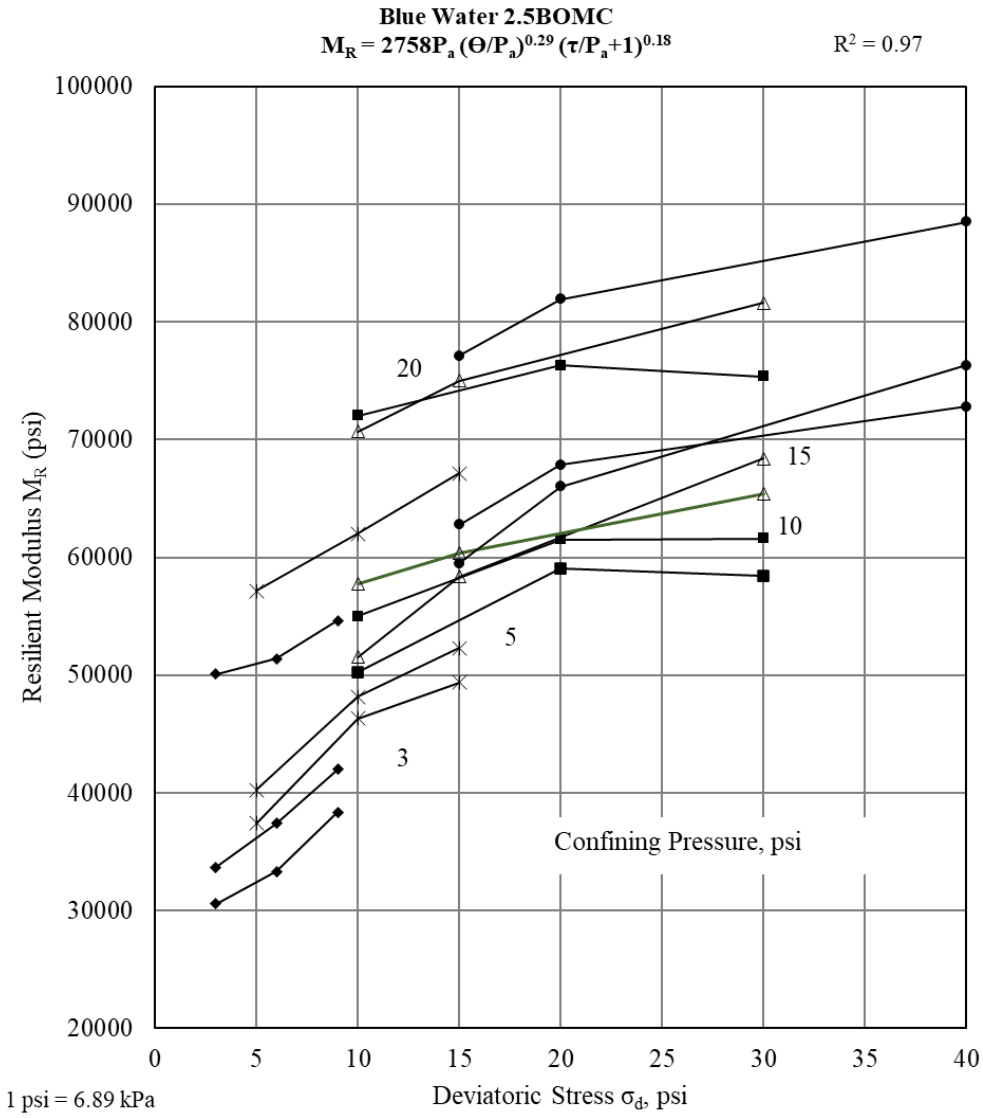

Figure A.3. 2. Detailed M_R test results at 2.5BOMC for Blue Water limestone

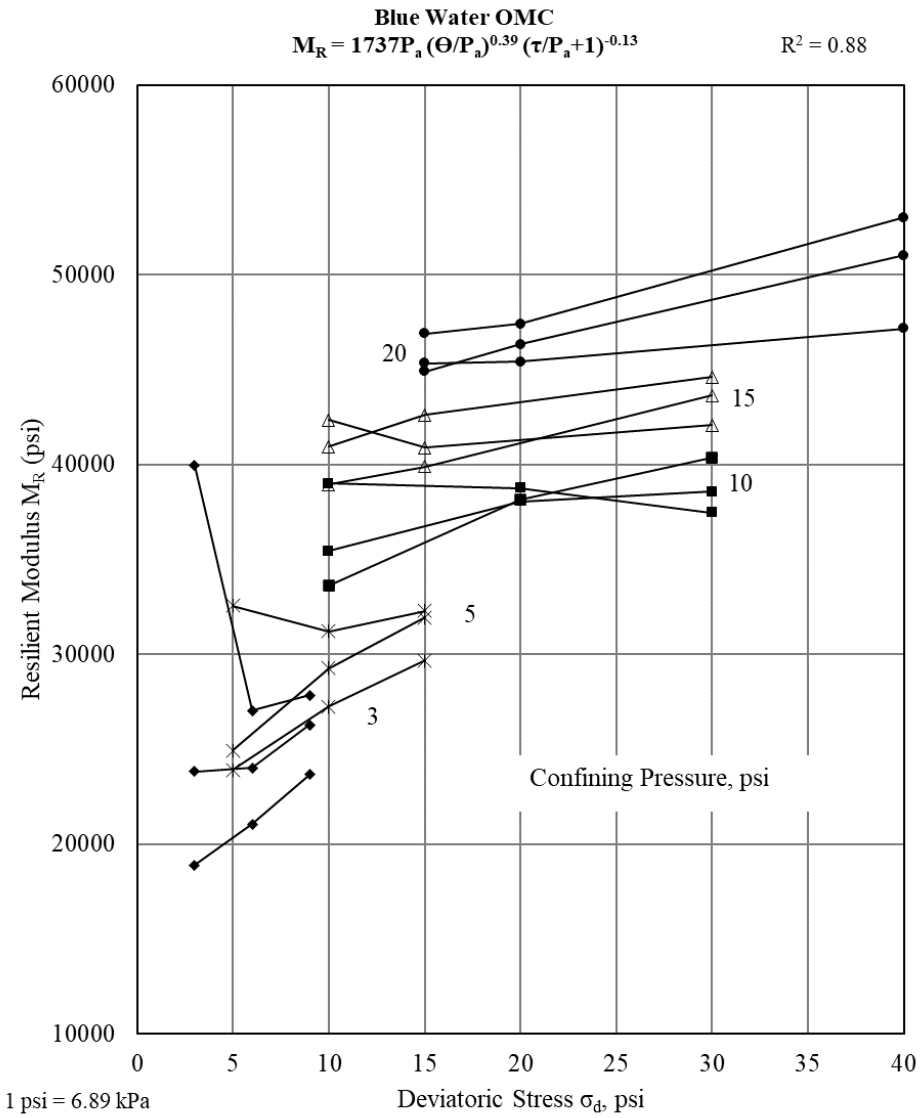

Figure A.3. 3. Detailed M_R test results at OMC for Blue Water limestone

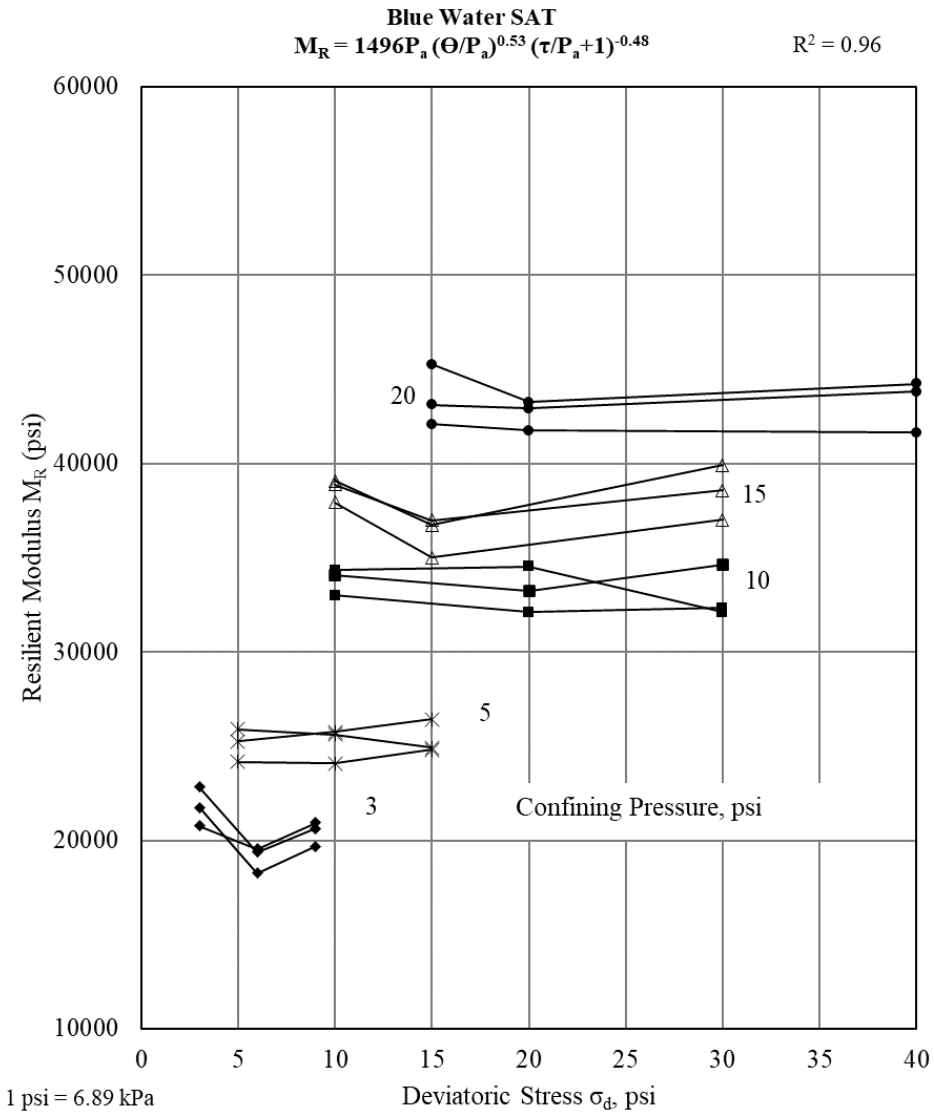

Figure A.3. 4. Detailed M_R test results at SAT for Blue Water limestone

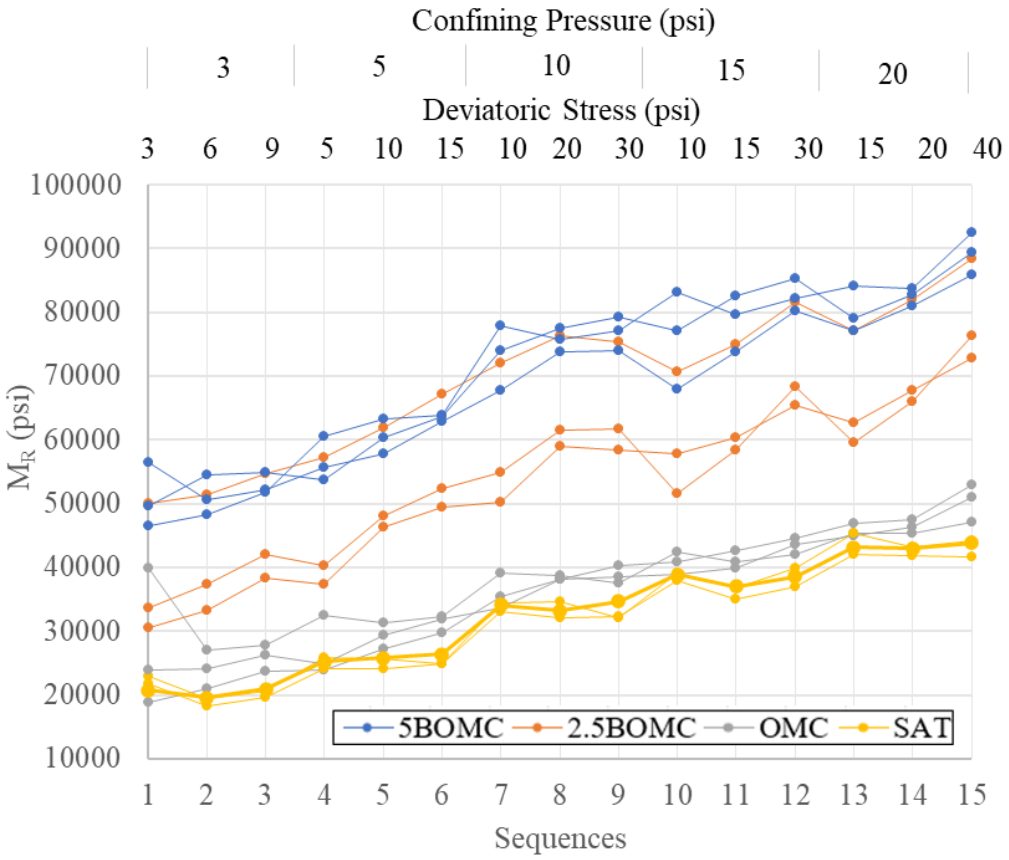

Figure A.3. 5. Final M_R test results for Blue Water limestone

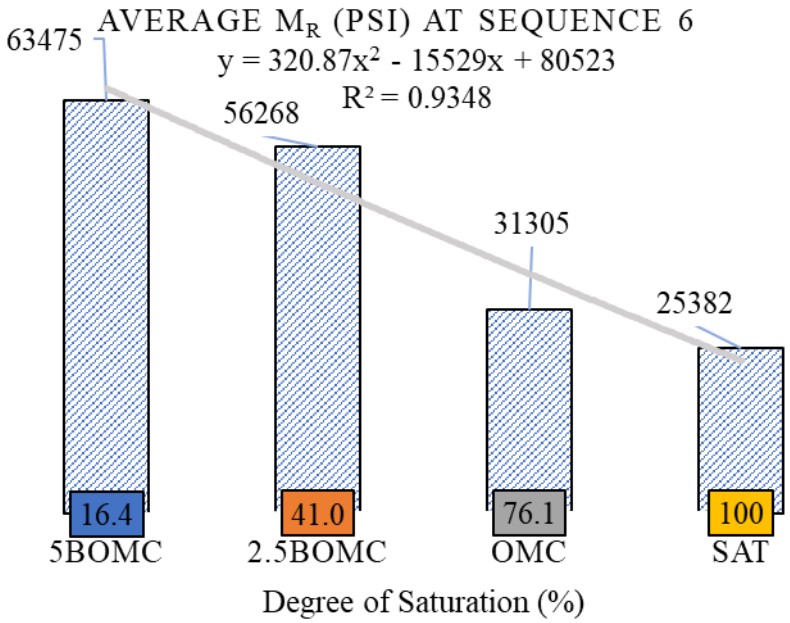

Figure A.3. 6. Final triaxial shear maximum strengths for Blue Water limestone

A.4 For Brooklyn limerock

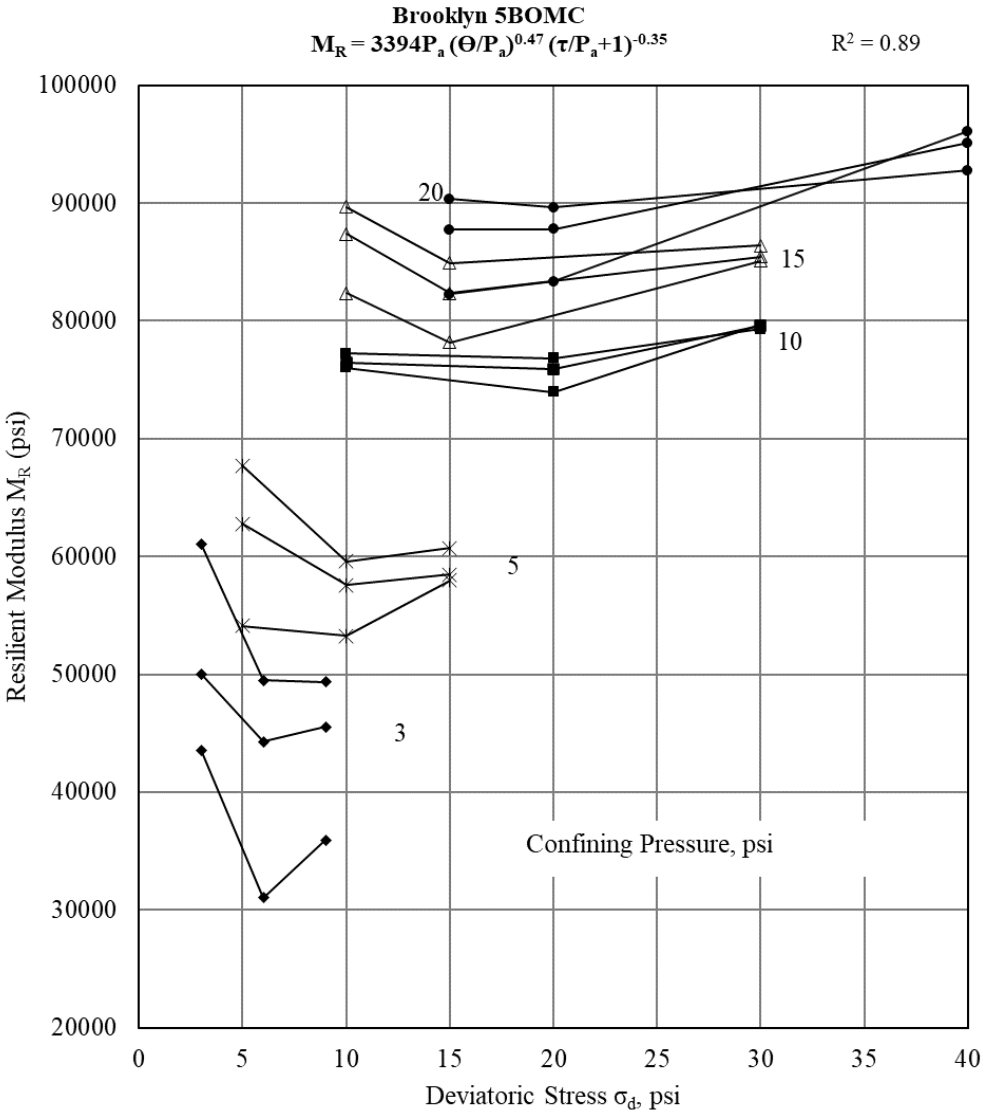

Figure A.4. 1. Detailed M_R test results at 5BOMC for Brooklyn limerock

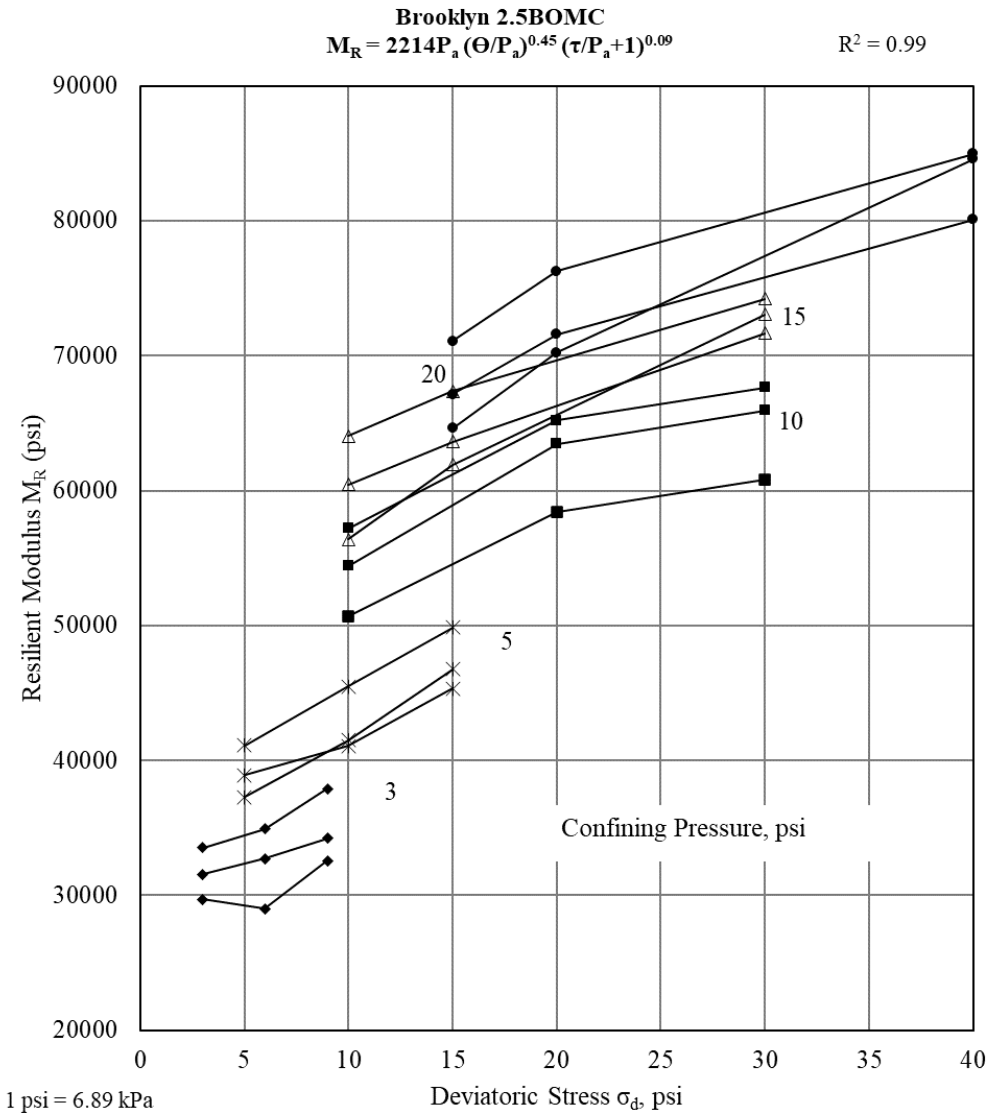

Figure A.4. 2. Detailed M_R test results at 2.5BOMC for Brooklyn limerock

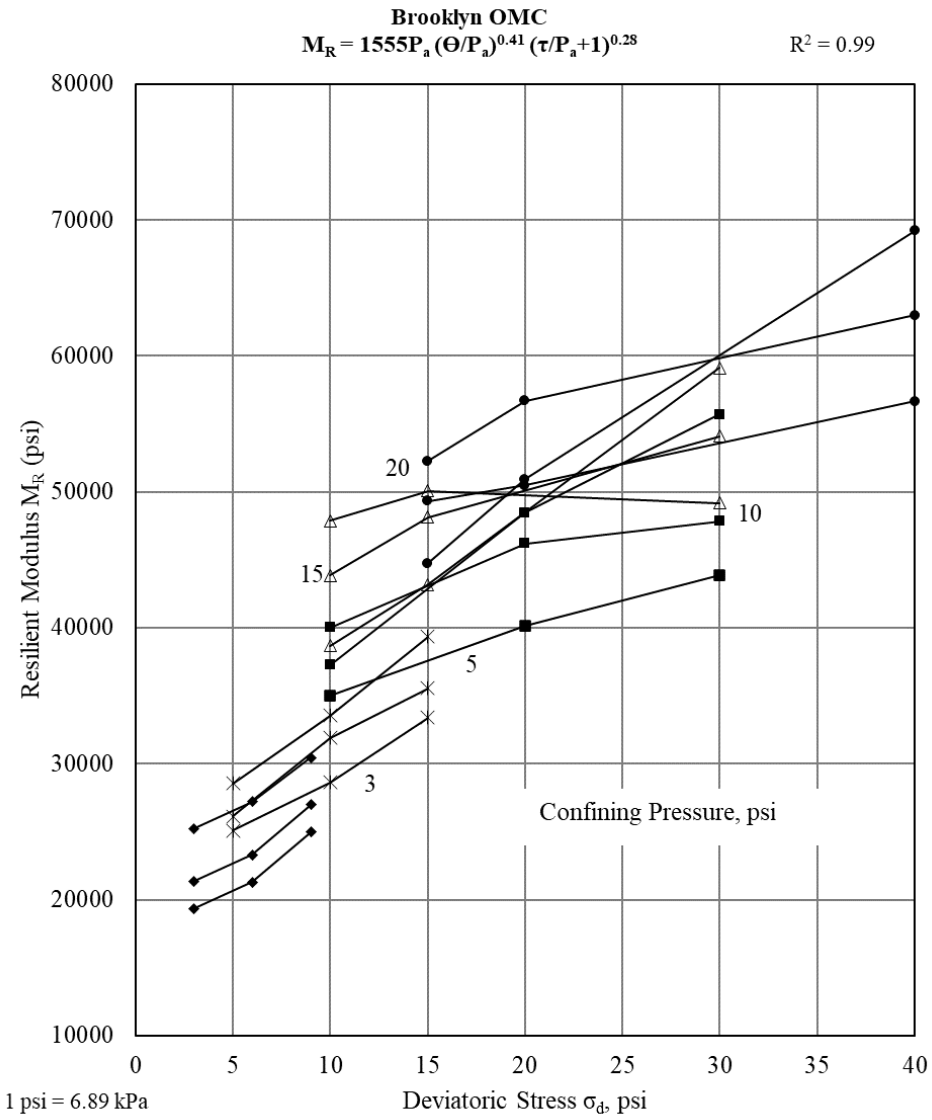

Figure A.4. 3. Detailed M_R test results at OMC for Brooklyn limerock

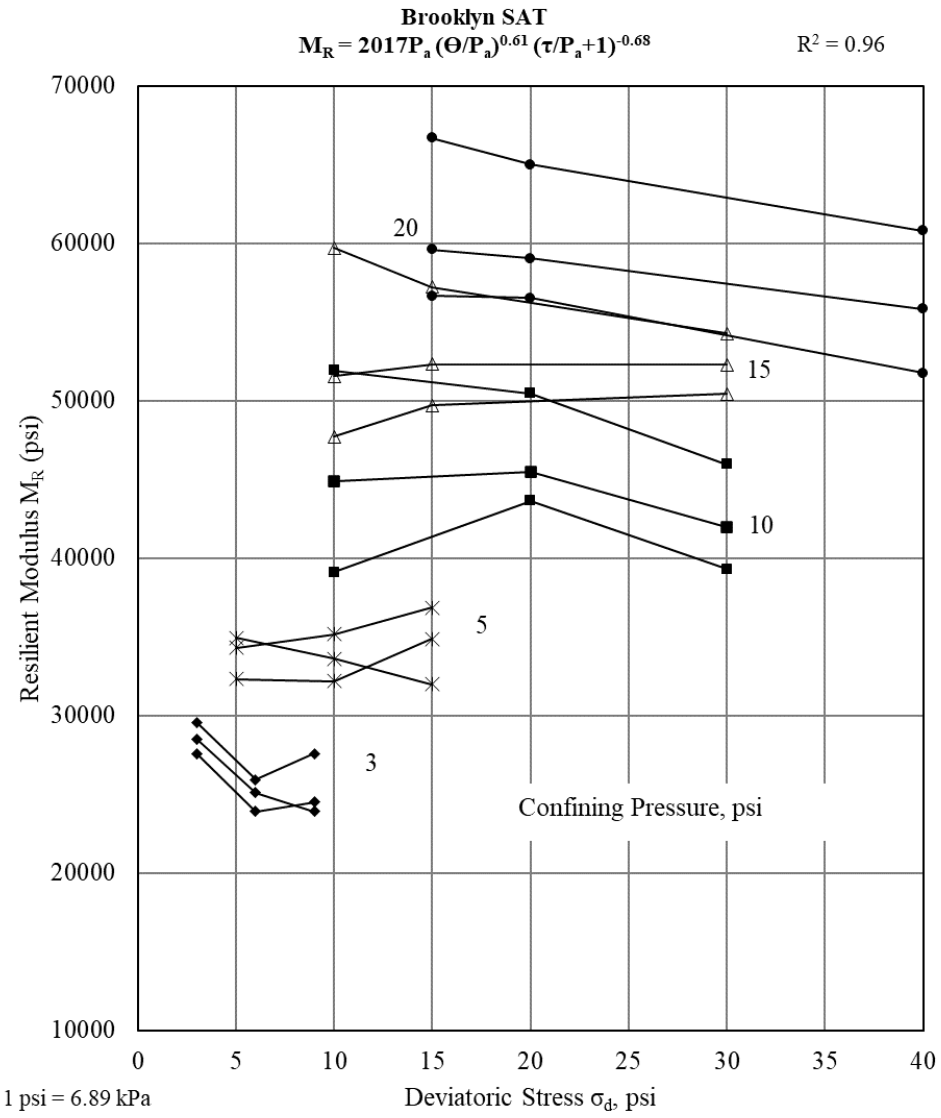

Figure A.4. 4. Detailed M_R test results at SAT for Brooklyn limerock

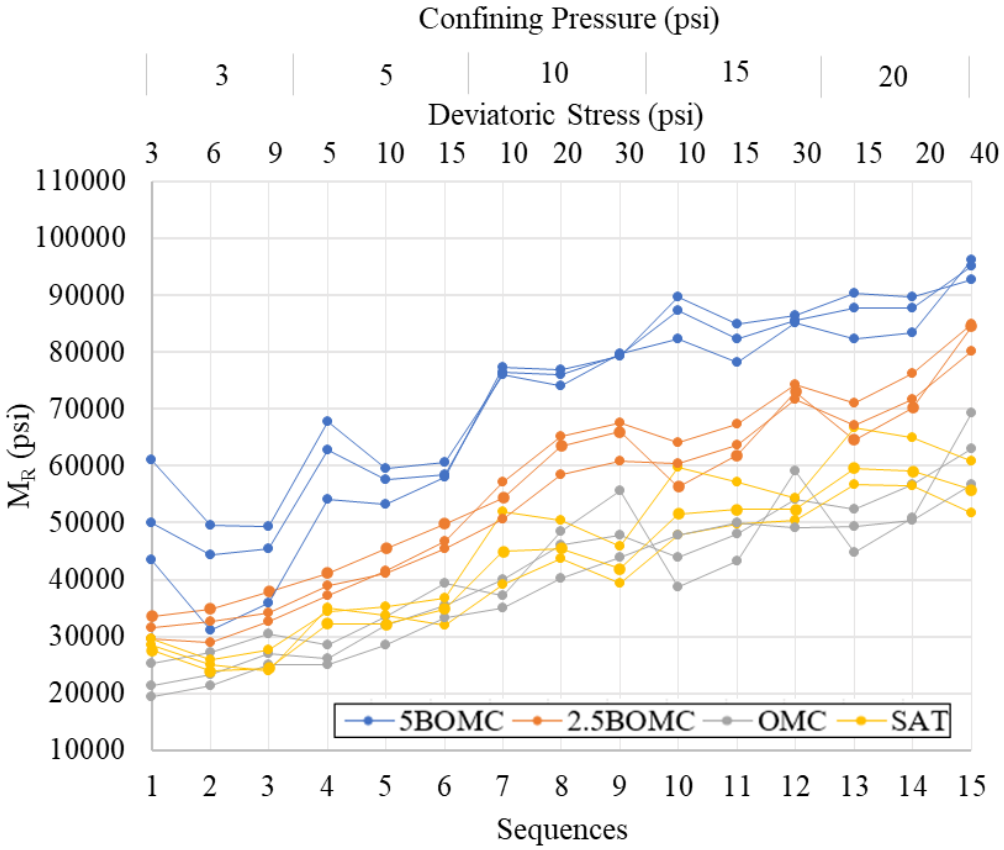

Figure A.4. 5. Final M_R test results for Brooklyn limerock

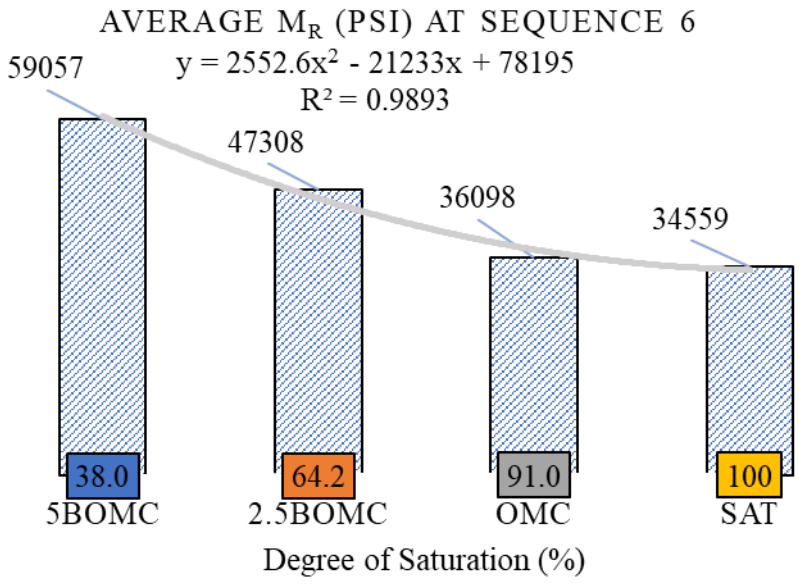

Figure A.4. 6. Final triaxial shear maximum strengths for Brooklyn limerock

A.5 For Calica limerock

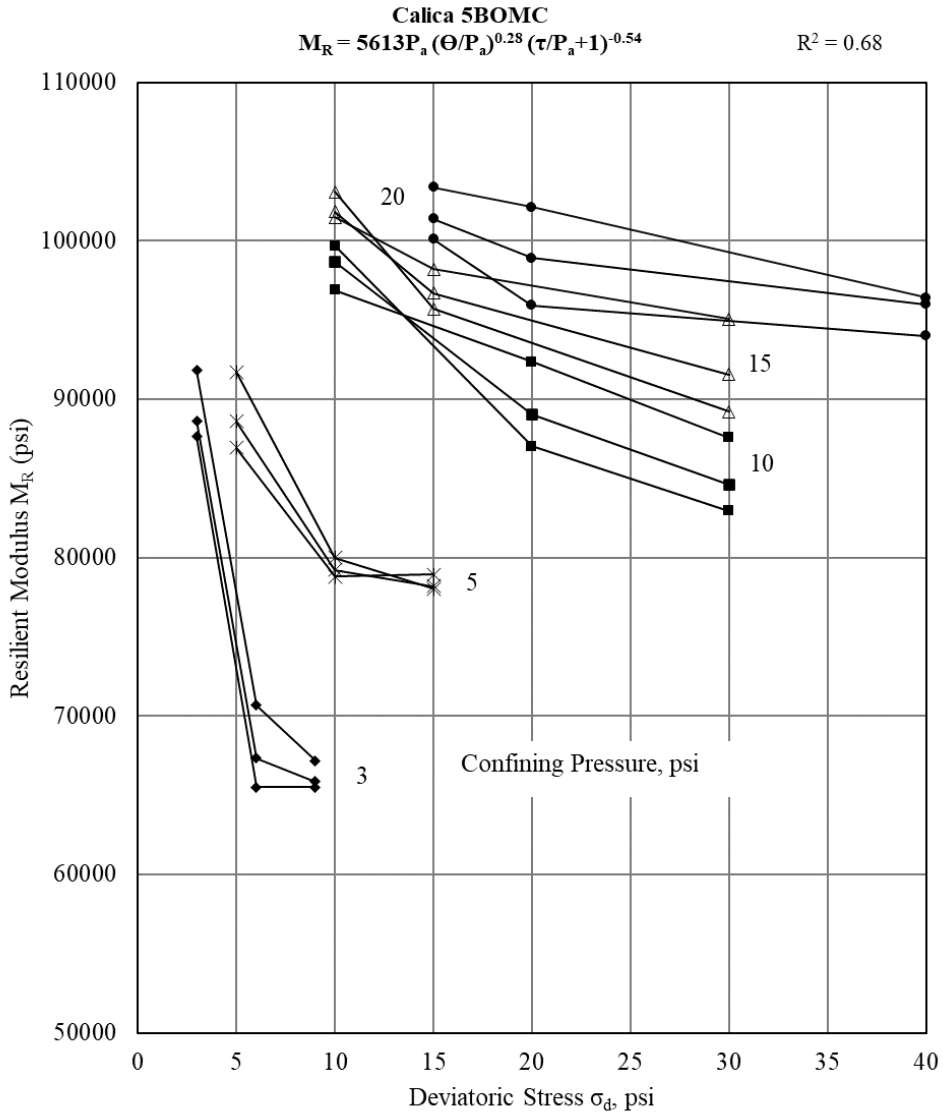

Figure A.5. 1. Detailed M_R test results at 5BOMC for Calica limerock

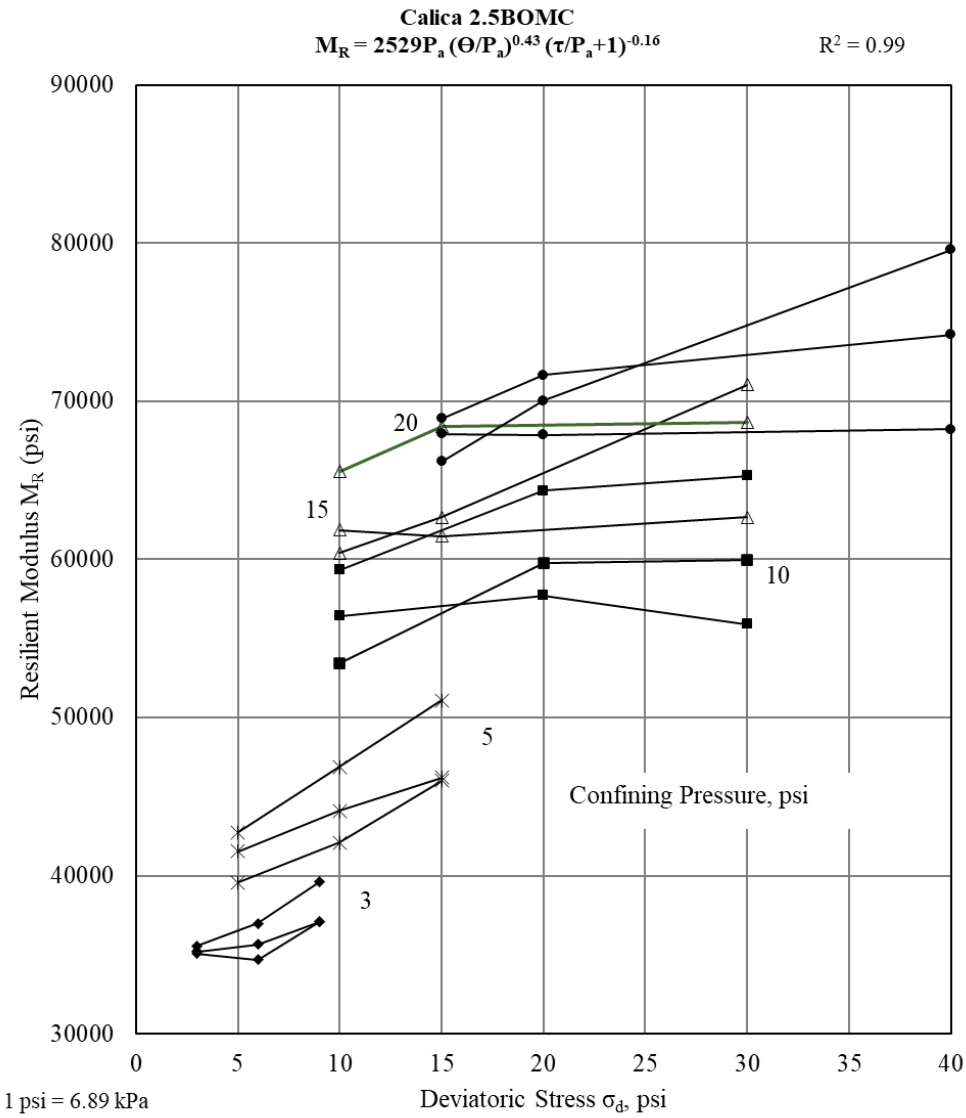

Figure A.5. 2. Detailed M_R test results at 2.5BOMC for Calica limerock

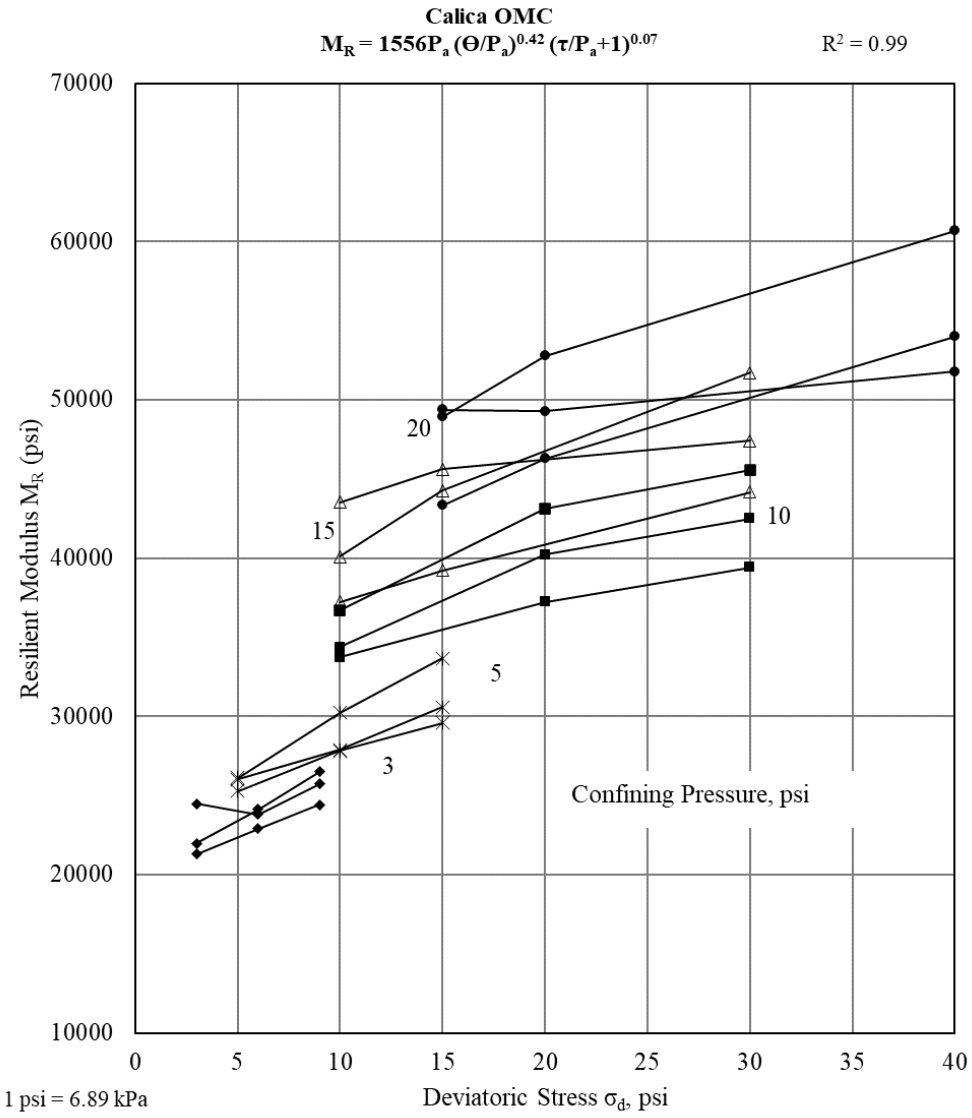

Figure A.5. 3. Detailed M_R test results at OMC for Calica limerock

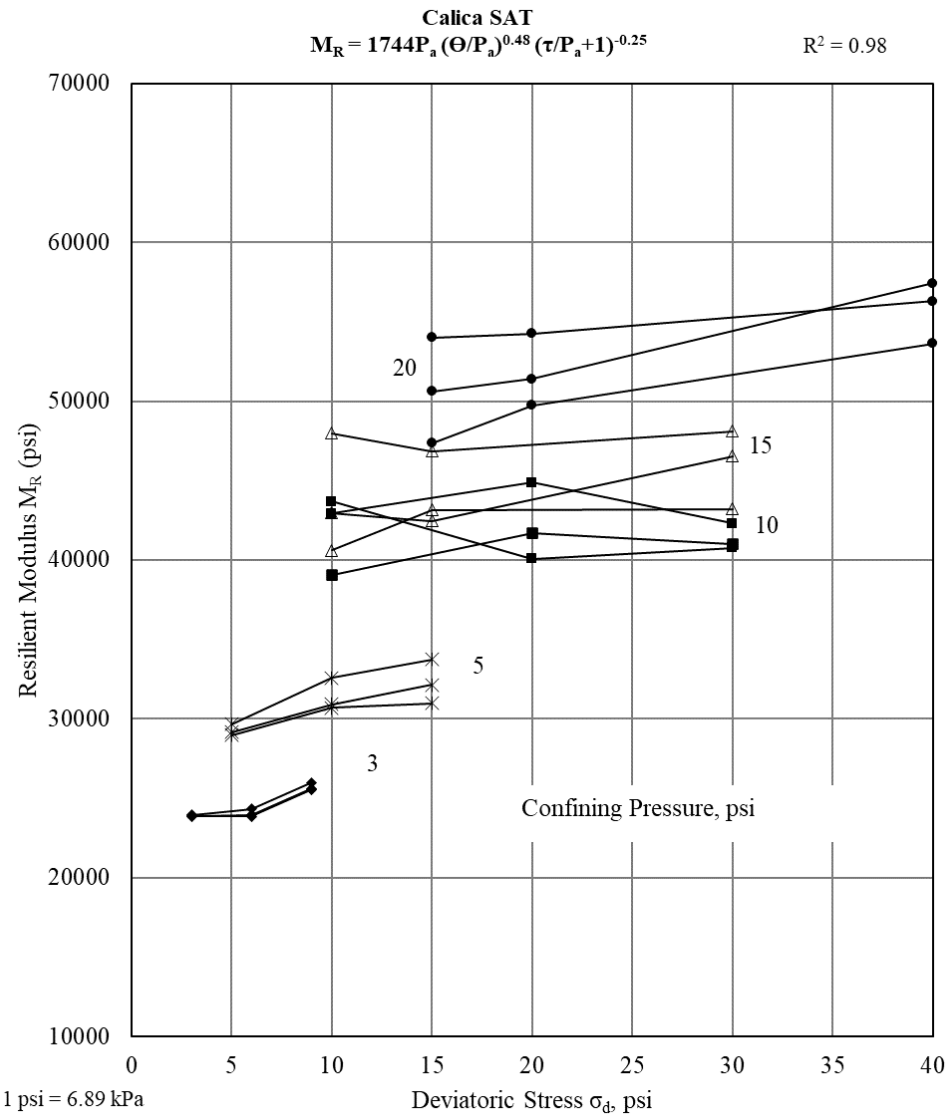

Figure A.5. 4. Detailed M_R test results at SAT for Calica limerock

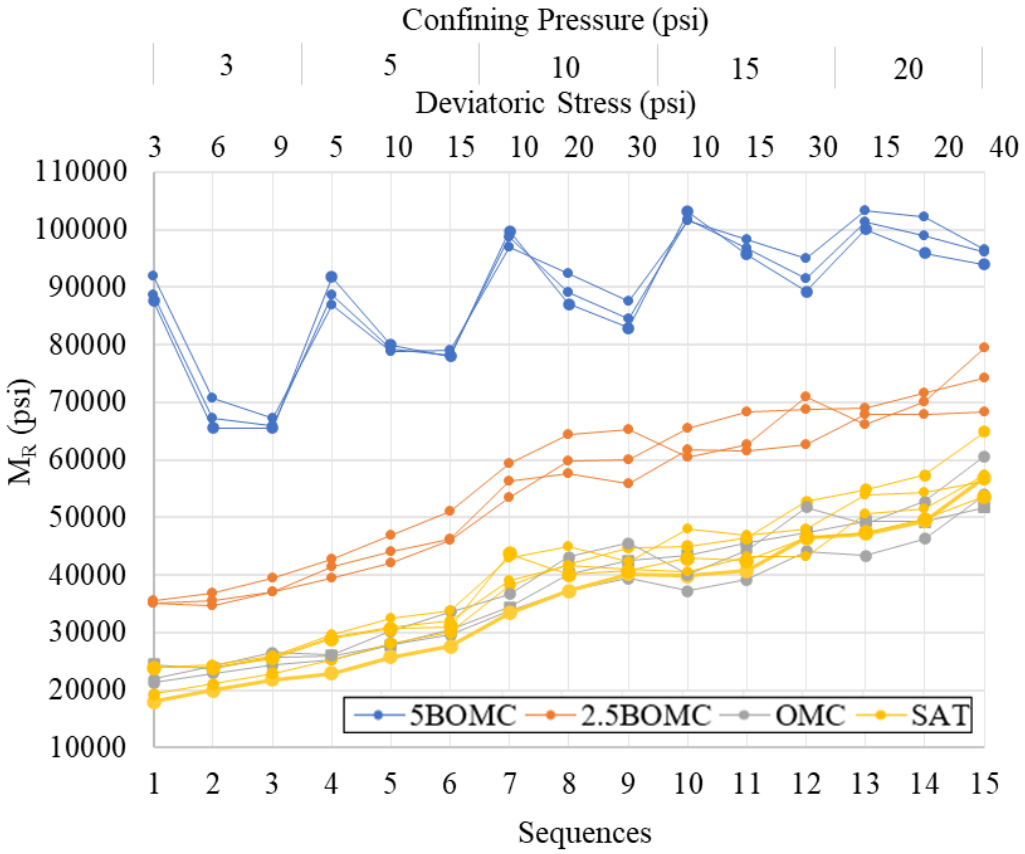

Figure A.5. 5. Final M_R test results for Calica limerock

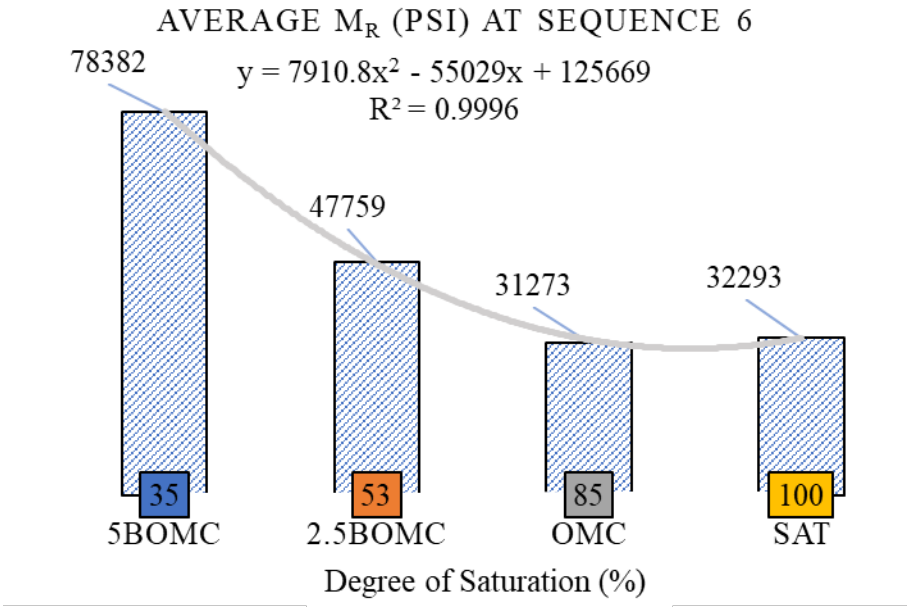

Figure A.5. 6. Final triaxial shear maximum strengths for Calica limerock

A.6 For JACO limerock

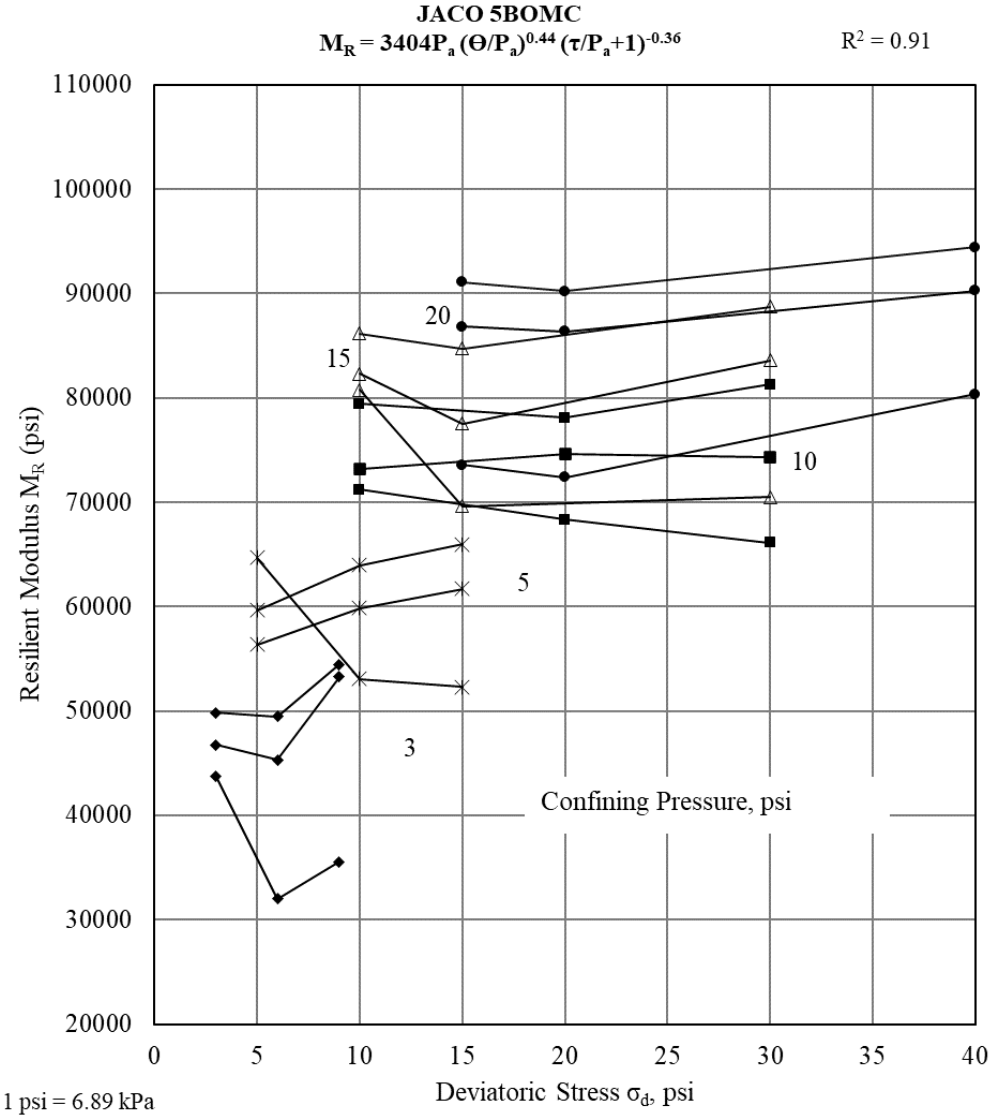

Figure A.6. 1. Detailed M_R test results at 5BOMC for JACO limerock

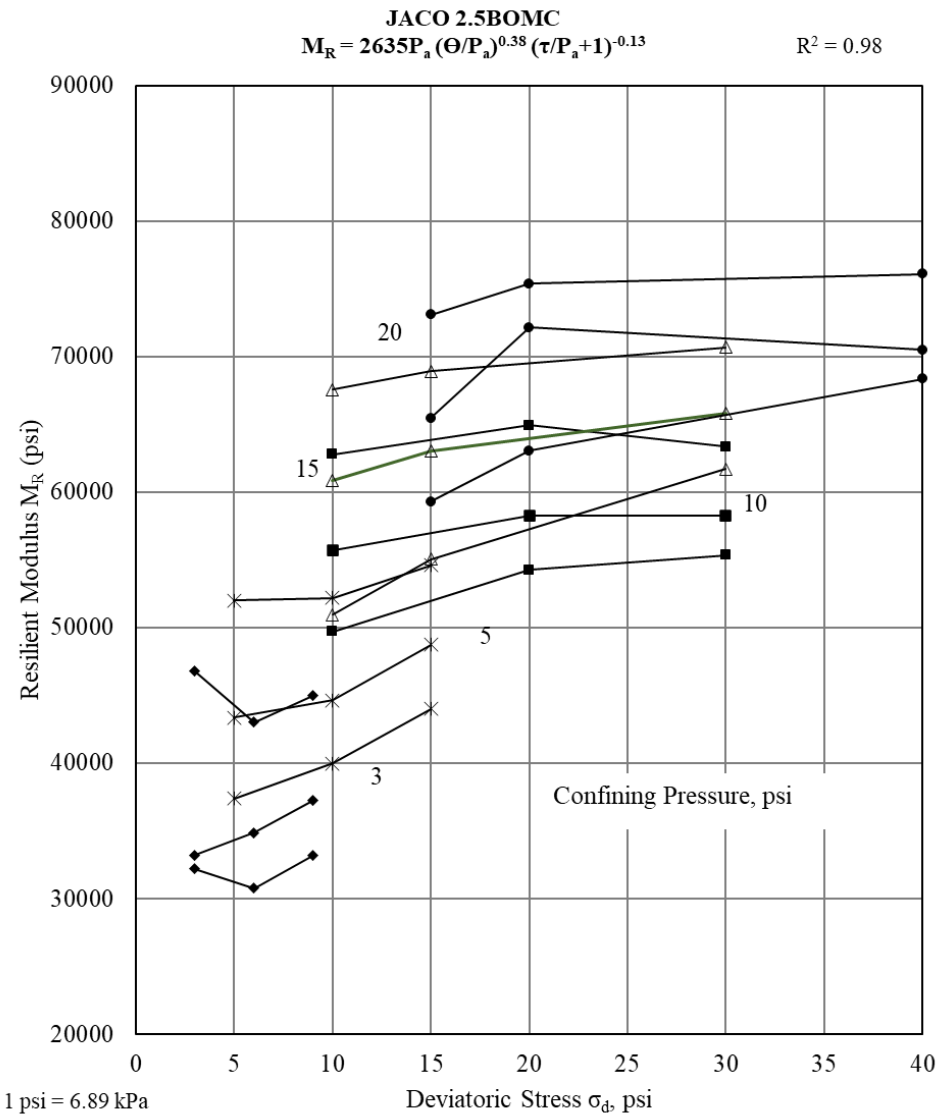

Figure A.6. 2. Detailed M_R test results at 2.5BOMC for JACO limerock

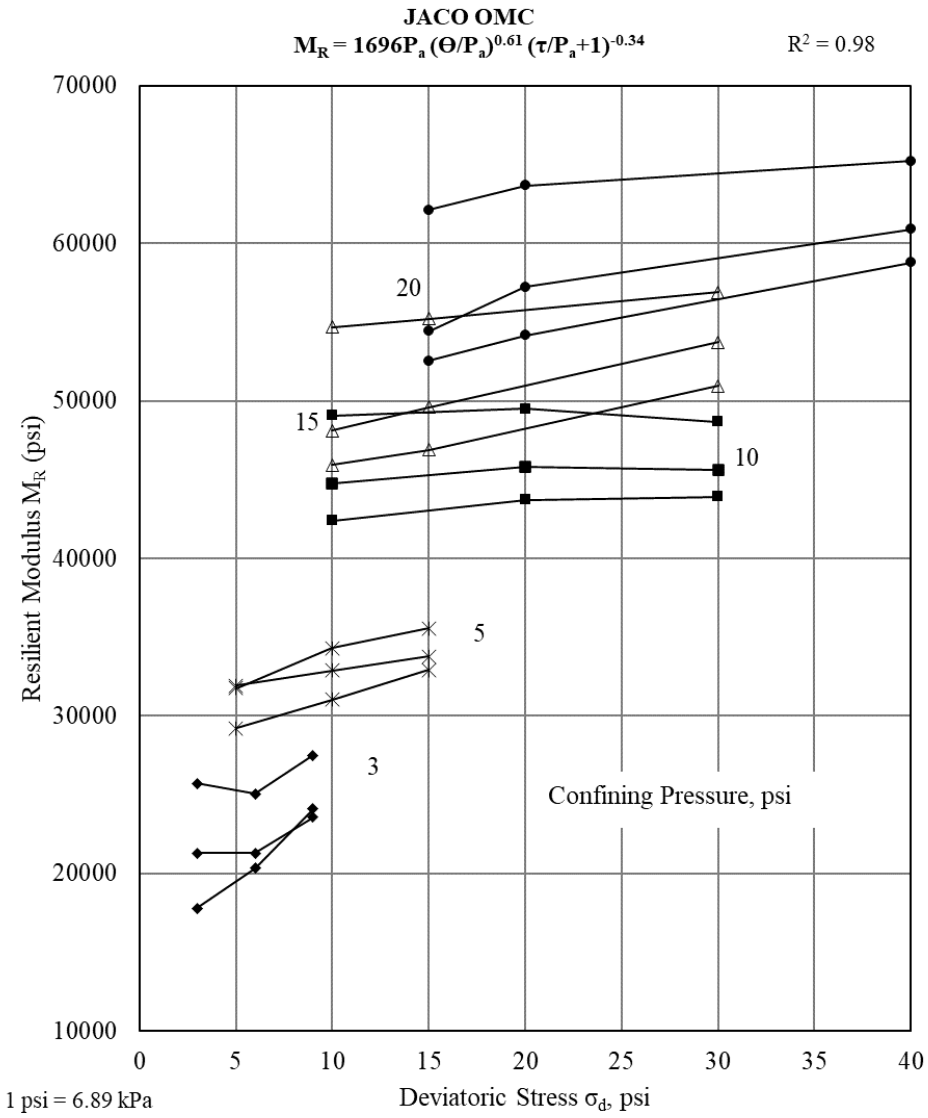

Figure A.6. 3. Detailed M_R test results at OMC for JACO limerock

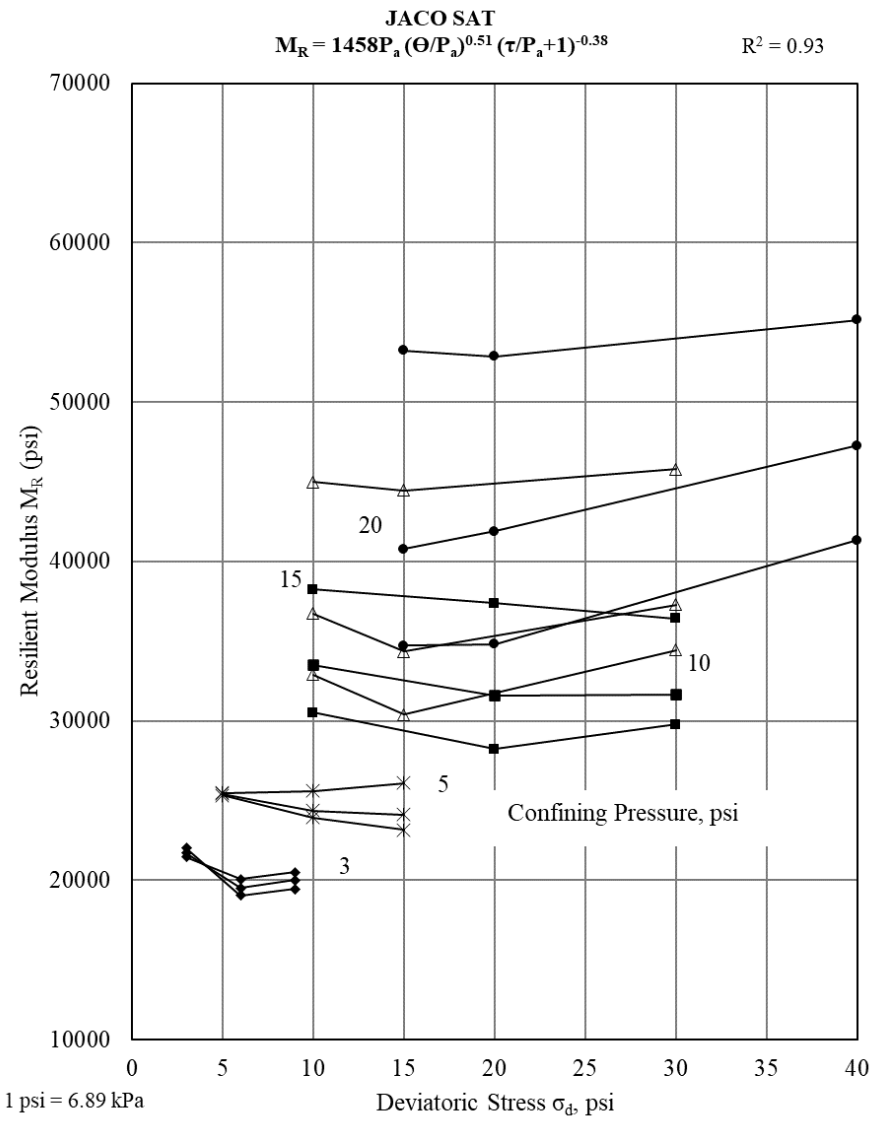

Figure A.6. 4. Detailed M_R test results at SAT for JACO limerock

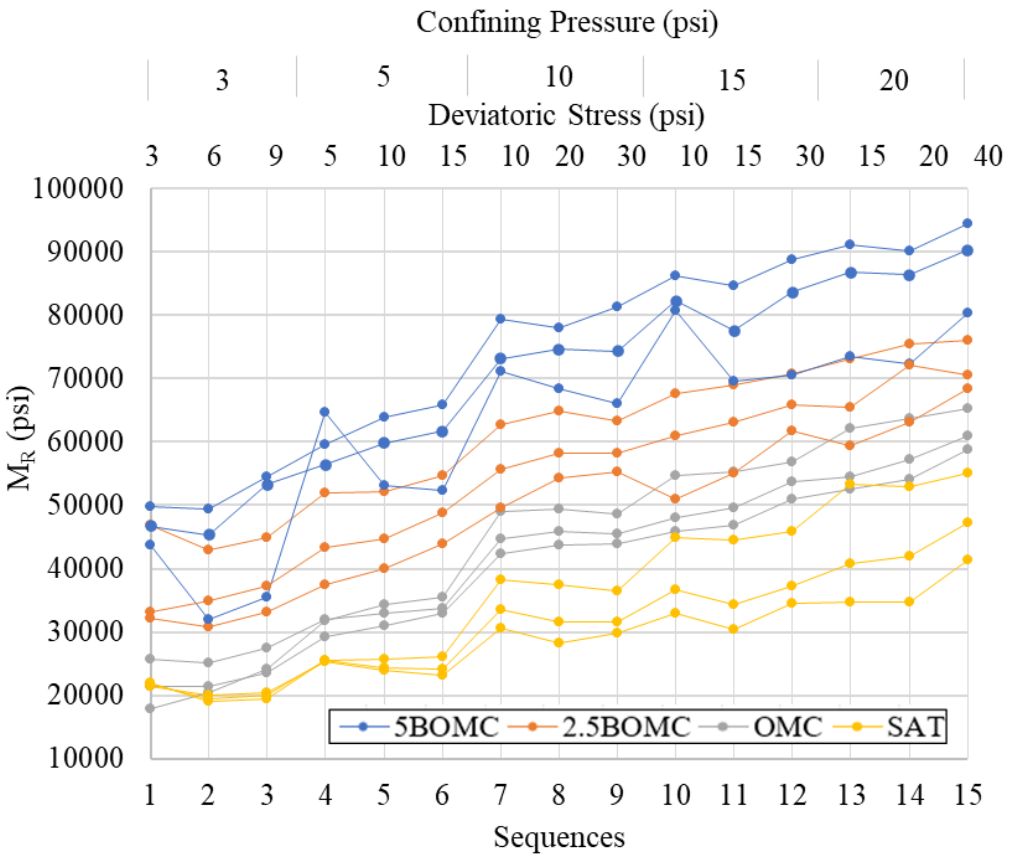

Figure A.6. 5. Final M_R test results for JACO limerock

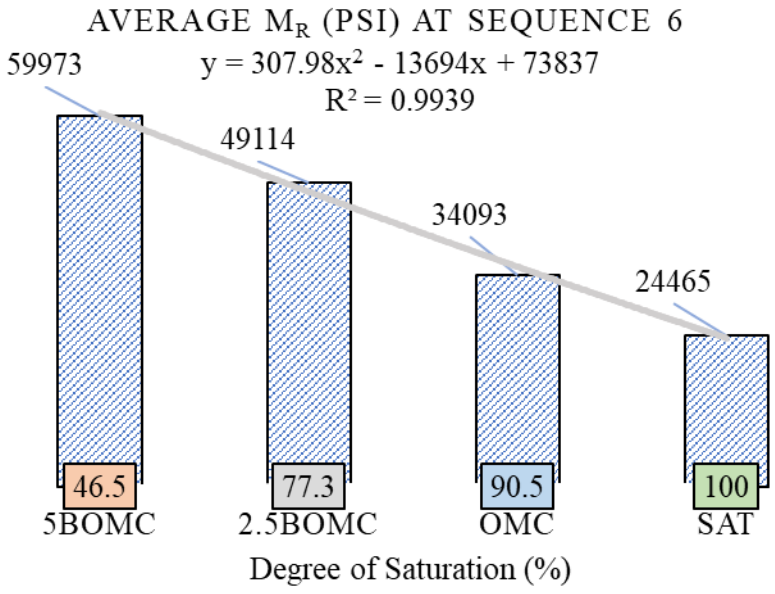

Figure A.6. 6. Final triaxial shear maximum strengths for JACO limerock

A.7 For North Florida limerock

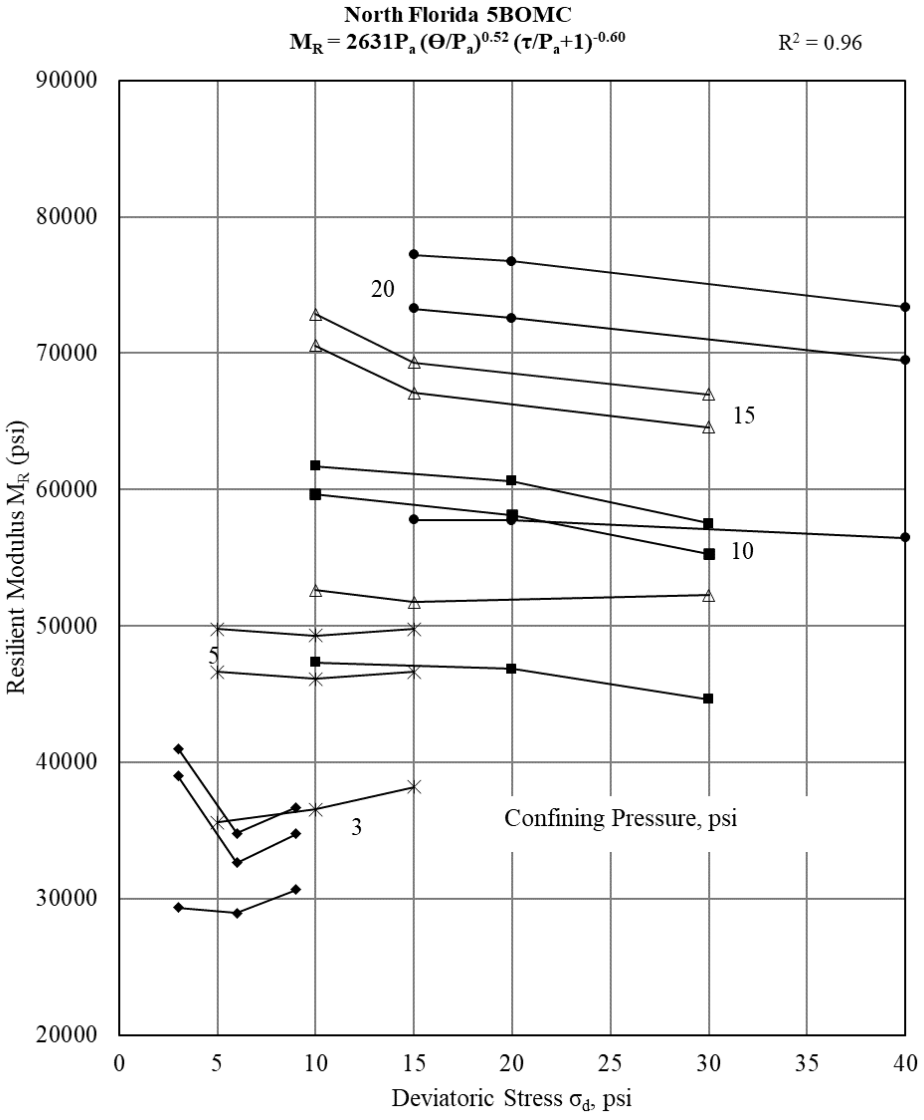

Figure A.7. 1. Detailed M_R test results at 5BOMC for North Florida limerock

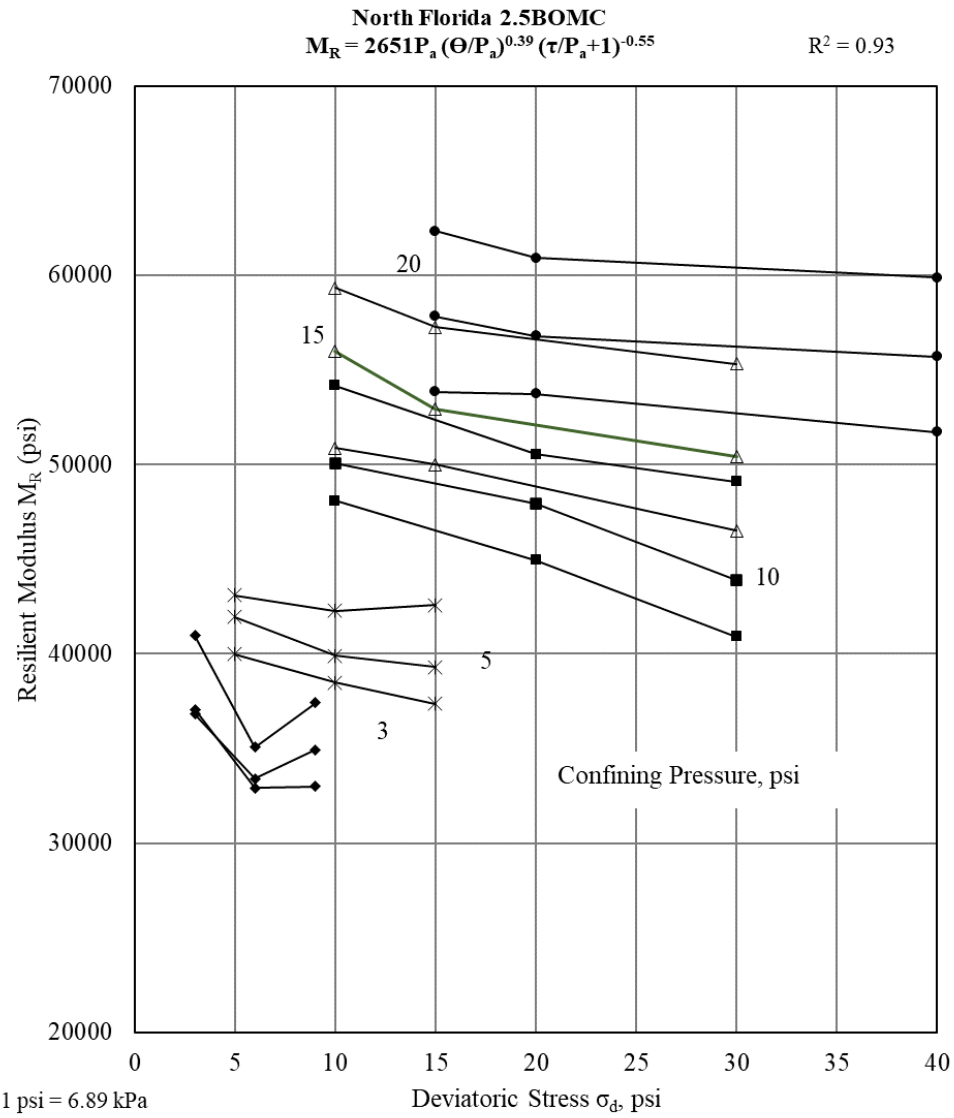

Figure A.7. 2. Detailed M_R test results at 2.5BOMC for North Florida limerock

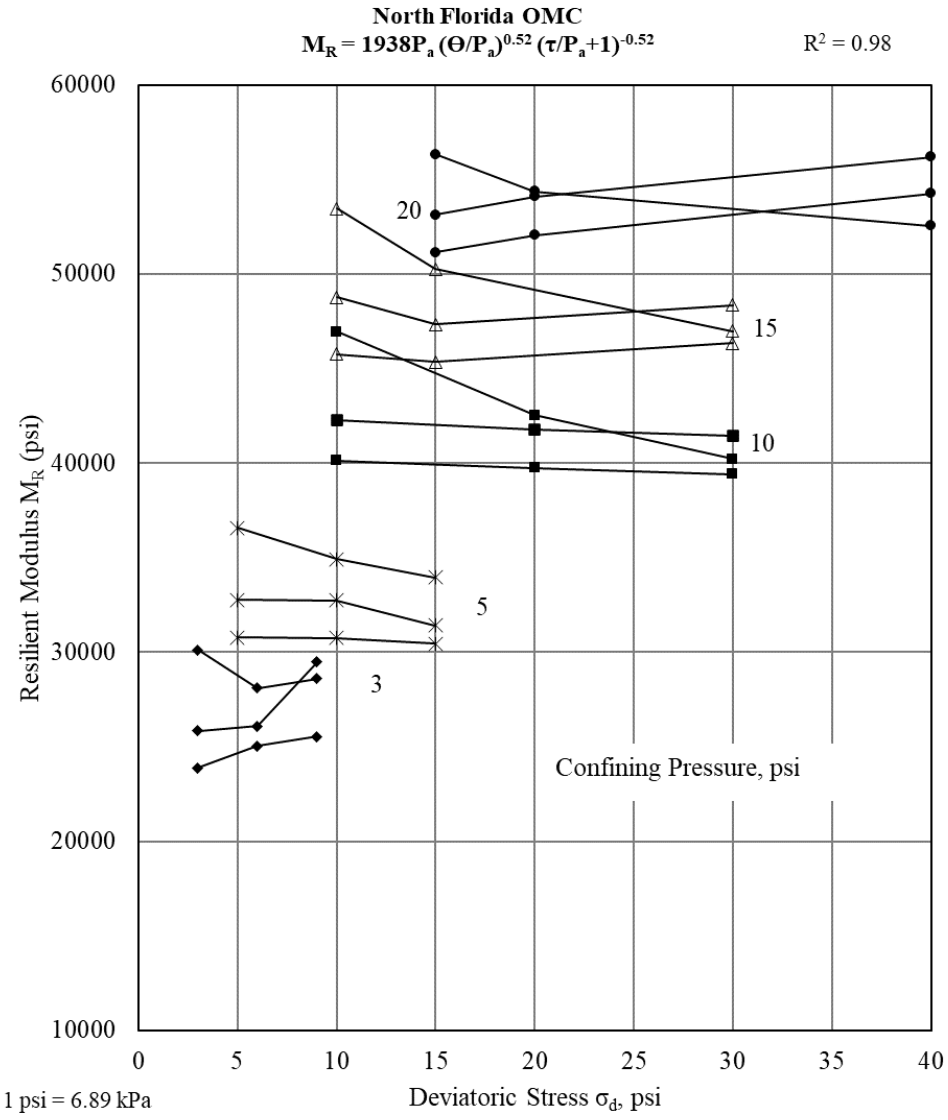

Figure A.7. 3. Detailed M_R test results at OMC for North Florida limerock

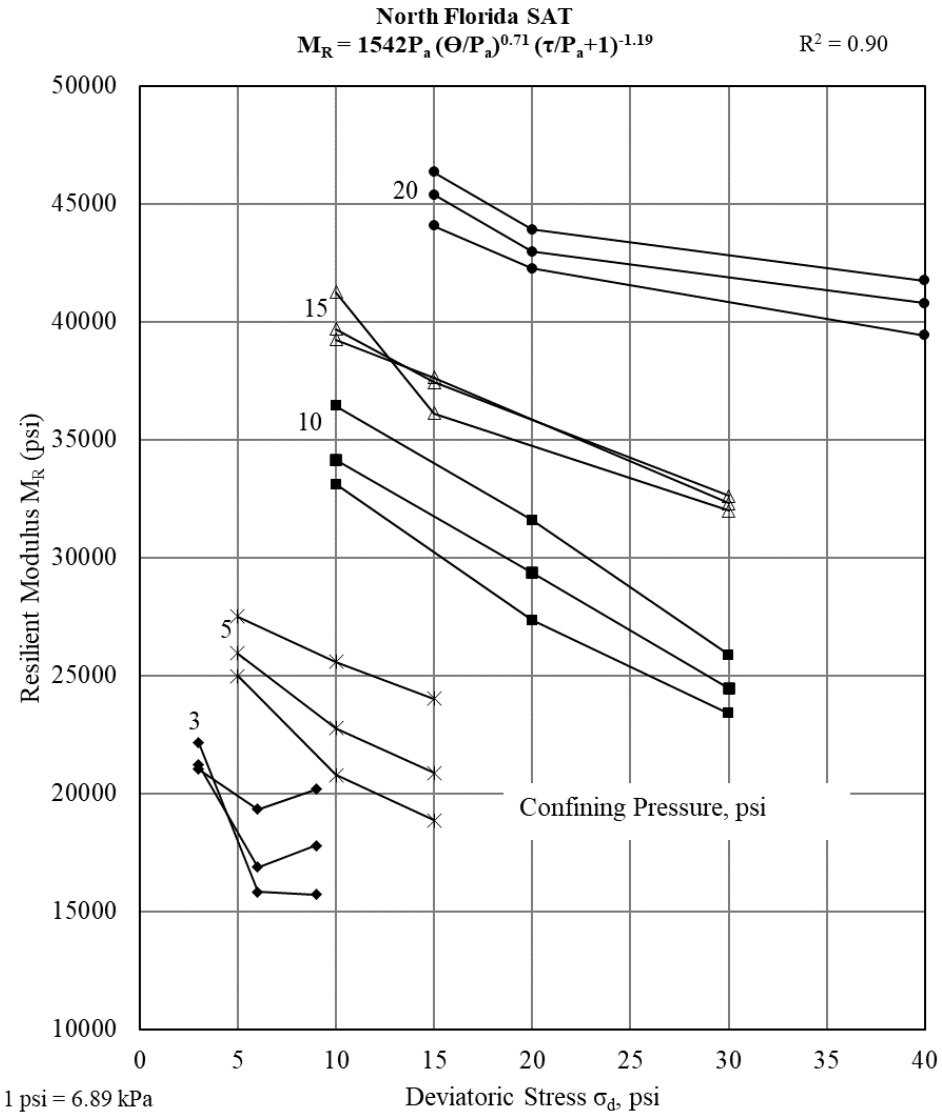

Figure A.7. 4. Detailed M_R test results at SAT for North Florida limerock

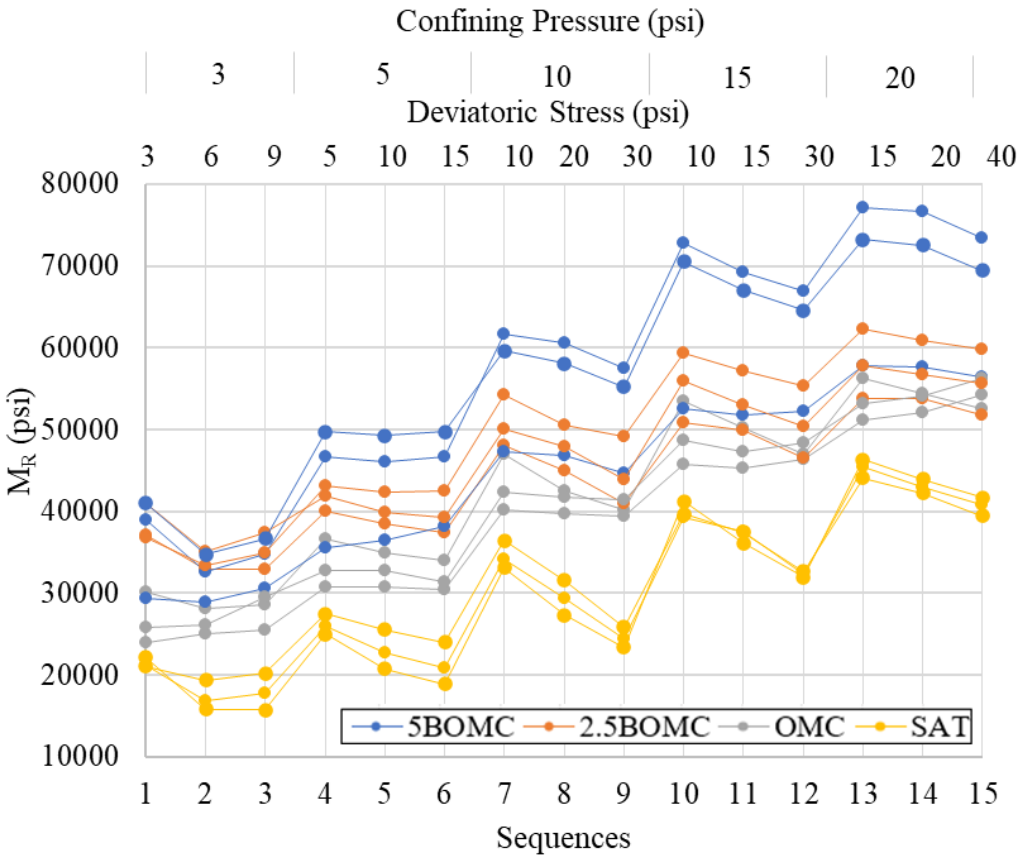

Figure A.7. 5. Final M_R test results for North Florida limerock

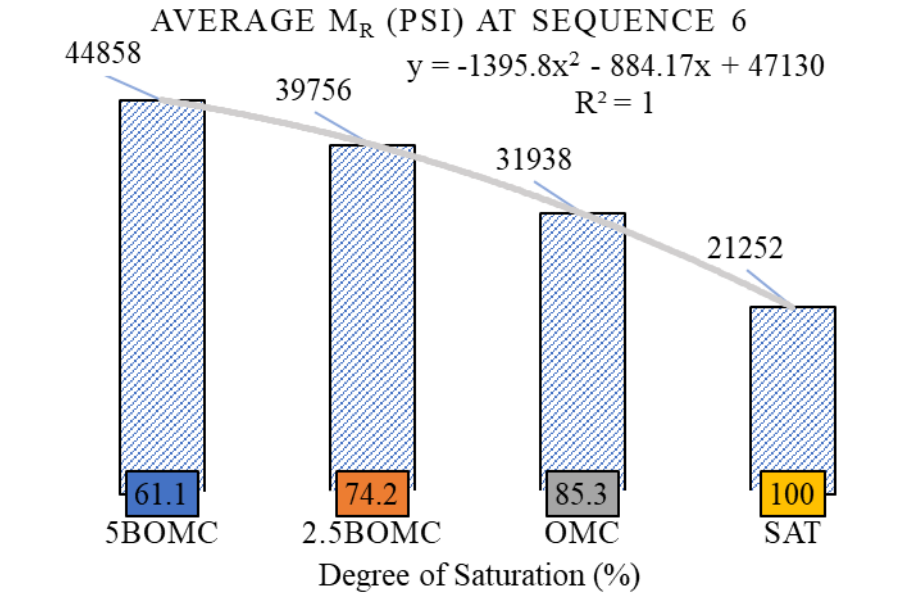

Figure A.7. 6. Final triaxial shear maximum strengths for North Florida limerock

APPENDIX B – Significance Testing

B.1 Statistical Significance – Multiple T-tests

Multiple hypothesis t-tests were conducted with a 95% confidence level to determine whether the average resilient modulus for each base aggregate obtained at moisture contents below and above OMC was statistically greater and less, respectively, than the resilient modulus obtained at OMC.

The Hypotheses were:

- Multiple T-test – Example for Calica limerock
  - -2.5BOMC results: $n_{-2.5\%} = 3$; $_{-2.5\%} = 47759$; $S_{-2.5\%} = 2868$; CL = 95%; α = 0.05
  - OMC results: $n_{omc} = 3$; $_{omc} = 31273$; $S_{omc} = 2129$; CL = 95%; α = 0.05
  - Hypothesis:
  - Using t-table (1-sided test) and α = 0.05
  - SE ($_{-2.5\%}$ - $_{omc}$) =
  -
  -
  - From t-table (1 Tailed test), 3 and = 8 à p-value = 0.003

Conclusion: The p-value (0.003) is less than α (0.05). Therefore, reject the null hypothesis. This means that we are 95% confident that the resilient modulus values of Calica limerock at -2.5%BOMC are statistically greater than the ones at OMC.

- **Multiple t-test – Results for all seven base materials**
  - **For Calera limestone**

	Calera		
	-5%	-2.5%	SAT
n =	3	3	3
n_{omc} =	3	3	3
$\bar{y}$ =	71597	58010	34575
$\bar{y}_{omc}$ =	33509	33509	33509
S =	43	2016	260
S_{omc} =	2421	2421	2421
CL =	95%	95%	95%
α =	0.05	0.05	0.05
U =	0	0	0
U_{omc} =	0	0	0
SE =	1398	1819	1406
t_{calc} =	27	13	1
d_f =	2.0	3.9	2.0
d_f rounded down =	2	3	2
p-value =	0.001	<0.0005	0.200

Figure B.1. 1. Multiple t-test results for Calera limestone

- **For Tuscumbia limestone**

	Calica		
	-5%	-2.5%	SAT
n =	3	3	3
n_{omc} =	3	3	3
$\bar{y}$ =	78382	47759	32293
$\bar{y}_{omc}$ =	31273	31273	31273
S =	478	2868	1376
S_{omc} =	2129	2129	2129
CL =	95%	95%	95%
α =	0.05	0.05	0.05
U =	0	0	0
U_{omc} =	0	0	0
SE =	1260	2062	1463
t_{calc} =	37	8	1
d_f =	2.2	3.7	3.4
d_f rounded down =	2	3	3
p-value =	<0.0005	0.003	0.200

Figure B.1. 2. Multiple t-test results for Tuscumbia limestone

- **For Blue Water limestone**

	Blue Water		
	-5%	-2.5%	SAT
n =	3	3	3
n_{omc} =	3	3	3
$\bar{y}$ =	63475	56268	25382
$\bar{y}_{omc}$ =	31305	31305	31305
S =	554	9532	898
S_{omc} =	1411	1411	1411
CL =	95%	95%	95%
α =	0.05	0.05	0.05
U =	0	0	0
U_{omc} =	0	0	0
SE =	875	5563	965
t_{calc} =	37	4	-6
d_f =	2.6	2.1	3.4
d_f rounded down =	2	2	3
p-value =	<0.0005	0.025	0.005
	<	<	<

Figure B.1. 3. Multiple t-test results for Blue Water limestone

- **For Brooklyn limerock**

	Brooklyn		
	-5%	-2.5%	SAT
n =	3	3	3
n_{omc} =	3	3	3
$\bar{y}$ =	59057	47308	34559
$\bar{y}_{omc}$ =	36098	36098	36098
S =	1455	2305	2449
S_{omc} =	3013	3013	3013
CL =	95%	95%	95%
α =	0.05	0.05	0.05
U =	0	0	0
U_{omc} =	0	0	0
SE =	1932	2190	2242
t_{calc} =	12	5	-1
d_f =	2.9	3.7	3.8
d_f rounded down =	2	3	3
p-value =	0.004	0.008	0.200

Figure B.1. 4. Multiple t-test results for Brooklyn limerock

- **For Calica limerock**

	Calica		
	-5%	-2.5%	SAT
n =	3	3	3
n_{omc} =	3	3	3
$\bar{y}$ =	78382	47759	32293
$\bar{y}_{omc}$ =	31273	31273	31273
S =	478	2868	1376
S_{omc} =	2129	2129	2129
CL =	95%	95%	95%
α =	0.05	0.05	0.05
U =	0	0	0
U_{omc} =	0	0	0
SE =	1260	2062	1463
t_{calc} =	37	8	1
d_f =	2.2	3.7	3.4
d_f rounded down =	2	3	3
p-value =	<0.0005	0.003	0.200

Figure B.1. 5. Multiple t-test results for Calica limerock

- **For JACO limerock**

	JACO		
	-5%	-2.5%	SAT
n =	3	3	3
n_{omc} =	3	3	3
$\bar{y}$ =	59973	49114	24465
$\bar{y}_{omc}$ =	34093	34093	34093
S =	6984	5324	1499
S_{omc} =	1356	1356	1356
CL =	95%	95%	95%
α =	0.05	0.05	0.05
U =	0	0	0
U_{omc} =	0	0	0
SE =	4107	3172	1167
t_{calc} =	6	5	-8
d_f =	2.2	2.3	4.0
d_f rounded down =	2	2	4
p-value =	0.015	0.021	0.0005

Figure B.1. 6. Multiple t-test results for JACO limerock

- **For North Florida limerock**

	North Florida		
	-5%	-2.5%	SAT
n =	3	3	3
n_{omc} =	3	3	3
$\bar{y}$ =	44858	39756	21252
$\bar{y}_{omc}$ =	31938	31938	31938
S =	5984	2634	2600
S_{omc} =	1805	1805	1805
CL =	95%	95%	95%
α =	0.05	0.05	0.05
U =	0	0	0
U_{omc} =	0	0	0
SE =	3609	1844	1827
t_{calc} =	4	4	-6
d_f =	2.4	3.5	3.6
d_f rounded down =	2	3	3
p-value =	0.025	0.010	0.005

Figure B.1. 7. Multiple t-test results for North Florida limerock

B.2 Practical Significance

- **Low Traffic Roads**

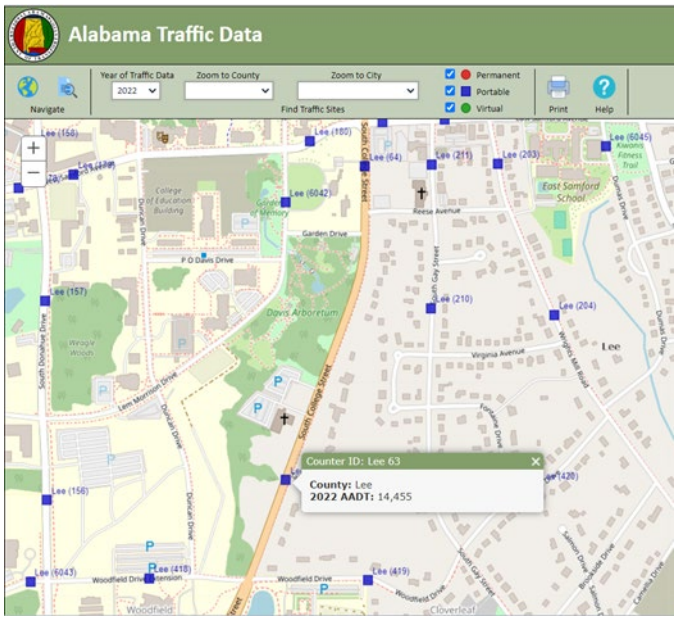

Figure B.2. 1. 2022 Annual Average Daily Traffic (AADT) of south college street Auburn, AL

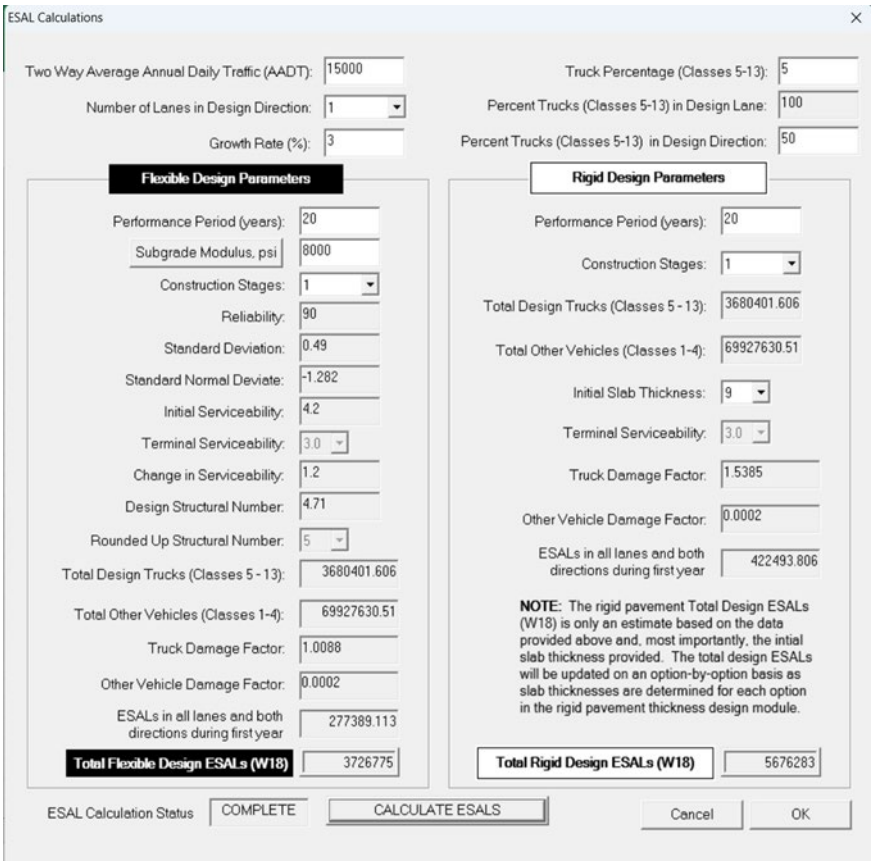

Figure B.2. 2. ESALs calculations for south college street Auburn, AL

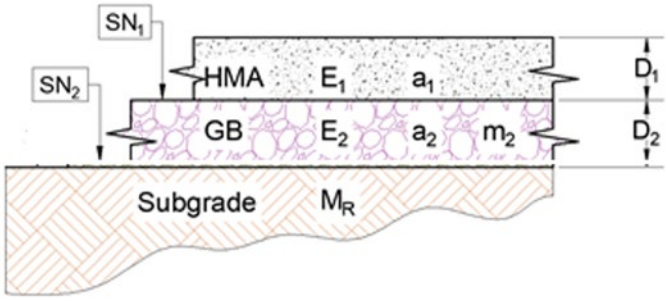

Figure B.2. 3. 2-layer pavement section

	AADT	15000
	W18	3700000
GB - Mr (psi)	**SN1**	**D1 (in)**
30000	2.67	5.0
29000	2.71	5.0
28000	2.75	5.1
27000	2.80	5.2
26000	2.84	5.3
25000	2.89	5.4
24000	2.94	5.5
23000	3.00	5.6
22000	3.06	5.7
21000	3.12	5.8
20000	3.19	5.9

Figure B.2. 4. Sensitivity Analysis - HMA thickness (D1) calculations based on GB M_R change

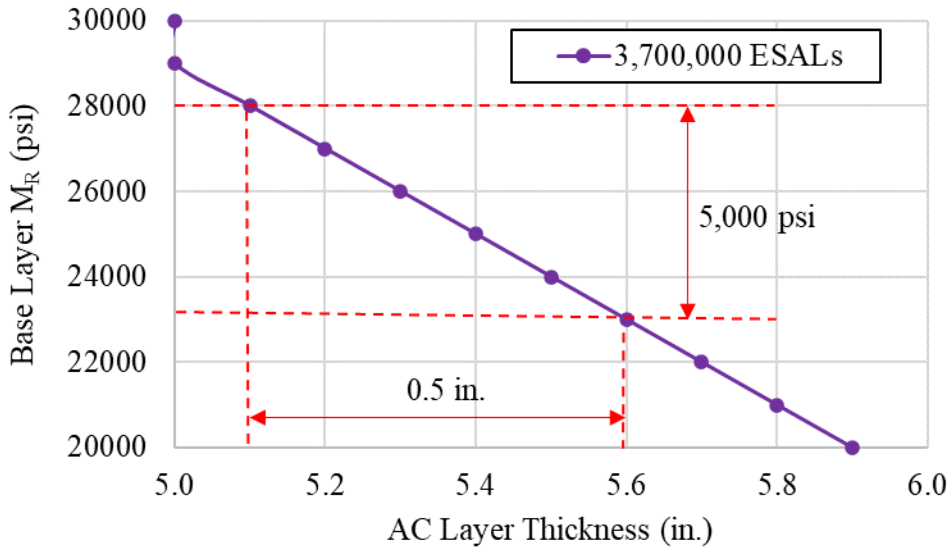

Figure B.2. 5. Sensitivity analysis results for low traffic

- **High Traffic Roads**

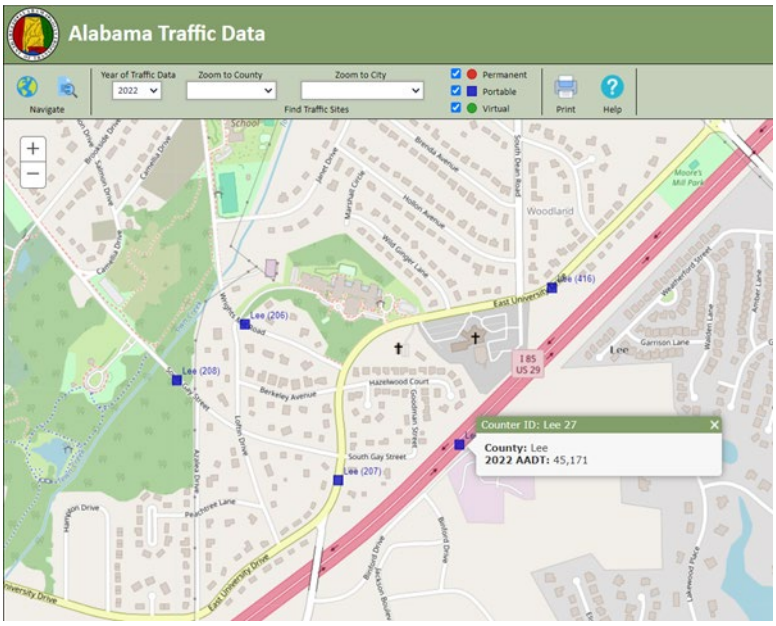

Figure B.2. 6. 2022 Annual Average Daily Traffic (AADT) of I-85

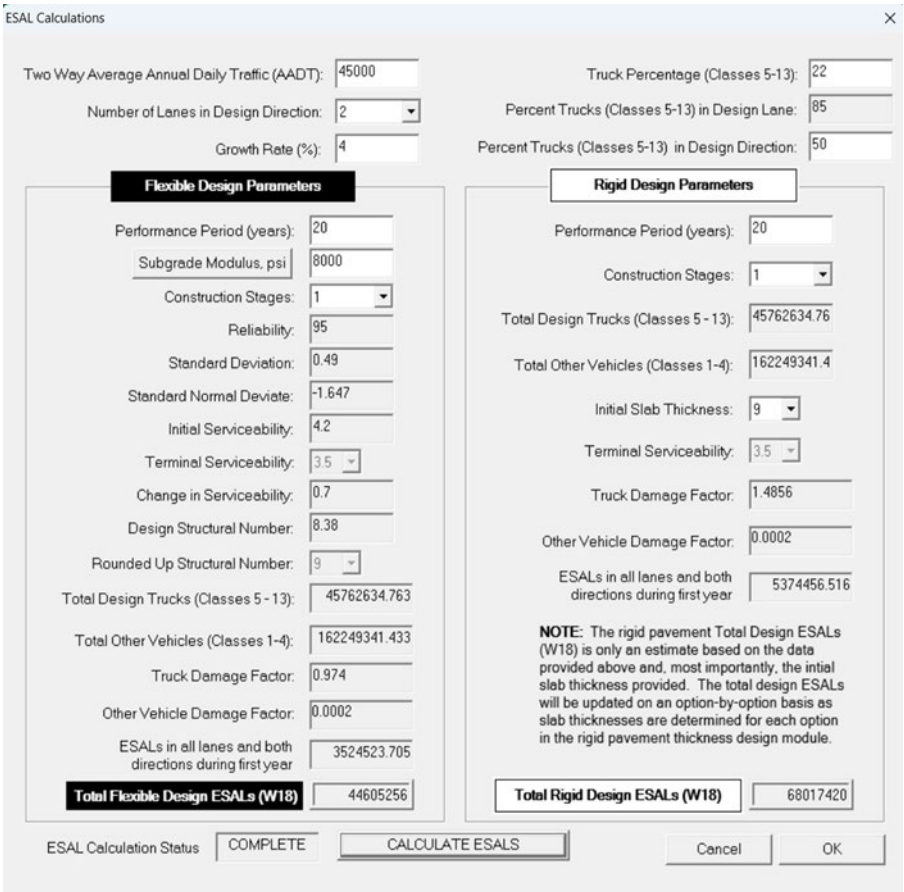

Figure B.2. 7. ESALs calculations for I-85

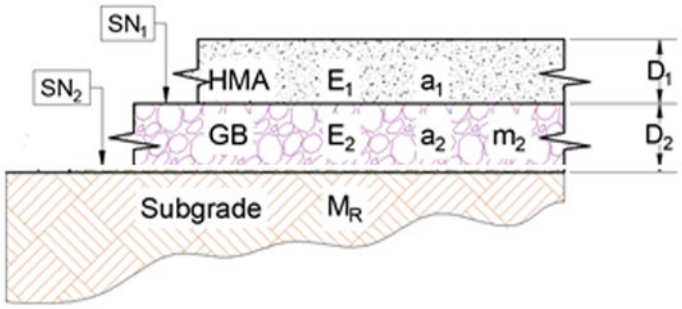

Figure B.2. 8. 2-layer pavement section

	AADT	45000
	W18	44600000
GB - Mr (psi)	**SN1**	**D1 (in)**
30000	4.261181	7.9
29000	4.320179	8.0
28000	4.381519	8.1
27000	4.445363	8.2
26000	4.511893	8.4
25000	4.581315	8.5
24000	4.653864	8.6
23000	4.729809	8.8
22000	4.809459	8.9
21000	4.893171	9.1
20000	4.981364	9.2

Figure B.2. 9. Sensitivity Analysis - HMA thickness (D1) calculations based on GB M_R change

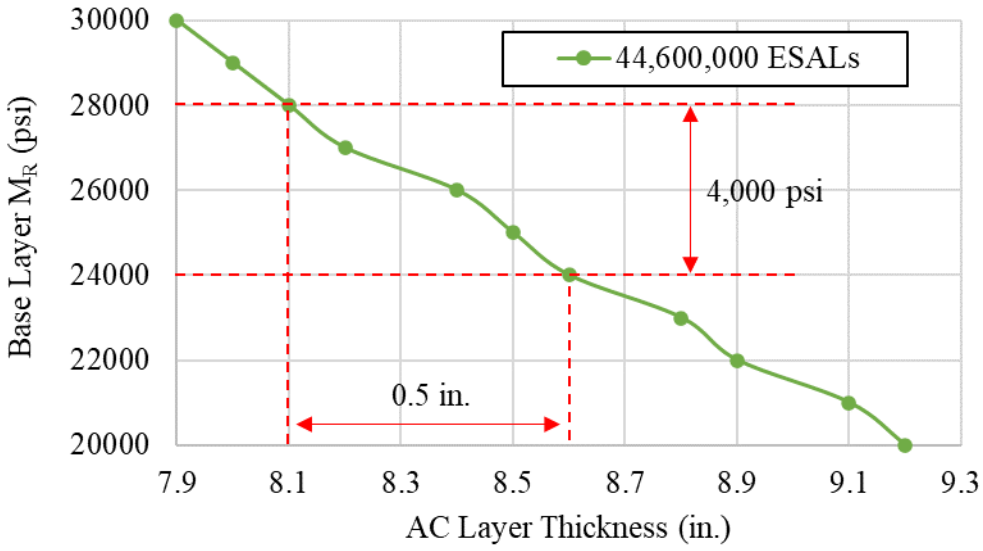

Figure B.2. 10. Sensitivity analysis results for high traffic